2038-5625

Italian Journal of Agrometeorology

Rivista Italiana di Agrometeorologia

n. 2 – 2022

Cover photo by Graziano Lampa

Italian Journal of Agrometeorology

n. 2 - 2022

Firenze University Press

The ***Italian Journal of Agrometeorology*** (***IJAm - Rivista Italiana di Agrometeorologia***) is the official periodical of the Italian Association of Agrometeorology (AIAM) and aims to publish original scientific contributions in English on agrometerology, as a science that studies the interactions of hydrological and meteorological factors with the agricultural and forest ecosystems, and with agriculture in its broadest sense (including livestock and fisheries).

SUBSCRIPTION INFORMATION
IJAm articles are freely available online, but print editions are available to paying subscribers. Subscription rates are in Eur and are applicable worldwide.
Annual Subscription: € 50,00 Single Issue: € 25,00

CONTACT INFORMATION
Please contact ordini@fupress.com, if you have any questions about your subscription or if you would like to place an order for the print edition. Information on payment methods will be provided after your initial correspondence.

Published by
Firenze University Press – University of Florence, Italy
Via Cittadella, 7 - 50144 Florence - Italy
http://www.fupress.com/ijam

Italian Journal of Agrometeorology
Rivista Italiana di Agrometeorologia

Firenze University Press
www.fupress.com/ijam

OPEN ACCESS

Citation: C. Kittas, W. Baudoin, E. Kitta, N. Katsoulas (2022) Sheltered horticulture adapted to different climate zones in Radhort Countries. *Italian Journal of Agrometeorology* (2): 3-16. doi: 10.36253/ijam-1655

Received: May 12, 2022

Accepted: June 4, 2022

Published: January 29, 2023

Data Availability Statement: All relevant data are within the paper and its Supporting Information files.

Competing Interests: The Author(s) declare(s) no conflict of interest.

Sheltered horticulture adapted to different climate zones in Radhort Countries

Constantinos Kittas[1,*], Wilfried Baudoin[2], Evangelini Kitta[1], Nikolaos Katsoulas[1]

[1] *University of Thessaly, Greece, University of Thessaly, Department of Vegetal Production and Rural Environment, Phytokou Street, 38444 Volos, Greece*
[2] *Former FAO Senior Officer , Plant Production and Protection Division Rome, Italy*
*Corresponding author. E-mail adress: ckittas@uth.gr

Abstract. Over the last decade, the total population of the sub-Saharan region of Africa has been increasing rapidly at a rate of more than 3% annually, with urbanization expected to be approximately 40% of the total population by 2050. Parallel growth has not been achieved in the agricultural sector in West Africa, with vegetable production and consumption being amongst the lowest in the world. This has aggravated the already food insecurity and malnutrition situation in the region. In this context, and within the framework of their agricultural development policies, 10 countries of West Africa (Burkina Faso; Cabo Verde; Côte d'Ivoire; Guinée; Guinée Bissau; Mali; Mauritanie; Niger; Sénégal; Chad), established the "African Network for Horticultural Development "RADHORT" (Réseau Africain pour le Développement de l'Horticulture), in order to cooperate for the diversification and intensification of horticulture in the region. The countries of RADHORT cover different climate zones ranging from the arid climate (desert), to the Sahelian zone (semi-arid), to the dry tropical zone (with long dry season and short rainy season), and to the wet tropical zone (humid zone with bimodal rainfall). Temperatures and global radiation are very suitable for vegetable production in tropical countries throughout the year, but open air cultivation can be severely hampered by high temperatures, winds, heavy rainfall, while being exposed to pest and disease infestation. Sheltered cultivation will help to moderate negative effects of climate factors on the crop, improve water productivity and the efficiency of eco-friendly pest and disease management. The paper analyses and discusses different technical options of sheltered cultivation to be tested in RADHORT countries, as a means to enhance horticulture crops productivity and quality for meeting the growing demand of an expanding rural and urban population.

Keywords: greenhouse, nethouse, protected cultivation, Tropics.

INTRODUCTION

The total population of the sub-Saharan region of Africa has been increasing rapidly at a rate of more than 3% annually during last decade, with an urbanization rate expected to be approximately 40% of the total population by 2050 (Saghir and Santoro, 2018). Parallel growth has not been achieved in the agricultural sector in West Africa, with vegetable production,

availability and consumption being amongst the lowest in the world. This has compounded the already food insecure and malnutrition situation in the region.

In this context, the intensification and development of the horticulture sector has considerable potential for contributing to enhanced food and nutrition security at global level. It would be based on the sustainable use of available land and water resources and would generate employment and income, contributing significantly towards improving the livelihood particularly of small-scale farmers, women and youth. To this end, and within the framework of their agricultural development policies, 10 countries of West Africa, have joined together and committed themselves to the intensification and diversification of horticultural crops in the region. To this effect they established the African Network for Horticultural Development "RADHORT" (Réseau Africain pour le Développement de l'Horticulture)[1], as a framework to facilitate regional cooperation and integration. RADHORT is a major result of a project for the development of horticultural production in West Africa implemented since 1988 by FAO under the FAO-Belgium Cooperation Program (GCP/RAF/244/BEL). The member states of RADHORT are Burkina Faso, Cabo-Verde, Ivory Coast, Guinea, Guinea-Bissau, Mali, Mauritania, Niger, Senegal and Chad (FAO, 2016)[2]. The countries of RADHORT are located in the Tropics.

However, they cover different climate zones ranging from desert, semi-desert to subtropical and tropical.

The scope of RADHORT is the development of the horticultural sector with the aim of achieving intensification and development of horticulture production in support of improved food and nutrition security in the context of the rapidly increasing population of African countries and the rising urbanization rate.

Within the effort for the development of the horticultural sector in RADHORT countries, a description and an analysis are made in this article of different technical options for the rational design and equipment of sheltered cultivation based on the climatic features prevailing in the region covered by the RADHORT countries. These technical options could be a basis for applied research at regional level with the aim of promoting sheltered cultivation as part of an innovation toolbox in support of sustainable crop intensification in the West Africa region.

[1] http://www.fao.org/agriculture/crops/thematic-sitemap/theme/hort-indust-crops/radhort/presentationgenerale/en/

[2] The constitutional act of RADHORT has been undersigned by the Ministers of agriculture of the ten founder countries and the acceptance instrument has been deposited at FAO for record and custody.

THE CLIMATE CHARACTERISTICS OF RADHORT COUNTRIES

The countries of RADHORT are located in the Tropics. However, looking at the map of Climate zones of Africa (Figure 1, http://www.synergy-energy.co/africa-climate-map.html), it is noted that, according to Köppen- Geiger climate classification (Köppen, 1936), the RADHORT countries (Burkina-Faso, Cabo Verde, Guinea, Guinea Bissau, Mali, Ivory coast, Mauritania, Niger, Chad and Senegal), cover different climate zones ranging from the arid climate (desert), to the Sahelian zone (semi-arid), to the dry tropical zone (tropical with long dry season and short rainy season), to the wet tropical zone (humid zone with bimodal rainfall).

This situation illustrates the fact that there is very large variation of climate features within the RADHORT countries.

WHY GREENHOUSES IN THE TROPICS?

The tropics are a belt of the earth surrounding the Equator. They are delimited in latitude by the Tropic of Cancer in the Northern Hemisphere at 23°26'13.1" (or 23.43696°) N and the Tropic of Capricorn in the Southern Hemisphere at 23°26'13.1" (or 23.43696°) S; these latitudes correspond to the axial tilt of the Earth.

In tropical regions, the temperatures and the global radiation are very suitable for vegetable production throughout the year. However, open field cultivation can be severely hampered by adverse weather conditions, including high temperatures, drying winds, high pest and disease incidence, as well as heavy rainfall and high relative humidity (von Zabeltitz, 2011).

The aim of promoting sheltered cultivation is to intensify the production of safe vegetables of better quality, allowing to reduce the applications of synthetic chemical pesticides and saving on water and land resources. Crop production under sheltered cultivation permits continuous crop production throughout the year with efficient use of inputs: water, fertilizers, labor, space and the implementation of biological control as part of integrated plant protection management (IPM). With respect to water, which is a serious limiting factor in several RADHORT countries, it was reported by Katsoulas et al. (2012), that crops grown in a nethouse consumed about 20-40% less water than in the open field. The same reduction occurs for crops in unheated simple (low tech) greenhouses, while for crops under sophisticated (high tech) greenhouses, water saving against open field can exceed 60% (Nederhoff and Stangellini, 2010).

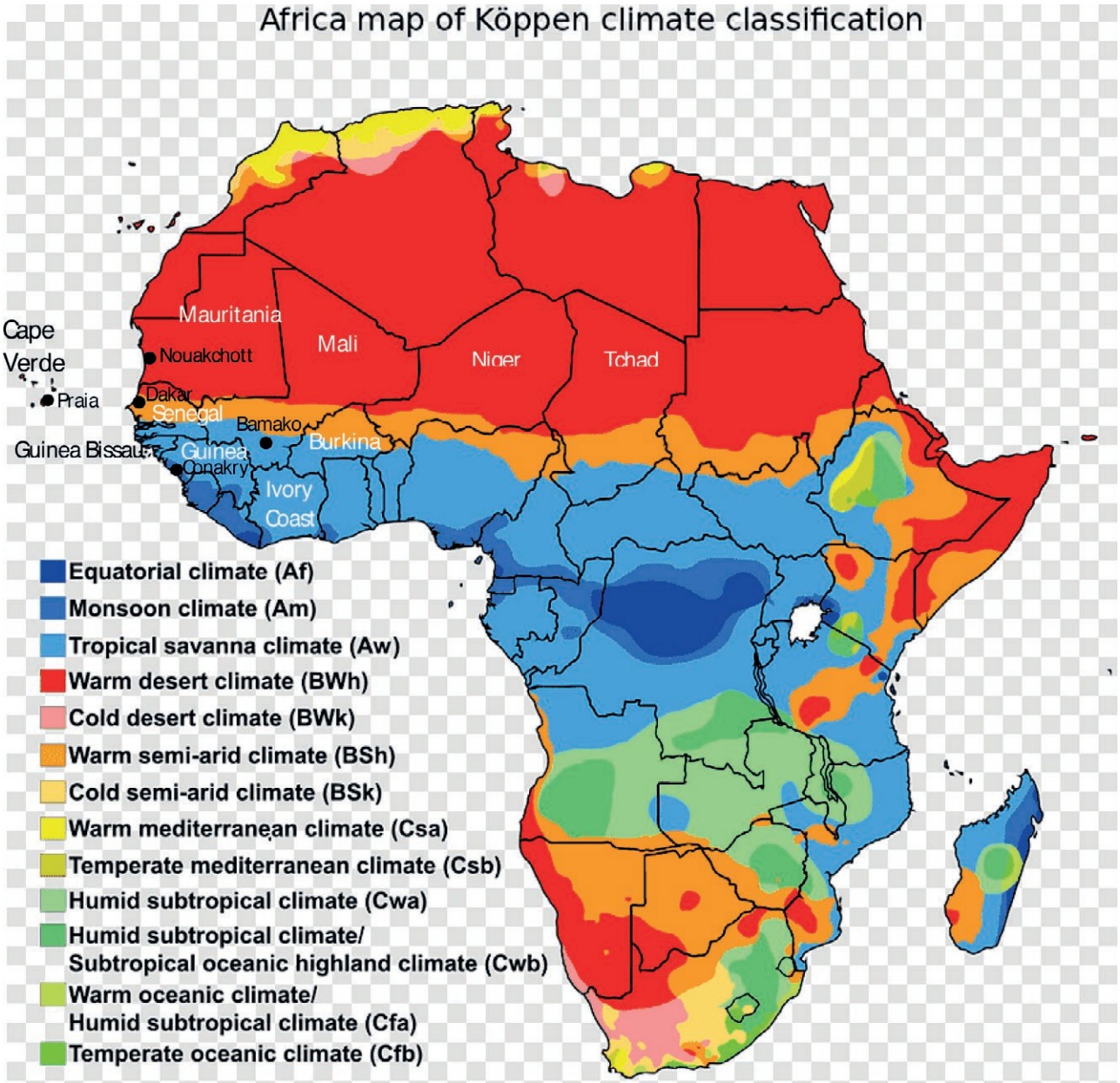

Fig. 1. Climatic Zones of Africa and RADHORT countries.

Sheltered cultivation can be defined as any agricultural activity taking place under a protective structure. A protective structure is defined as any structure designed to modify the environment under which plants are grown.

Protective structures are generally classified in two main groups:

Greenhouses, referring to structures covered (at least the roof) with non-porous materials and nethouses, which are covered with porous materials.

Greenhouses, besides the cover sheets, can be equipped with screen nets, which are used either for insect proofing or shading. Insect-proof nets can be applied on the openings of the greenhouses, while shading nets can be added on top of the greenhouse roofs to prevent overheating.

Nethouses offer a physical protection of the crop against adverse climate factors (e.g. wind, dust, etc) and insect pests while also offering a cooling effect by reducing the incoming solar radiation.

The development and use of efficient, cheap but cost-effective technologies for adapted protective-shelter structures is crucial for the expansion of protected culti-

vation in the tropics. This means that imported turnkey greenhouses from countries with subtropical or temperate climate can be avoided. Instead, the design of constructions, which are adjusted to local climate parameters and built with locally available materials, including *Bambusa vulgaris*, *Casuarina equisetifolia*, *Borassus flabellifer*, should be investigated and promoted for the different climate zones (FAO, 1999).

Vegetable production in tropical climates under adapted shelter structures with selected covering materials will result in higher yield of better quality, secured harvest all year round, less susceptibility to diseases, less insect damage, less physical damage and flooding by heavy rain-fall, reduced water consumption, more efficient use of fertilizers, less chemical pest and disease control and a more comfortable working environment. The increase in productivity and better quality produce obtained with fewer and cost-effective inputs are expected to lead to an increase of revenue for the farmers. In fact, a cost-benefit analysis conducted in Kenya (Nakuru, 0°18'11.1564''S, 36°4'48.0900''E, warm-summer Mediterranean climate – Csb) comparing the profitability of tomato cultivation in low tech unheated greenhouses and in the open field (Wachira et al., 2014), demonstrated that average yields in greenhouse were about 10 times higher than in the open field.. Net profits per square meter were 13 times higher for tomato cultivation in greenhouse than in the open field even though fixed costs, i.e. the sum of all costs that do not vary with the production, were on average more than 60 times higher for greenhouse farming. Furthermore, a cost benefit analysis in warm semi-arid region (Rohtak, India, 28°53'40.09"N 76°35'21.01"E, BSh) (Duhan, 2016) showed that growing vegetables under low cost unheated greenhouses is more than 10 times more profitable as compared to open field production.

GENERAL RULES FOR TECHNOLOGIES OF PROTECTED HORTICULTURE IN TROPICS

Some general rules and technologies suitable for the climatic conditions prevailing in the RADHORT countries are presented as guiding principles for the rational development of protected agriculture in such countries.

Design criteria for greenhouses are based on the climate conditions in situ and climate control needs in line with the analysis of the limiting factors for plant growth, the general greenhouse structure and covering materials requirements, taking into consideration local standards if existing, as well as locally available, suitable and cost effective materials.

Climate Conditions for assessing the Regional Suitability for Greenhouse Cropping

Greenhouses have to be designed in regard to the needs of the plants and conditions of the different climate zones. To check the suitability of a region for protected cultivation, the climate data should be compared with those of other regions and with the main requirements of the plants to be grown in the greenhouses.

For vegetables, the main climate requirements and set points for climate control for thermophile species are (Kittas, 1995; von Zabeltitz and Baudoin, 1999):

- T_{max}: mean monthly maximum temperatures below 32-34°C
- T_{min}: mean monthly minimum temperatures greater than 12°C
- SR: mean minimum outside solar radiation 7.5 MJ/m^2/day.
- HR: relative humidity in the range of 70 to 90%

From the analysis of climate data in RADHORT countries, it can be concluded that, there is no need for heating since T_{min}> 12°C always and this is the case for all RADHORT countries. To the contrary, in the Tropics, the greenhouse design and equipment has to face a specific problem of climate control, which is the avoidance of greenhouse overheating.

By using the climate data of each area a climograph can be elaborated to assess the local suitability for greenhouse cropping (Kittas, 1995). More precisely, the climograph for selected sites will be obtained by combining the average maximum monthly outside temperature and the corresponding average global radiation for a given region during the 12 months of the year. By adopting 27°C and 33°C as reference temperature set points, the following climate control requirements can be defined to ensure good plant growth:

- T_{max}< 27°C a good ventilation is sufficient
- 27°C <Tmax< 33°C ventilation + shading are needed
- T_{max}> 33°C cooling is needed.

The General Design Requirements

Based on the climate control requirements for good plant growth, the following general design criteria and technical specifications have been elaborated for greenhouse cultivation in the tropics (Baudoin and von Zabeltitz, 2002):

- Cladding material: Plastic film, with the following desirable characteristics:
  - Long lasting: Longevity should be for a minimum of 3 to 4 years even with high global radiation.

  - Light diffusing: In order to increase homogeneity of the solar radiation but also to increase the shading effect of the cover.
  - Easy to clean from prevailing dust.
  - UV-Absorbent and if possible photo-selective against insects' infestation.
  - Antifog to avoid condensations on the cover.
  - Antidrip to avoid wetting the plants underneath.
  - IR reflectant for heat reduction purposes.
  - Covering film must not flutter in the wind, but has to be stretched and tightly fixed by simple stretching devices.
- Shade nets: They are usually white with Shading Intensity (S.I.), as required, between 20 and 40% and 2-3 years longevity.
- Ventilation: To be efficient, ventilation openings (ventilators) are needed at sidewalls and the ridge. Ridge ventilation is absolutely necessary, if mean maximum temperature is above 27°C. Efficient ventilation should aim at reducing the difference between inside and outside greenhouse temperature.
- Insect proofing: Ventilation openings have to be equipped with nets of 50 mesh against penetration of insects, without decreasing the ventilation efficiency for more than 30%. Therefore, the ventilation area must be adequately increased. The S.I. of insect proof nets is about 20%.
- Structural and geotechnical design: For the four prevailing climates (BSh, BWh, Aw, Am) the design has to favor the natural (passive) ventilation, which can be obtained by sidewall and ridge openings (equivalent to at least 30% of the floor area), both covered with insect-proof nets. In Aw and Am climates, it should be possible to close the vents in order to operate fan and pad evaporative cooling when needed (Franco et al., 2014). Gutter height: The gutter height should be about 2.5 to 3 m minimum. The higher the structure with ridge ventilation, the greater the ventilation efficiency by the chimney-effect. To the extent possible, the use of locally available and renewable construction materials is advisable to contain the investment cost. The greenhouse structure and foundation must be designed and calculated according to the "EN 1990 'Eurocode - Basis of structural and geotechnical design", against wind, pressure and suction forces, and crop loads.
- Rainwater collection: Gutters are necessary to not only drain off the rainwater but also for the collection and storage of rainwater, which can be recycled for irrigation and other purposes.
- Greenhouse irrigation: localized irrigation systems should be applied, to avoid increasing the air-humidity inside the greenhouse. It will help to control weed growth and contain the infestation of pests and diseases.

APPROPRIATE GREENHOUSE TYPES FOR RADHORT COUNTRIES

Climographs have been elaborated, using the meteorological data of Nouakchott (Mauritania), Dakar (Senegal), Praia (Cabo Verde), Conakry (Guinea)and Bamako (Mali) (Table 1), with a view to characterizing the suitability for selected greenhouse types in these sites, which could be extrapolated at regional level to iso-climate areas in the RADHORT countries. Ierapetra (35°00'42.70"N, 25°44'32.42"E) on the south coast of the island of Crete (south Greece), has been used as a reference location for comparison purposes. Ierapetra is the area with the highest concentration of protected crops in Greece with Mediterannean climate (dry summers and mild, wet winters), classified as Csa by the Köppen-Geiger system[3].

The analysis is based on the climograph of the following cities:

(1). Nouakchott, Mauritania (18°09'N 15°58'W, warm desert climate), classified as BWh in the Köppen-Geiger system vs. Ierapetra and Praia, Cabo Verde (14°55'N 23°31'W, warm desert climate, BWh) vs Ierapetra (Figure 2), with relatively lower maximum temperatures than the corresponding values in continental areas, due to the beneficial effect of sea breezes from the Atlantic.

(2). Dakar, Senegal (14°40'N 17°25'W, warm semi-arid climate, BSh) vs Ierapetra (Figure 3).

(3). Conakry, Guinea (9°31'N 13°42'W, monsoon climate, Am) and Bamako, Mali (12°39'N; 8°0'W, tropical savanna, Aw) vs Ierapetra (Figure 4).

a. Climograph of Nouakchott and Praia vs Ierapetra

The climate in Nouakchott is warm desert, it means hot and rather dry with very low rainfall over the year. From Figure 2, it can be suggested: (i) Greenhouse to be the highest possible for improving the chimney effect for higher ventilation rate; (ii) Ventilation needs to be very efficient throughout the year with openings up to 30-35% of the total floor area. The lateral and

[3] The major greenhouse types adapted to Ierapetra are: Tympaki type (similar to Parral), Tunnel and modified arched roof single layer polyethylene covered greenhouses equipped with vent openings for natural ventilation.

Table 1. Meteorological data of RADHORT countries and Ierapetra- Greece.

City, Country	Data	Units	1	2	3	4	5	6	7	8	9	10	11	12	Total
Ouagadougou Burkina Faso 12,37°N/1,53°W	Tmean	°C	25,1	28	31,4	33,2	32,4	29,7	27,5	26.5	27.4	29.1	28.2	25.4	
	Tmean	°C	25,1	28	31,4	33,2	32,4	29,7	27,5	22	21.8	25,1	28	31,4	
	Tmax	°C	33	36	38	39	38	35	32	31	33	36	36	33	
	HR	%	22,8	20,3	21,8	35,7	49,80	62,5	72,5	79	75,3	58,2	35,4	26,8	
	SR	MJ/m²/d	19,7	22,9	23,2	23	22,3	22	20,6	19,3	20,8	21,3	20,7	19,1	
	Rainfall	mm	0.1	0.5	5.9	26.5	66.8	97.5	176	214	121	33.5	1.2	0.2	743.2
Praia Cabo Verde 14,93°N/23,51°W	T_{mean}	°C	22.9	22.9	23.6	23.9	24.7	25.5	26.1	27.1	27.4	27.2	26.1	24.1	
	Tmin	°C	19.3	19.2	19.5	19.9	20.7	21.6	22.7	23.9	24.2	23.6	22.5	20.8	
	Tmax	°C	26.5	27.0	28.1	28.2	28.9	29.6	29.6	30.4	30.9	31.0	29.7	27.7	
	HR	%	65.7	63.3	62.6	64.5	65.2	68.5	73.3	76.0	76.8	72.9	69.8	70.1	
	SR	MJ/m²/d	16,6	18,9	22,6	24,2	26,3	25,8	22,6	20,9	19,4	18,2	16,3	14,9	
	Rainfall	mm	3.1	0.6	0.3	0.0	0.5	0.0	8.0	60.4	60.9	31.0	2.7	5.0	172.5
N'djamena Chad 12,11°N/15,0 7°E	Tmean	°C	23.4	25.9	29.9	32.9	32.9	30.9	28.3	27.0	28.2	29.4	26.8	24.2	
	Tmin	°C	14.3	16.6	21.0	24.8	25.8	24.7	23.1	22.4	22.7	21.8	17.8	14.8	
	Tmax	°C	32.4	35.2	38.7	41.0	39.9	37.2	33.5	31.6	33.7	36.9	35.8	33.5	
	HR	%	29	23	21	28	39	52	68	76	72	49	33	31	
	SR	MJ/m²/d	18,9	21,3	24,0	24,2	23,5	22,3	19,9	19,1	19,9	19,9	18,9	17,5	
	Rainfall	mm	0	0	1	3	6	9	13	15	9	3	1	0	60
Abidjan, Ivory Coast 5,33°N/ 4,03° W	Tmean	°C	26.8	27,7	27.9	27.7	26.9	25.8	24.7	24.5	25.6	26.8	27.4	27.0	
	Tmin	°C	23.5	24.6	24.9	24.9	24.6	23.7	22.9	22.1	22.3	23.6	24.4	23.8	
	Tmax	°C	30.5	31.0	31.1	31.2	30,4	28.7	27.4	26.9	27.6	29.2	30.5	30.3	
	HR	%	84	86	83	82	84	86	85	86	89	87	83	83	
	SR	MJ/m²/d	18,4	18,9	18,7	18,5	17,2	14,4	14,7	14,1	14,1	16,2	17,3	17,4	
	Rainfall	mm	3	4	9	11	19	22	12	8	11	14	16	9	138
Bissau, Guinea-Bissau 11,87°N/15,61°W	T_{mean}	°C	24.4	25.6	26.6	27.0	27.5	26.9	26.1	26.4	26.4	27.0	26.9	24.8	
	Tmin	°C	17.8	18.3	19.4	20.6	22.2	22.8	22.8	22.8	22.8	22.8	22.2	18.9	
	Tmax	°C	31.1	32.8	33.9	33.3	32.8	31.1	29.4	30.0	30.0	31.1	31.7	30.6	
	HR	%	45,5	49	54	58	64,5	75	80,5	84	81,5	78	67,5	53,5	
	SR	MJ/m²/d	17,8	20,4	22,9	23,8	23,3	21,5	19,7	18,1	18,9	19,7	17,9	16,7	
	Rainfall	mm	0.5	0.8	0.5	0.8	17.3	175	472	683	435	195	41	2.0	2020
Conakry Guinea 9,54°N/13,68°W	Tmean	°C	26,4	26,4	26,2	26,1	25,8	25,2	24,7	24,5	24,7	24,9	25	25,7	
	Tmin	°C	22,8	22,8	21,4	20,2	20,6	20,4	21,4	21	20,4	19,8	20	21,4	
	Tmax	°C	32.2	33.1	33.4	33.6	33.2	31.8	30.2	29.9	30.6	30.9	32.0	32.2	
	HR	%	56,6	61,9	66,7	73	82,3	86,4	86,8	87,3	87	86,5	83,1	66,7	
	SR	MJ/m²/d	20,1	21,8	23,7	23,3	20,3	17,6	14,8	14,2	17,6	18,6	18.5	18.9	
	Rainfall	mm	1	1	3	22	137	396	1130	1104	617	295	70	8	3784

City, Country	Data	Units	1	2	3	4	5	6	7	8	9	10	11	12	Total
Bamako Mali 12,65°N/8°W	Tmean	°C	24,8	27,9	30,9	32,5	31,4	28,6	26,3	25,7	26,1	27,3	26,9	24,9	
	Tmin	°C	16,6	19,8	22,8	25	23,8	22,2	20,6	20,4	20,2	19,6	18,8	16,8	
	Tmax	°C	33	36	39	40	39	35	32	31	32	35	35	33	
	HR	%	23,4	20,2	21,3	34,9	51,1	68,3	79,0	83,2	81,3	69	41,7	28,3	
	SR	MJ/m²/d	18,8	21,8	22,6	23	22,1	20,5	18,9	18,2	19,3	20,2	20,1	191	
	Rainfall	mm	0,6	0,7	2,1	19,7	54,1	132	224	290	196	66,1	5,2	0,5	991,3
Nouakchott Mauritania 18,08°N/15,98°W	Tmean	°C	21,3	22,6	24	24	25,3	26,6	27	28,3	29,3	28,6	25,6	22,7	
	Tmin	°C	15,6	15,2	17	17	18,6	20,2	24	25,6	25,6	22,2	19,2	17,4	
	Tmax	°C	29.1	30.8	33.5	34.8	34.3	34.7	32.4	33.0	36.1	36.7	34.0	31.0	
	HR	%	38,5	43,3	49,6	59,2	60,1	67,0	75,9	75,7	71,3	56,9	48,3	40,8	
	SR	MJ/m²/d	20,5	22,3	25,9	28,1	27,7	27,7	25,9	25,5	24,1	22,7	19,8	18,4	
	Rainfall	mm	0.7	1.5	0.2	0.1	0.3	1.9	6.3	36.8	36.3	6.3	2.0	2.8	95.2
Niamey, Niger 13,51°N/2,1°E	Tmean	°C	24,4	27,2	31,4	34,4	34,4	31,9	29,3	28	29,2	30,9	28,4	25,1	
	Tmin	°C	15,8	18,4	23,8	27,8	28,8	26,8	24,6	23	24,4	23,8	20,8	17,2	
	Tmax	°C	33	36	39	41	40	37	34	33	34	38	36	33	
	HR	%	21,6	17,4	17,0	25,3	40,9	54,5	66,9	74,7	69,5	47,1	27,4	24,4	
	SR	MJ/m²/d	19,7	22,9	24,5	25,2	25,1	23,9	21,8	20,5	21,5	21,78	20,74	18,86	
	Rainfall	mm	0,0	0,0	3,9	5,7	34,7	68,8	154	171	92,2	9,7	0,7	0,0	540,7
Dakar, Senegal 14,69°N/17,44°W	Tmean	°C	20,7	20,7	21	21,4	22,8	25,6	27,1	27,4	27,6	27,6	25,8	23,4	
	Tmin	°C	15,4	16,4	17	17,8	19,6	22,2	27,2	24,8	24,2	24,2	21,6	18,8	
	Tmax	°C	26	25	25	25	26	29	27	30	31	31	30	28	
	HR	%	70,2	74,90	78,50	83,00	82,90	82,30	79,70	83,00	84,70	81,80	73,80	68,60	
	SR	MJ/m²/d	17,6	20,9	23,6	24,9	24,2	22,4	20,2	19,2	19,2	19,9	17,9	16,5	
	Rainfall	mm	1,0	2,0	0,3	0,0	0,1	14,0	51,0	154	133	26	9,2	1,0	391,6
Ierapetra, Greece 35.01°N/25.74°E	Tmean	°C	13	13,3	14,7	17,3	21	25,8	28,3	28,1	25,1	21,7	18,3	14,8	
	Tmin	°C	9,7	10	11,5	13,9	17,3	22,2	24,4	24	21,4	18	14,7	11,6	
	Tmax	°C	16,3	16,6	17,9	20,7	24,7	29,4	32,2	32,1	28,8	25,4	21,9	18	
	HR	%	68	67	65	61	60	57	58	59	60	65	67	70	
	SR	MJ/m²/d	8,3	10,9	14,7	18,6	22,6	25,9	26,3	24,5	19,7	13,9	10,4	8	
	Rainfall	mm	101	70,7	44,8	20	10,4	1,3	0,3	0,7	13,7	41,7	62,8	118	484,4

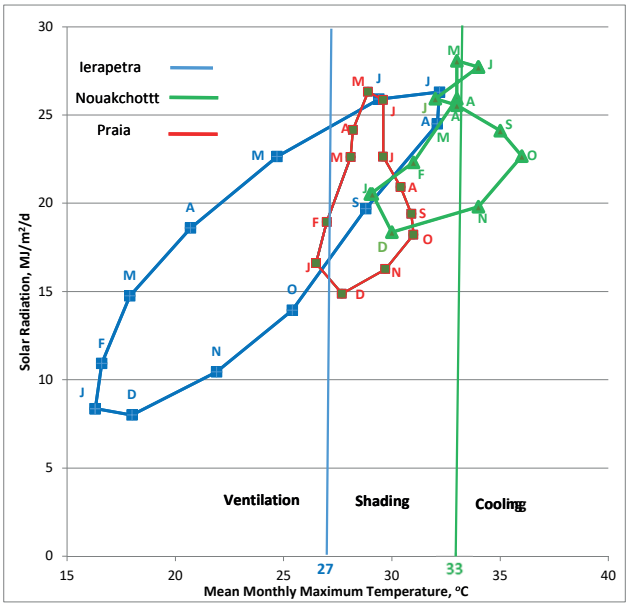

Fig. 2. Climograph of Nouakchott ((Mauritania, 18°09'N and 15°58'W, warm desert climate), Praia (Cabo Verde, 14°55'N and 23°31'W, warm desert climate) and Ierapetra (Greece, 35°00'42.70"N, 25°44'32.42"E, cold semi-arid climate).

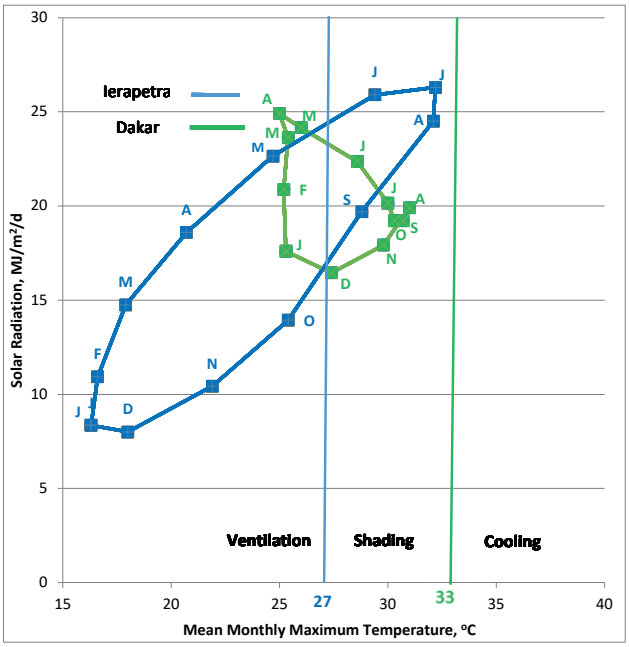

Fig. 3. Climograph of Dakar, Senegal, 14°40'N and 17°25'W, warm semi-arid climate) vs Ierapetra (Greece, 35°00'42.70"N, 25°44'32.42"E, cold semi-arid climate).

roof vents should be kept permanently open and shading of the greenhouse should be applied using nets with SI= 30%[4]. (iii) The combined action of natural ventilation and shading can increase the transpiration of the plants, which is beneficial for the crops due to the outside low humidity. It should be stressed that all ventilator openings must be covered with insect proof nets (50 mesh). (iv) From March to mid-November) an evaporative cooling system is necessary. . The diurnal relatively high air temperatures combined with the absence, practically, of rainfall lead to diurnal values of air relative humidity no greater than 30- 40%. Consequently, a satisfactory performance of an evaporative cooling system is assured for a greenhouse installed in such an area (Watson et al., 2019).

However, this requires additional investment for more sophisticated technical options like fan and pad cooling, or a high-pressure fog system, both of which also improve the hygrometric status of the greenhouse environment. Fan and pad greenhouse cooling is based on hot and dry air being sucked through a wet pad posed at one side of the greenhouse and electric ventilators at the opposite site (Franco et al., 2014). The high pressure fog cooling system occurs by spraying a fine mist that will evaporate and cool down the air by absorbing the heat inside the greenhouse[5] (Kumar et al., 2009). The use of photovoltaic panels for powering the ventilators and the pump is an option that has to be validated as a cost effective investment.

The climate in Praia (Cabo Verde) is also classified warm desert. However, as compared to Nouakchott the maritime effect is pronounced and induces lower temperatures and even less rainfall. Figure 2 shows that shading of greenhouses is necessary throughout all the year. Furthermore, the shading has a beneficial effect since it enhances transpiration of stressed crops. Black plastic mulching against weeds is advisable. It will reduce inside air humidity and help to prevent fungal diseases.

b. Climograph of Dakar vs Ierapetra

The climate in Dakar (Senegal) is warm semi-arid (BSh). Figure 3 shows that for half of the year, from December to May, a very good ventilation is sufficient. For the rest six months shading is necessary. Nevertheless, considering that insect proof nets in the ventilation openings against insects are indispensable, shading of greenhouses throughout all the year is suggested to avoid too high temperatures inside.

[4] SI: Shading Intensity

[5] The latent heat of evaporation of water at 25°C is approximately 2500 J/g, it means that evaporation of 1 gram of water at 25 °C will absorb approximately 2500 Joules (580 calories) from the ambient air

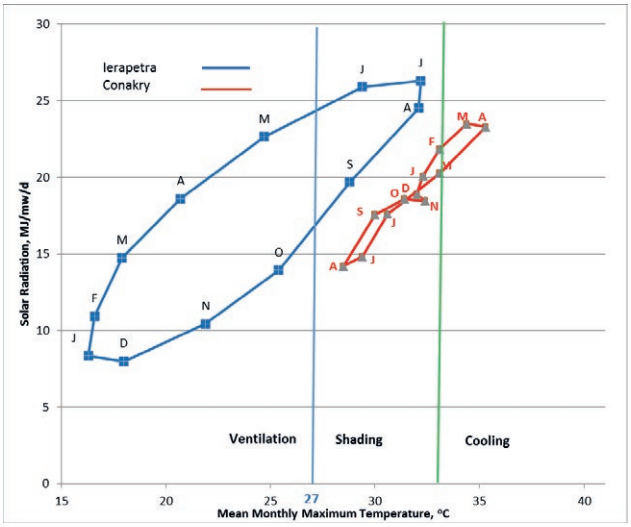

Fig. 4. Climograph of Conakry (Guinea, 9°31'N and 13°42'W, monsoon climate) and Bamako (Mali, 12°39'N and 8°0'W, tropical savanna) vs Ierapetra (Greece, 35°00'42.70"N, 25°44'32.42"E, cold semi-arid climate).

c. Climograph of Bamako and Conakry vs Ierapetra

The climate in Bamako (Mali) is tropical savanna and in Conakry (Guinea) it is monsoon.

From Figure 4 we can conclude and suggest:

For Conakry: Cultivation is possible from June to February (9 months), in a greenhouse, equipped with efficient ventilation system and shading. For the rest of the year i.e. from mid-February to mid-May, the mean maximum temperatures are slightly over 33°C. Such mean maximum temperatures, for a short period, do not justify the use of an evaporative cooling system, taking into consideration its cost and low efficiency due to the high outside relative humidity (HR>60%). So, it may eventually be possible to produce vegetables in Conakry all year round under greenhouses the higher ,the better(gutter at least 3.5-4 m), with roof openings and the whole lateral side opened and an external roof shade net with a S.I. of 30-35 %. The ventilation openings must to be equipped with nets to protect against insects, birds, and rodents, and should be increased by at least 10% to reach 40% of the floor area in order to avoid decreasing the ventilation efficiency too much.

For Bamako, the case is a more difficult:

- From October to June (9 months), it is necessary to cool the greenhouse by using for example the fan and pad system since outside temperatures are too high The corresponding outside humidity during this period is low, which favours an efficient evaporative cooling system.
- The rest of the year i.e. from July to September (3 months), it is possible to produce vegetables under greenhouses the higher, the better (gutter at least 3.5-4 m), with roof openings and the whole lateral side opened and shade net with a SI of 30%. The ventilation openings must to be equipped with nets to protect against insects, birds, and rodents, and should be increased by at least 10% to reach 40% of the floor area in order to avoid decreasing the ventilation efficiency too much.

Summing up for greenhouse types

From the analysis, using the climagraphs of the above mentioned cities for characterising the suitable greenhouse types, it can be concluded that for RADHORT countries:

- In warm desert and warm semi arid areas (BWh and BSh) a greenhouse should be the highest possible (resistant enough to strong winds), equipped with lateral and roof vents, with openings corresponding to 30-35% total floor area, permanently opened throughout all the year and always equipped with shade nets SI 30%. Additionally, in continental BWh areas an evaporative cooling system is necessary for 3-4 months during the year.
- In tropical savanna (Aw), greenhouses with combined rooftop ventilation and shading system could be sufficient for 7 to 9 months. An evaporative cooling system (fan and pad or high-pressure fog) is necessary for the rest of the year (3 to 5 months) in such areas. For monsoon (Am) climate areas it could be possible to produce vegetables all year round in greenhouses: the higher possible, with combined roof and lateral ventilation openings of a total ventilation area equivalent to 40% of the floor area permanently opened and covered with insect proof nets and the roof shaded with nets of SI of 30%.
- In the Sahelian environment of the RADHORT countries, an adapted greenhouse should be:
  - High (2.5-3 m minimum at gutter height) and must have:
  - Lateral and roof openings of 30-35% of the total floor area needed for good ventilation, covered with 50 mesh insect proof nets and remain permanently open.
  - Shading nets on roof with SI≈30%
  - Plastic or straw mulching.
- For all options, plastic or straw mulching would provide additional advantages for saving irrigation water and reducing the relative humidity inside the

greenhouse and helping to control fungal diseases and weed growth.

These types of greenhouses and equipment recommended for the RADHORT climate environment are different from the greenhouses successfully used in Ierapetra. This illustrates the fact that greenhouses and their management have to be "tailored" to the local conditions and needs.

NETHOUSES IN TROPICS

Nethouse cultivation may constitute an alternative, to open field production in warm climates. It could be a less expensive option than greenhouse cultivation. Nethouses are usually covered with shade nets and SI of 20-30% or with insect-proof screens[6] of 50 mesh, i.e. 50 open spaces per inch in each direction, delineated by the threads.

Insect-proof nets are recommended, in order to avoid insect damage and thereby limit the use of plant protection products. For many advantages, nethouses are used to (Kitta, 2014):

- reduce high radiation levels and wind speed;
- modify positively the crop physiological response due to relatively good ventilation and adapted shading avoiding too high temperatures . The inside air temperature should not be very different from the temperature outside;
- lead to enrichment in diffuse radiation inside the growing environment, resulting in better uniformity and higher level of radiation captured by the plants;
- keep the leaf temperature lower as compared to the open field thereby avoiding photo-synthesis inhibition;
- protect against sunburns, that affect the quality of the produce;
- protect the crop from hail, sand storms, and physical damage caused by heavy rain;
- minimize the invasion of insects, thus, allowing a significant reduction in plant protection products application;
- avoid the entrance of different types of predators, including birds and rodents.

All the above advantages lead to increased overall yield levels of better quality, reduced water consumption and increased water use efficiency (WUE) and water productivity (kg/m^3). Related experiments in warm Mediterranean climates show that the production in nethouses is almost doubled (for tomatoes from five to ten kg per m^2), and water consumption is reduced by 40% (Kitta et al., 2014b). Similar results were mentioned by Saidi et al. (2013) for tomato growing under nets in East Africa climate (Njoro-Kenya, temperate Mediterranean climate classified as Csb by the Köppen-Geiger system). Furthermore, Simon et al. (2014) found similar results for cabbage under nets in Mediterranean climate (Montpellier, Csa climate type), instead for subequatorial climate (Cotonou Benin, tropical savanna climate, classified as Aw by the Köppen-Geiger system), they propose periodical removal of nets (during the rainy season), to increase productivity.

In terms of productivity, the best shading or insect proof net is white with shading intensity between 20 and 30% (Kitta et al., 2014). However, it is important to note that nethouses are shelter options that are efficient for production essentially outside the rainy periods.

In conclusion, compared to a greenhouse, a nethouse is a relatively simple and cheap construction. Associated to adequate horticultural techniques and practices (quality seed and planting material, irrigation, fertilization and integrated phytosanitary protection), it is a production technology that leads to a significant increase of crop yield and quality, and the efficient use of water and other inputs, when operated, in the tropics, outside the raining period.

Attention must be paid to the fact that nethouses protect, to a certain extent, against restrictions and constraints of open field production. It should be emphasized that the only device used for climate modification is the covering net. Nethouses are basically different from greenhouses, which are more capital expensive but more efficient and more flexible when equipped appropriately with climatic control devices according to the investment potential in each case. According to von Zabeltitz (2011), the plants under nethouses are permanently wetted when raining, which favors diseases occurrence. Therefore, nethouses may be limited to regions with very low rainfall during the cropping season.

Appropriate Nethouses for Sub-Saharan (RADHORT) countries

The suitability of nethouse cultivation in RADHORT countries, is based on the following analysis.

a. For Nouakchott, Mauritania (18°09'N, 15°58'W, warm desert climate BWh), taking into account that there is almost no rainy period in the desert climate of Nouakchott and simultaneously the outside maximum temperatures, are not excessive from

[6] Insect proof screens of 50 mesh have a SI of about 20%

mid-November till July (Fig. 2), growing vegetables under a nethouse covered with insect proof nets or shading nets is proposed, as a valuable alternative solution to open field production. For the rest of the year, between July and mid- November it would be possible to produce vegetables under nethouses by growing heat resistant species, like sweet potato. Therefore, it is possible to grow vegetables under a nethouse year round with satisfactory yield levels, provided water for irrigation is secured. In fact, for desert areas of RADHORT countries, the limiting factor for vegetable cultivation is not only the climate but also the water availability. If we consider that the incoming solar radiation is more or less stable for Nouakchott and in the order of 20 MJ/m^2/day, the water needs (E) for a vegetable production under a nethouse with a transmissivity factor of 70% (so, shading intensity of 30%) is of about:
E=0.67*0.7*20/2.5=3.8 mm/ day= 3.8 l/m^2/day.[7]
So, for a growing vegetable season of 150 days, 571.5 mm of water are needed. For two production cycles, the total amount of water needed is 1143 mm, equivalent to 1,143 l/m^2 (1,143 m^3/m^2) for a production cycle of 300 days.
From available climate data, the total precipitation quantity for Nouakchott is only 94 mm and therefore, even if all the rainwater is collected, this quantity covers only about 13% of the water needs for irrigation. So, the irrigation should be based on well or river water, mainly from the Senegal River.

b. For Dakar, Senegal (14°40'N 17°25'W, warm semi-arid climate, BSh) and Praia, Cabo Verde (14°5'N 23°31'W, warm desert climate, BWh), we can conclude from climate data of Table 1, that, due to the raining interval, the convenient period for vegetables under nethouses is from November to June-July, practically for a period of 8 months, since the rainy season usually extends from July to October (4 months). However, a possible solution to extend the growing period during the rainy season, could be to cover only the roof of the nethouse with a removable 50 micron-thick transparent polyethylene film[8]. This may result, however, in reducing light transmittance by two cladding materials. (von Zabeltitz, 2011). The temperatures in non-raining period are convenient for vegetable production under nethouses provided that water for irrigation is available. Giving that the radiation regime in the BWh and BSh climate zones is about 20 MJ/m^2/day, a total quantity of water for a vegetable production in nethouses for a period of 8 months, is around 900 mm (= 240*0.67*0.7*20/2.5) or 0,900 m^3/m^2. For Dakar, almost half of this quantity could be captured from harvesting the rainwater, which is about 400-500 mm/year, mainly from the roofs of adjacent buildings and eventually stored in farm ponds lined with plastic taking into account that farm ponds have some important limitations , like cost and space. The remaining half could be pumped either from rivers or from aquifers. In Praia, because of the prevalence of salty underground water, the situation is more difficult since the only source of water could be from collecting rainwater[9], which, nevertheless, is less than 200 mm/ year. For covering the water needs of a 9-month vegetable production cycle, about 1,0 m^3/m^2 of nethouse is needed. (=270*0.67*0.7*20/2.5).

c. For Conakry, Guinea (9°31'N; 13°42'W, monsoon climate Am) and Bamako, Mali (12°39'N; 8°0'W, tropical savanna climate, Aw) the raining period is extended from May to October. Therefore, only a limited period of 6 months (from November to April) is suitable for vegetable production under a nethouse. In Am and Aw climates, there is no problem of water availability due to abundant rainwater quantity provided it is properly harvested. However, in these climate zones, abundant and heavy rainfall can also be a limiting factor, besides the high temperatures regime occurring during the non-raining period. Therefore, possible period for nethouse vegetable production is short, only 6 months (between November and April) with an increased shading factor in the order of 40%, but with eventual risk of lower productivity. For the other six months, a nethouse is not well adapted. Vegetable production in the rainy season can be improved by growing in a greenhouse as rain-shelter with roof ventilation and open sidewalls. An alternative option, less expensive, would be to cover only the roof of the nethouse with a removable transparent IR reflectant polyethylene sheet of 50 micron.

[7] According to de Villele (1974) the following simplified relation can be used for the estimation of water needs (E) of crops under cover in Mediterranean areas: E = K 0.67 t RSo /λ (mm/day), where: K = crop coefficient, t = transmissivity of the cover to solar radiation, RSo = outside solar radiation (MJ m^{-2} day^{-1}), λ = latent heat of vaporization of water (=2,5 MJ/mm/m^2)

[8] The polyethelene file should possibly be an NIR reflective in order to reduce the transmission of SR and thereby avoiding the overheating of the greenhouse

[9] On the Island of Santiago and other Islands of Cabo Verde rainwater is stored in retention ponds and small lakes behind dams in the mountainous areas.

Summing up for nethouse cultivation in RADHORT countries

In all 5 cities people grow vegetables during the rainy season in the open field particularly leafy vegetables like amaranth, nightshade and also fruit vegetables like okra and root vegetables like sweet potato.

Practically speaking, a nethouse is useful all year round. Additional protection against the rain could be obtained by covering only the roof of the nethouse with a PE film of 50 micron. This can suffice for a few months in climates of Dakar and Praia (BSh) and maybe not needed in Nouackchott (BWh). Instead in Bamako (Aw) and Conakry (Am), a nethouse with a permanent covered roof, will be more adequate to contain the impact of the extended rainy season on the crops.

In conclusion, growing vegetables under a nethouse is possible in all climates and seasons of the RADHORT countries. It is a technological progress as compared to growing in open field without any means of protection. It offers the different advantages as cited by Kitta, 2014. To protect the crop against the rain, it is possible but not compulsory, to cover the roof of the nethouse with a PE film of 50 micron during the rainy season.

ECONOMIC ASSESMENT FOR SHELTERED CULTIVATION IN RADHORT COUNTRIES

From an economic point of view, the cost of inputs will largely vary according to the countries and cities within the countries and the volatility of market prices for imported items. Prices for structure components can be lower when sourced from local markets. Indicatevely, for Spain (Almeria) and Greece (Ierapetra), the investment for a simple greenhouse equipped with only static ventilation, drip irrigation system and shading nets (no cooling) ranges from 15 to 17 €/m^2 and the corresponding net profit for tomato production is of 5 to 6 €/m^2/year. The corresponding investment for a nethouse varies between 7 to 8 €/m^2, incluging the structure, covering net and drip irrigation pipes, with a net income for pepper production of the order of 2 to 3 €/m^2/year. Considering that cost of a technology package of sheltered cultivation will vary according to countries and areas, the return on investment will also be case specific.

The promotion of sheltered horticulture in RADHORT countries would require business case studies, which would be used to document and justify the access to credit and eventual subsidies to facilitate the adoption of innovative production technologies in support of sustainable horticulture intensification.

Factors to consider in order to asses the return on investment are, *inter alia*:

- higher yield levels per unit of area, as a result of year-round cultivation;
- higher income per unit of area, as a result of precision production planning in accordance to market demand and better prices;
- better quality and higher proportion of marketable yield;
- higher income as a result of premium prices obtained in niche markets for quality and labeled produce, which offers traceability;
- higher water productivity (less expenses for water and energy per kg of produce);
- higher labor efficiency (all days can be working days);
- less expenses for chemical pest and disease control;
- less dammage by birds, rodents and other predators;
- less expensive and easier weed control;
- less fertiliser requirements, as a result of reduced drainage of soluble minerals;
- less physical damage to crops due to heavy rain and wind;
- use of high quality seeds and/or seedlings of adapted cultivars;

CONCLUDING REMARKS

Vegetable production in RADHORT countries can be intensified and the quality improved by adopting adequate shelter structures and covering materials. The demand for vegetables is rapidly increasing in light of the population growth and the urbanization process. With improved health consciousness, the demand for quality vegetables is expected to further rise over time with higher pro-capita consumption, which today is far below the 400 grams of daily intake, as recommended by WHO-FAO. However, sheltered horticulture in the RADHORT area is still very limited and in most cases non-existent with only some exceptions.

Based on cost-benefit analysis, sheltered horticulture should be further investigated as an option to reduce the use of plant protection products, while increasing productivity and quality per unit of land and water. At the same time, it will foster entrepreneurship and create additional job and income opportunities for prospective farmers, women and youth.

Moreover, there are obvious environmental challenges for enhancing the development of sheltered horticulture. The most important are: the non- chemical protection of vegetables against insects, diseases and weeds

with physical means such as insect proof nets, appropriate cover and mulching; the reduced water consumption for irrigation. By increasing the productivity by unit of land area, the encroachment on nature is contained. On the other hand, a negative environmental impact of sheltered horticulture is mainly related to the use and disposal of plastic waste. However recycling processes help to wave this inconvenience.

Ultimately and importantly, increasing the production of high quality fruit and vegetables all year round in sheltered cultivation, will contribute to attaining the Sustainable Development Goals (SDGs) of the United Nations (2015), essentially SDG 2 for improved food and nutrition security and SDG 1, reducing poverty, while protecting the environment and human health. As such, sheltered cultivation complies with the agroecology principles. Low- tech, cost-effective, properly designed greenhouses and nethouses constructed using locally available materials, whenever available, is a promising choice for the smallholders especially in urban and peri-urban areas of RADHORT's cities, to meet the increasing market demand for fresh vegetables. However, in order to be applied rationally, its development should be paired with capacity building and applied research, backed up by policy support and mobilization of needed resources including incentives and easy access to credit.

Sheltered horticulture is proposed as a regional thematic subject area for research, capacity building and development, to be implemented on the basis of the RADHORT regional cooperation agreement and commitment.

REFERENCES

Baudoin, W.O., von Zabeltitz, C.H.R. 2002. Greenhouse constructions for small-scale farmers in tropical regions. Acta Hortic. 578: 171-179.

de Villele, O. 1974. Besoins en eau des cultures sous serre- Essai de conduite des arrosages en fonction de l' ensoleillement. Acta Hortic. 35, 123-135. DOI:0.17660/ActaHortic.1974.35.16

Duhan, P.K. 2016. Cost benefit analysis of tomato production in protected and open farm. International Journal of Advanced Research in Management and Social sciences. 12(5): 140-148.

FAO, 2016. Réseau Africain pour le Dévelopement de l'Horticulture (RADHORT). http://www.fao.org/3/a-i5719f.pdf.

Climate map. http://www.synergy-energy.co/africa-climate-map.html

FAO, 1999. C. von Zabeltitz, W.O. Baudoin. Greenhouses and shelter structures for tropical regions. https://scholar.google.it/scholar?q=fao+agp+paper+154.

Franco, A., Valera, D.L., Peña, A., 2014. Energy Efficiency in Greenhouse Evaporative Cooling Techniques: Cooling Boxes versus Cellulose Pads. Energies, 7: 1427-1447.

Katsoulas, N., Rigakis, N., Kitta, E., Baille, A. 2012. Transpiration of a sweet pepper crop under screenhouse conditions. Acta Hortic. 957: 91-97.

Kitta, E. 2014. Ecophysiological and Agronomic Response of Horticultural Crops Grown under Screens in a Mediterranean Climate. PhD Diss., Polytechnical University of Cartagena, Spain.

Kitta, E., Baille, A., Katsoulas, N., Rigakis, N., González-Real, M.M. 2014a. Effects of cover optical properties on screenhouse radiative environment and sweet pepper productivity. Biosystems Engineering, 122: 115-126.

Kitta, E., Baille, A., Katsoulas, N., Rigakis, N. 2014b. Predicting reference evapotranspiration for screenhouse-grown crops. Agricultural Water Management, 143: 122-130.

Kittas C. 1995. A simple climograph for characterizing regional suitability for greenhouse cropping in Greece. Agricultural and Forest Meteorology, 78: 133-141.

Köppen, W.P. 1936. Das geographische System der Klimate. Handbuch der Klimatologie, W.P. Köppen and R. Geiger, Eds., Vol. 1, Part C, Gebrüder Borntraeger, C1-C44.

Kumar, K.S., Tiwari, K.N., Madan K. Jha, 2009. Design and technology for greenhouse cooling in tropical and subtropical regions: A review. Energy and Buildings 41: 1269-1275

Nederhoff, E. and Stanghellini, C., 2010. Water Use Efficiency of Tomatoes. Practical Hydroponics and Greenhouses, (115): 52-59. https://search.informit.org/doi/10.3316/informit.484066941930798

Saghir, J., Santoro, J. 2018. Urbanization in Sub-Saharan Africa. Meeting Challenges by Bridging Stakeholders. Report of Project on prosperity and development. Center for Strategies & International Studies. 7 pp.

Saidi, M., Gogo, E.O., Itulya, F.M., Martin, T., Ngouajio, M. 2013. Microclimate modification using ecofriendly nets and floating row covers improves tomato (Lycopersicon esculentum) yield and quality for small holder farmers in East Africa. Agric Sci 4(11): 577-584.

Simon, S., Komlan, F., Adjaïto, L., Mensah, A., Coffi, H.K., Ngouajio, M., Martin, T. 2014. Efficacy of insect nets for cabbage production and pest manage-

ment depending on the net removal frequency and microclimate. Int J Pest Manag 60(3): 208-216.
United Nations, 2015. Transforming our world: the 2030 Agenda for Sustainable Development, 41 pp.
von Zabeltitz, Ch., Baudoin, W.O. 1999. Greenhouses and Shelter Structures for Tropical Regions. Food and Agriculture Organization of the United Nations, FAO Plant Production and Protection Paper 154, Rome: FAO.
von Zabeltitz, Ch. 2011. Integrated Greenhouse Systems for Mild Climates Climate Conditions, Design, Construction, Maintenance, Climate Control. Berlin Heidelberg: Springer-Verlag.
Wachira, J.M., Mshenga, P.M., Saidi, M. 2014. Comparison of the profitability of small- scale greenhouse and open-field tomato production systems in Nakuru-North District, Kenya. Asian J Agric Sci 6(2): 54-61.
Watson, J.A., Gómez, C., Bucklin, R.A., Leary, J.D., McConnell, D.B. 2019. Fan and Pad Greenhouse Evaporative Cooling Systems. CIR1135 Technical Report, University of Florida.

Italian Journal of Agrometeorology
Rivista Italiana di Agrometeorologia

Firenze University Press
www.fupress.com/ijam

Citation: S. Sharafi (2022) Predicting Iran's future agro-climate variability and coherence using zonation-based PCA. *Italian Journal of Agrometeorology* (2): 17-30. doi: 10.36253/ijam-1557

Received: January 29, 2022

Accepted: July 16, 2022

Published: January 29, 2023

Data Availability Statement: All relevant data are within the paper and its Supporting Information files.

Competing Interests: The Author(s) declare(s) no conflict of interest.

Predicting Iran's future agro-climate variability and coherence using zonation-based PCA

Saeed Sharafi

Assistant Professor, Department of Environment Science and Engineering, Arak University, Arak, Iran
Corresponding author. E-mail: s-sharafi@araku.ac.ir

Abstract. The effects of climate changes on agroecosystems can cause relevant issues. Using principal component analysis (PCA) we determined the 67 agricultural climate indicators (ACI) at 44 of Iran's synoptic stations under current (1990-2019) and future (2025, 2050, 2075, and 2100) conditions. Based on UNESCO aridity index, the agroecological zonation (AEZ) was used to classify Iran's regions (very dry, dry, semidry and humid climates). Using the PCA method, the first 5 principal components were determined by including data sets for temperature (winter, spring, summer and autumn maximum and winter minimum temperature), precipitation (winter and summer precipitation), reference evapotranspiration (ET_{ref}), and the degree of growth days in spring and winter, which explained about 96 percent of the total variance. For each climate empirical equation for ET_{ref} was selected. In order to accurate evaluation of ET_{ref} were used The Penman-Monteith based on FAO_{56} ($PM\text{-}FAO_{56}$) for the very dry climate, the Hargreaves equation for the semidry climate, and the Penman 1 and 2 equations for the dry and humid climates, respectively. According to the results, the first component alone, with an eigenvalue of 41.15, explained more than 74 percent of the total variance. Based on the results of zoning by the PCA outcomes, the stations for 1990-2019 were classified into 7 zones. While 2025, 2050, 2075, and 2100 were classified in 6, 7, 6, and 5 zones, respectively. Under the future climatic conditions of the country, in terms of climatic indicators, the similarity between the stations will increase and the climatic diversity of the country will decline compared to current conditions. The results demonstrated that the PCA method would be valuable for monitoring AEZ in semidry climates at reasonably long periods.

Keywords: agro-climatic indicators, agro-ecological zonation, empirical equation, reference evapotranspiration.

INTRODUCTION

Climate change and variability affects agriculture more than any other human activity. Given the role of agriculture in food production, investigating the impacts of climate change on agriculture give some important elements to evaluate the world's future food security (Anwar et al., 2007; Challinor et al., 2005; Choudhary et al., 2012; Torriani et al., 2007). In other words, these changes have a direct effect on agriculture and food security

(Brown & Funk, 2008; Schmidhuber & Tubiello, 2007). Therefore, this sector is the most vulnerable, especially in semi dry climates (Sharafi & Mir Karim, 2020).

The effect of fluctuation on climatic parameters on crops, variety and phonological stage. Therefore, climate change can reduce economic incomes by reducing production in the agricultural sector and thus reduces individuals' purchasing power, especially that of poor communities (Blazquez & Domenech, 2018). Solaymani (2018) confirmed the negative impact of rainfall-temperature variability on food availability and access to food due to a reduction in the supply of agricultural products, a commodity inflation pressure and a reduction in household income in Malesia. Moreover, results suggest that the climate variability shocks lead to a reduction in the consumption and welfare of all household groups, particularly in rural areas.

On the basis of the aridity index of UNESCO, the climate of Iran is classified as dry climatic region (Sharafi & Ghaleni, 2021b), and therefore, its agriculture is highly dependent on precipitation and temperature. According to Rahim (2014) and Mohammed & Scholz (2019), the changes in precipitation patterns, directly and indirectly might reduce crop yield (Sánchez-Martín et al., 2017). Such changes exemplify just how much weather during the growing season, alongside long-term changes in climate, are having a significant impact on regional and global crop production (Newlands & Zamar, 2012). The effects of climate change on crop production are usually studied through crop physiology and ecology sciences. In a comprehensive review of the physiological mechanisms of crop response, various aspects of the impacts of climate change on these processes have been presented. More details of the responses of different species of crops as well as related physiological mechanisms can be reviewed from various resources (Nassiri et al., 2006; Kamali 2007). Although these studies are important in revealing crop growth responses to climate change, they do not provide data about the regional effects of climate change on crop production (e.g. rainfed wheat). Therefore, another part of this study investigates the effect of climate change on crop production on a regional scale to provide complete information about the production situation, and future climate limitations and barriers to crop production. The complexity of such studies has led to far fewer scientific references than in the first group of studies (Hammer et al., 2001; Nassiri et al., 2006; Gholipoor 2008; Sharafi et al., 2016).

Several researchers have evaluated the dependence of different empirical ET_{ref} equations on various meteorological parameters over different climates (Güçlü et al. 2017; Saggi and Jain 2019; Shiri et al. 2019; Ndiaye et al. 2020; Sharafi and Mohammadi Ghaleni 2021a, b). Sharafi and Mohammadi Ghaleni (2021b) evaluated different empirical equations for ET_{ref} in different climates of Iran. Their results found that the simplest regression model (MLR) based on minimum and maximum temperature data was more precise than the empirical equations. They also recommended the solar radiation–based Irmak equation as the best substitute for the PM-FAO_{56} model, especially in dry and semidry climates. Furthermore, accurate measurement of ET_{ref} is used as an indicator to understand the concepts of climate change. To better evaluate ET_{ref} in each climate, it is necessary to be aware of the climatic conditions, the quality of the weather data, and the related costs (Sharafi et al., 2016).

However, the study of the impacts of regional climate change on crop production is based on determining ACIs in the current situation, predicting future climatic conditions based on different scenarios by the current climate and climate change indicators, such as the GCM, calculation of ACIs under the conditions of climate change, comparison with the current conditions, and finally evaluation of future climatic conditions for plant growth and production (Antle, 1996; Holden & Brereton, 2004), but, the results of studies have confirmed that the PCA is suitable for analysis of agricultural climatic indicators on the regional scale and classification of stations studied in terms of similar agro-climatic characteristics (Gholipoor, 2009; Nassiri & Koocheki, 2006). PCA is a statistical method that converts a set of interdependent variables into a set of independent (non-interdependent) variables (Johnson, 1998). Many researchers have used this method to homogenize interdependent climate variables and use them in subsequent statistical analysis (Briggs & Lemin, 1992; Fovell and Fovell, 1993). PCA can also establish a functional relationship between variables and a close relationship between the Pearson correlation coefficient of determination and graphical data distribution (Chatterchi & Hadi, 2012). The aim of this study is to develop and introduce ACIs by PCA on a regional scale and station zoning under future climatic conditions in very dry, dry, semi dry and humid climates. In the development of these indicators, criteria such as the availability of the required climatic parameters at the regional level and a simple and accurate working method have been considered. The introduced indicators can be calculated and applied for future time series with observational numerical values for climatic parameters under future climatic conditions (2025, 2050, 2075 and 2100) of Iran.

MATERIAL AND METHODS

Study area

Iran located in geographical coordinates between 25° and 39° north latitudes and 44° and 63° east longitudes, with an area of about 1.65 × 106 km^2. The long-term monthly climatic data of precipitation (mm), temperature (maximum and minimum), relative humidity, wind speed, sunshine duration, and solar radiation from 1990 up to 2019 in 44 synoptic stations have been used in this study. Data have been sourced from the Iranian Meteorological Organization of Iran (IRIMO). Some records of data input were incomplete, or not available for some stations, therefore only stations with long climatic period length remained. Due to the widespread geographical distribution of selected stations, complete coverage for different Iranian climatic regions is given. The studied synoptic stations were divided into four climatic regions, namely, very dry (13 stations), dry (15 stations), semi dry (11 stations), and humid climates (5 stations) (Table 1).

ET_{ref} evaluation

The methods for calculating ET_{ref} according to the type of input data (temperature, relative humidity, wind speed, precipitation, geographical coordinates, and altitude of each station) include seven hybrid methods based on Penman (1948), two temperature-based methods, three hybrid radiation-temperature-based methods, and a radiation-based method (Zare et al., 2006; Sharafi and Ghalenee, 2021b).

According to Sharafi and Ghaleni's (2021a) results, the ET_{ref} were estimated by empirical equations of the PM-FAO_{56} for very dry climate, the Hargreaves equation for the semidry climate, and the Penman 1 and 2 equations for the dry and humid climates, respectively (Table 1). At the same time, the Penman-Monteith method is a suitable method in most parts of the country due to its comprehensiveness (Sharafi and Ghalenee, 2021b). This method has been used in studies by Sun and Song (2008), Gong et al. (2008), Celestin et al. (2020), and others. Since the condition for using this estimator is the normality of the studied variable (ET_{ref}), the Kolmogorov-Smirnov test was used. To evaluate the accuracy and measurement of the obtained results, there are similar statistics for measuring the validity of the models, among which is the coefficient of determination (R^2), the root of square errors (RMSE), and mean bias error (MBE) (Jacovides, 1998). Based on the mentioned statistics, the most appropriate method was proposed for each climate and was considered as the basic method for the studied stations (Table 1).

The slope of the line and the coefficient of determination of ET_{ref} values (mm y^{-1}) in the 5 climates are: very dry (19.91, R^2 = 0.6); dry (-18.43, r = 0.72); semi dry (17.54, R^2 = 0.83); semi humid (9.34, R^2 = 0.87); and humid (57.3, R^2 = 0.91). The stations were divided according to ET_{ref} values. In 2019, the maximum value of ET_{ref} was detected in Chabahar (14.56 mm d^{-1}) and Abadan (13.38 mm per day); and the lowest value of ET_{ref} was at the Bandar Anzali (2.08 mm d^{-1}) and Rasht stations (2.67 mm d^{-1}), respectively.

Table 1. The values of estimated error of ET_{ref} in models used for Iran's climate.

Code	Abs.	Climate	R^2	RMSE (mm day^{-1})	MBE (mm day^{-1})	Suggested model	Reference
(1)	P-M_{FAO56}	Very dry	0.92	1.33	-0.37	$ET_{ref} = \frac{0.48(R_n - G)\gamma \frac{900}{T+273} U_2 (e_{sa} - e_{a)}}{\Delta + \gamma(1 + 0.34U_2)}$	Allen et al. (2006)
			0.29	2.12	-0.86		
(2)	P-M1	Dry	0.43	0.73	-0.24	$ET_{ref} = (2.625 + 0.000479U_2)(e_{sa} - e_a)$	Penman (1948)
			0.97	1.62	-0.77		
(3)	H-G	Semidry	0.77	0.88	0.15	$ET_{ref} = 0.0162(K_r), R_a, TD^{0.5}(T + 17.8)$	Hargreaves (1975)
(4)	P-M2	Humid	0.68	0.68	0.03	$ET_{ref} = [\frac{\Delta}{\Delta + \gamma} R_n(0.27)(1 + 0.01U_2)(e_{sa} - e_a)]$	Penman (1948)
			0.9	0.387	0.08		
Average			0.74	1.12	0.195		

ET_{ref}; reference evapotranspiration (mm day^{-1}), △; the slope of saturation vapor pressure curve (mb °C^{-1}), R_n; net solar radiation (MJ m^{-2} day^{-1}); G; soil heat flux density (mm day^{-1}), γ; psychometric constant (kPa °C^{-1}), T_{mean}; mean daily temperature (°C), U_2: wind speed measured at 2 m height (m s^{-1}), R_a; extraterrestrial radiation (mm day^{-1}), λ; latent heat of vaporization (MJ kg^{-1}), e_{sa}; saturation vapor pressure (k Pa), e_a; actual vapor pressure (k Pa) and (e_s-e_a); saturation vapor pressure deficit (k Pa).

M-K test

Table 1 shows the seasonal climatic trends and significance at the level of 1 and 5%. According to the M-K test results, many stations show an increase in mean temperature the autumn, winter, spring and summer seasons. The slope of the warming trend was much steeper in winter and summer. In dry and very dry climates, the trend of increasing mean temperature was observed during four seasons. In general, during the last 30 years, in humid, semi dry, dry and very dry climates, about 75, 86, 81 and 89 percent of precipitation, respectively, occurs in autumn and winter, respectively. Therefore, the study of this climatic parameter has a very important role in better assessment and understanding of drought indicators. Accordingly, in all studied climates, a trend of reduced precipitation was observed, especially in winter; however, in semi dry and dry climates, this declining trend was more severe. Also, a decrease in precipitation in spring season was observed for stations in humid climate. On the other hand, in most semi dry and very dry climates, the amounts of increase in precipitation were reported in autumn season, although these values were not significant. According to the results of preliminary studies, ET_{ref} values in most of the stations studied in different climates have an increasing trend, which had an increasing and significant trend in winter and summer. The difference in ET_{ref} values in humid and very dry climates is about 2452 mm per year (Table 2).

GCM scenario

Three basic scenarios evaluate climate change impact: delta perturbation, analogue, and GCM. To a certain degree, they reflect the history of climate construction since the construction method was recognized in line with the types of available data. Delta perturbation and analogue have the simplest scenarios, whereas the GCMs are the most complex. For synthetic scenarios, a random alteration in a particular weather parameter is applied to an obtained time series. Presently, GCMs are the only reliable methods accessible for simulating the physical processes that detect the global climate situation (IPCC, 2014). Researchers depend on weather data that can be derived from GCM, which needs to be converted to a local scale using statistical or dynamical downscaling methods (Mukherjee & Siddique, 2019).

The UKMO (Version 3.0) GCM was developed at the Hadley Centre for Climate Prediction and Research, which is a part of the UK Meteorological Office. The model is one of a breed of coupled Ocean–Atmosphere GCMs (OAGCM) that require no flux corrections to be made. The GCM consists of a linked atmospheric model, ocean model and sea ice model. However, for the present study we used only the atmospheric component of the model. By implementing UKMO-GCM for the years 2025, 2050, 2075, and 2100, the monthly values of minimum and maximum temperature, wind speed, and precipitation for different stations were calculated and the effects of climate change were determined based on the scenario defined in the model on these climatic parameters (Nassiri et al., 2006). Then, using the results of the implementation of GCM of all ACIs calculated in the current situation, again for the years 2025, 2050, 2075, and 2100, the values were calculated and by comparing these values and their differences with the current conditions, the effects of climate change on the indicators were determined (Antle, 1996).

ACI

In general, the weight of the parameters is estimated based on the relative importance of the parameters. Most of the qualitative indicators developed for the parameters used are considered unequal weights with a sum equal to one (Sarkar and Abbasi, 2006). According to an aggregation function used to calculate ACIs, the weight of each parameter has a large effect on the calculated final number (Sutadian et al., 2017; Sarkar and Abbasi, 2006; Uddin et al. 2021). In order to determine the weight for agricultural climate parameters, PCA method was used. In this method, by considering the mean values of specific vectors (α_i) related to the first 5 principal components, the weight vector related to qualitative parameters i to j (Ω_i) was calculated using Equation (5):

$$\Omega_i = \sum_{i=1}^{j} \lambda_i \alpha_i \Big/ P^{(j)} \tag{5}$$

Where λ_i is the variance of the principal component of i and $P^{(j)}$ is the cumulative variance (Eq. 6) to the principal component of j.

$$P^{(j)} = \sum_{i=1}^{j} \lambda_i \tag{6}$$

The final weight of the parameters was calculated according to the calculated Ω_i values for each parameter i (Casillas-García et al. 2021). The aggregation of ACI is the last stage in the development of an index. In this step, using the sub-indexed parameters and the weights related to each parameter, a number was obtained as a

Tab 2. Seasonal climatic trends at the selected weather stations over Iran.

Class	Station	Tmean				Precipitation				ET_{ref}			
		Aut.	Win.	Spr.	Sum.	Aut.	Win.	Spr.	Sum.	Aut.	Win.	Spr.	Sum.
Humid	Babolsar	0.07△	0.26▲	0.11▲	0.23▲	-0.05▽	-0.06	-0.07▽	0.02●	0.00●	0.14▲	0.04●	0.12▲
	Bandar Anzali	0.05●	0.23▲	0.07△	0.16▲	-0.05▽	-0.14▼	-0.07▽	0.05△	-0.03○	0.11▲	-0.01○	-0.01○
	Ramsar	0.07△	0.27▲	0.10△	0.29▲	0.04●	0.09△	-0.04○	0.03●	-0.01○	0.16▲	0.05●	0.15▲
	Rasht	0.07△	0.20▲	0.09△	0.19▲	-0.03○	-0.04○	-0.08▽	0.03●	-0.03○	0.11▲	0.02●	0.04●
	Gorgan	-0.05▽	0.09△	0.07△	0.12▲	-0.11△	-0.09	-0.14△	-0.06▽	0.01●	0.19▲	0.15▲	0.24▲
Semi dry	Urmia	0.02●	0.19▲	0.12▲	0.13▲	0.02●	0.02●	-0.08▽	0.04●	0.04●	0.21▲	0.14▲	0.18▲
	Nowzheh	0.07△	0.18▲	0.07△	0.13▲	0.05△	-0.18▼	-0.03○	0.06△	0.04●	0.18▲	0.05△	0.15▲
	Sanandej	0.06△	0.20▲	0.13▲	0.18▲	0.00●	-0.26▼	-0.03○	0.14▲	0.05△	0.20▲	0.12▲	0.23▲
	Saqez	0.00●	0.11▲	-0.06▽	-0.05○	0.01●	-0.15△	-0.12△	0.10△	-0.01○	0.14▲	0.03●	-0.01○
	Arak	0.03●	0.12▲	0.07△	0.02●	-0.01○	-0.22▼	0.01●	0.06△	-0.02○	0.13▲	0.02●	0.08△
	Kermanshahan	0.09△	0.17▲	0.14▲	0.24▲	0.01●	-0.11▼	-0.01○	0.07△	0.08△	0.18▲	0.14▲	0.28▲
	Khoramabad	-0.02○	0.04●	0.04●	0.13▲	0.04●	-0.12▼	0.02●	0.08△	-0.01○	0.06△	0.07△	0.18▲
	Ilam	0.03●	0.10△	0.09△	0.19▲	0.03●	-0.11▼	0.01●	0.08△	0.03●	0.12▲	0.10△	0.23▲
	ShahreKurd	-0.06▽	0.09△	-0.11▼	-0.16▼	0.04●	-0.08▼	0.03●	0.16▲	-0.06	0.11▲	-0.07▽	-0.16▼
	Qazvin	0.04●	0.18▲	0.08△	0.12▲	0.06△	-0.05○	-0.01○	0.08△	0.04●	0.20▲	0.09△	0.12▲
	Zanjan	0.04●	0.22▲	0.06△	0.09△	0.05●	-0.06	-0.02○	0.12▲	0.04●	0.23▲	0.07△	0.13▲
Dry	Khoy	0.07△	0.15▲	0.15▲	0.27▲	-0.03○	-0.15▼	-0.09▽	0.10△	0.07△	0.16▲	0.13▲	0.26▲
	Tabriz	0.04●	0.18▲	0.11▲	0.17▲	-0.06	-0.14▼	-0.10▼	0.08△	0.05△	0.19▲	0.11▲	0.18▲
	Dezful	0.00●	0.07△	0.08△	0.16▲	0.03●	-0.24▼	-0.02○	0.15▲	0.19▲	0.39▲	0.26▲	0.39▲
	Birjand	0.01●	0.10△	0.05●	0.04●	0.06△	-0.06▽	0.05△	0.10△	0.01●	0.12▲	0.05●	0.05●
	Fassa	0.04●	0.10△	0.05●	0.04●	-0.01○	-0.05○	-0.01○	0.02●	-0.20▼	-0.24▼	-0.18▼	-0.26▼
	Isfahan	0.05●	0.13▲	0.09△	0.11▲	0.00●	-0.05○	0.04●	0.02●	0.05●	0.14▲	0.09△	0.10△
	Qom	0.00●	0.09△	0.03●	0.03●	0.02●	-0.07▽	0.04●	0.06△	0.01●	0.11▲	0.04●	0.06△
	Mashhad	0.12▲	0.24▲	0.16▲	0.26▲	-0.01○	-0.05○	0.05●	0.18▲	0.09△	0.23▲	0.14▲	0.28▲
	Sabzevar	0.05●	0.18▲	0.08△	0.11▲	-0.03○	-0.13▼	0.04●	0.06△	0.05●	0.18▲	0.08△	0.13▲
	Semnan	0.01●	0.12▲	0.09△	0.09△	0.03●	-0.08▽	0.00●	0.07△	-0.02○	0.10△	0.06△	0.05●
	Shahroud	0.06△	0.17▲	0.11▲	0.12▲	-0.05▽	-0.07▽	-0.11▼	0.11▲	0.03●	0.15▲	0.09△	0.10△
	Shiraz	0.06△	0.13▲	0.10△	0.13▲	0.04●	-0.06▽	0.01●	0.13▲	0.07△	0.14▲	0.11▲	0.16▲
	Tehran	0.05△	0.20▲	0.10△	0.13▲	0.03●	-0.08▽	-0.02○	0.13▲	-0.01○	0.13▲	0.03●	0.03●
	Torbat Heydarieh	0.00●	0.09△	0.03●	0.01●	0.01●	-0.10▽	0.02●	0.10△	-0.02○	0.09△	0.02●	0.00●
	Kerman	0.12▲	0.17▲	0.09△	0.14▲	0.05●	-0.15▼	-0.01○	0.03●	0.12▲	0.19▲	0.09△	0.15▲
Very dry	Bam	0.07△	0.17▲	0.13▲	0.21▲	-0.01○	-0.07▽	-0.02○	-0.08▽	0.02●	0.15▲	0.10△	0.21▲
	Iranshahr	0.05●	0.10△	0.06△	0.07△	0.01●	-0.04○	0.01●	0.00●	0.02●	0.08△	0.03●	0.06△
	Tabass	0.11▲	0.17▲	0.17▲	0.21▲	0.02●	0.04●	0.01●	0.04●	0.11▲	0.15▲	0.17▲	0.23▲
	Yazd	0.11▲	0.20▲	0.12▲	0.16▲	0.03●	-0.13▼	0.04●	0.15▲	0.11▲	0.20▲	0.11▲	0.18▲
	Zabol	0.05●	0.11▲	0.10△	0.19▲	0.00●	-0.09▽	0.06△	-0.06▽	0.03●	0.14▲	0.09△	0.18▲
	Zahedan	0.06△	0.14▲	0.10△	0.09△	0.00●	-0.05▽	0.02●	0.14▲	0.05△	0.15▲	0.07△	0.09△
	Abadan	0.07△	0.15▲	0.15▲	0.31▲	0.01●	-0.14▼	0.03●	-0.02○	0.06△	0.14▲	0.16▲	0.34▲
	Ahwaz	0.09△	0.17▲	0.17▲	0.27▲	-0.03○	-0.12▼	-0.01○	-0.04○	-0.04○	0.05△	-0.02○	-0.15▼
	Bandar Abbas	0.03●	0.08△	0.03●	0.02●	0.10△	-0.06▽	0.05●	0.11▲	-0.28▼	-0.30▼	-0.31▼	-0.35▼
	Bandar Lengeh	0.12▲	0.20▲	0.12▲	0.26▲	0.09△	-0.10▼	0.03●	0.02●	0.05●	0.13▲	0.07△	0.22▲
	Bushehr	0.07△	0.16▲	-0.01○	0.00●	0.05●	-0.08▽	0.03●	0.30▲	0.02●	0.12▲	-0.17▼	-0.31▼
	Chabahar	0.06△	0.13▲	0.06△	0.00●	-0.02○	-0.08▽	-0.01○	-0.05○	-0.13▼	-0.09▽	-0.18▼	-0.25▼
	Jask	0.11▲	0.21▲	0.10△	0.08△	0.05●	-0.14▼	0.14▲	-0.06▽	0.17▲	0.25▲	0.14▲	0.14▲

COlOur map
Kendall's Tau (τ) -∞ -0.20 -0.05 0.00 0.05 0.20 +∞

▲, significant at 1% with increasing trend; ▼, significant at 1% with decreasing trend; △, significant at 5% with increasing trend; ▽, significant at 5% with decreasing trend; ●, not significant with increasing trend; ○, not significant with decreasing trend.

score for the quality of the parameter. The aggregation function of ACI can be additive functions, multiplicative functions or a combination of these two functions (Sutadian et al., 2016).

In order to evaluate 67 agricultural climate indicators, 36 temperature variables including; the minimum temperature in winter (12 variables), the maximum temperature in winter (12 variables), winter precipitation (6 variables), summer precipitation (6 variables), the maximum temperature in spring, summer, and autumn (12 variables), ET_{ref} (12 variables) in different seasons, degree of growth days in spring and winter (4 variables) and forest day in spring, fall and winter seasons (3 variables) (Appendix 1). The PCA technique was used to evaluate ACIs at 44 stations in Iran. SAS software (V.13.1) was used to perform PCA (Rosenzweig et al., 1995). For this purpose, 67 ASCII data files were first placed in a set. The PRIN COMP PROC command was used to provide principal components of the data. The principal components were implemented in the correlation matrix because the analyzed variables had very different numerical values and their mean and standard deviation were very different due to measurement in different units. It should be noted that the application of PCA on the coefficient of determination matrix is equivalent to the application of this technique on standardized data (Fovell & Fovell, 1993). According to the PCA results, eigenvalues and eigenvectors related to each of the principal components were calculated and evaluated (Nassiri et al., 2006). ACIs of different stations, calculated based on the results of the GCM model under climate change conditions, were also exposed to PCA after becoming 67 indicators and their principal components under climate change conditions were determined. Finally, all ACIs calculated under the current conditions and different scenarios of climate change along with their principal components were compared and the effect of climate change on these indicators was evaluated (Appendix 1).

RESULTS AND DISCUSSION

Statistical analysis of ACIs

Having implemented PCA, the first 5 principal components explained about 100 percent of the total variance. In general, statistically speaking, there is no specific method for selecting the number of components that should be retained, so selecting 5 components in this study was a judgment call. Note, however, that the simplest criterion for selecting the number of components is to retain a number that can explain 95 percent of the total variance. Accordingly, the presence of 4 principal components was sufficient to explain 95 percent of the total variance. Further analysis showed that it is not necessary to add a new component because by excluding the fifth component, the statistical accuracy of the next analysis was not much reduced. Table 2 presents the eigenvalues of the coefficient of the determination matrix and the part of the total variance explained by each of the 5 principal components. According to the results, the first component with an eigenvalue of 41.15 alone explained more than 75 percent of the total variance. These values are reduced in subsequent components, respectively, and finally the fifth component, with an eigenvalue less than one, explained a small amount of the total variance percentage. Furthermore, the first four principal components can explain 98.85 percent of the total variance; however, as mentioned earlier, the presence of the fifth component only improved the accuracy of this analysis and subsequent analysis (Table 3).

Appendix 1 presents eigenvalues for each of 67 variables in 5 principal components. As shown, the first principal component is filled with load temperature variables (variables 1 to 36 of Appendix 1). Load or loading is the power (with values from -1 to +1) of the coefficients related to each of the variables integrated into a principal component. The highest load of the second principal component is related to the winter minimum temperature, the winter precipitation, and the variables of autumn, winter and spring precipitation and ET_{ref} (variables 4, 12, and 37-60 of Appendix 1). The maximum load of the third principal component is the winter minimum, average, and maximum temperature (variables 16, 20, and 24 of Appendix 1). The fourth principal component showed its highest load for the summer minimum, average, and maximum temperature, the spring maximum temperature, and the winter minimum, average, and maximum precipitation and ET_{ref}

Table 3. Eigenvalues of the correlation matrix and amount of variance described by each of the 5 principal components.

PCA	Eigenvalue	Difference*	Ratio of total variance	Cumulative ratio of total variance**
PCA 1	0.7689	0.7358	32.0756	40.8927
PCA 2	0.9265	0.1563	6.2138	9.3025
PCA 3	0.9734	0.0542	2.0022	3.0531
PCA 4	0.9814	0.0191	0.2093	1.0526
PCA 5	0.9991	0.0148	0.1208	0.8409

* The difference between the eigenvalues of two successive components.

** The cumulative value of the ratio of variance described by successive components.

Table 4. The description of information for each of the 5 principal components.

PCA	Description information
PCA 1	The sum information of temperature (min, max, and mean)
PCA 2	The winter minimum temperature and ET_{ref}
PCA 3	The winter minimum and average ET_{ref}, the winter minimum temperature
PCA 4	The winter precipitation, the summer ET_{ref}, the spring, summer, and autumn maximum temperature
PCA 5	Growth degree days (GDD) in spring and winter, the summer precipitation

Table 5. The description of information for each of the 5 principal components of climate change (2025, 2050, 2075, and 2100).

PCA	Description information
PCA 1	The summed information of temperature (min, max, and mean, respectively)
PCA 2	The summed information of precipitation, the summer ET_{ref}
PCA 3	The autumn minimum temperature, the summer maximum temperature
PCA 4	The winter ET_{ref}, growing degree days in spring

(variables 17, 18, 22, 17, 17, 40, 44, 48, 52, 56 and 60 in Appendix 1). The fifth principal component had a positive load for variable degree of growth days in winter and spring, and the spring minimum, maximum, and average precipitation (variables 32, 38, 39, 42, 46, 50, 54, and 58 of Appendix 1). Accordingly, Table 4 summarizes the information integrated into each of the 5 principal components, which together explain 99 percent of the total variance in agricultural climate data.

In this study, using the geographic information system related to the country's stations, after implementation of the program and based on the variables integrated into the 5 principal components, the stations were placed in seven climatic areas. Fig. 2 shows the location of these areas based on the first and second principal components, which together explain about 91 percent of the total variance among the data (Table 3). Therefore, according to the set of indicators of agricultural climatology used in this study, stations with the maximum climatic similarity were placed in a group. It is not possible to group the studied stations based on 67 indicators at a stage. Therefore, as mentioned earlier, at the first stage the indicators of agricultural climatology were placed in 5 principal components, and then, by the geographic information system based on the principal components, the stations of the same climate were placed in the same area.

Statistical analysis of agricultural climatic indices under conditions of climate change

The results of statistical analysis showed that under the conditions of climate change, 4 principal components will explain more than 96 percent of the total data variance, while in the current situation, to explain the variance of agricultural climate data, 5 principal components were defined (Table 3). The properties of the 4 components related to climate change conditions are presented in Table 5. Also, the first and the second, are the same in the current situation and under climate change conditions, but the other components are different (Table 5). Various researchers have cited temperature, precipitation, and the climatic indicators of their crops (e.g. the duration of the growing season or of the dry season) as the most important variables affecting crop growth and development.

The results show that under climate change conditions, the set of information about temperature, precipitation, and the indicators obtained from them will be the principal climatic components in Iran; however, the contribution of these components to explaining the properties of the studied stations compared with different current conditions is somehow different. These results are consistent with the study results of Solaymani et al. (2018), who examined the effects of climate change on Malaysian food security. Table 6 presents the eigenvalues and the amount of variance explained by each of the principal components under climate change conditions. Comparing these results with the values presented in Table 6 shows that under climate change conditions, the contribution of the first principal component (temperature information) to the explanation of total has declined and in contrast, the role of the second principal component (precipitation information) in overall variance has increased; in addition, the second principal component for 2050 has been much more effective than 2025 and 2100. In other words, the second principal component will have a decreasing trend of precipitation and an increasing trend of temperature. Therefore, it seems that under future climate change conditions of the country, the amount of precipitation and agricultural climate indicators related to it will be more important compared to the current situation, and in contrast to the role of temperature and its indicators, will be somewhat reduced compared to specific conditions. Accordingly, it can be concluded that although the increase in temperature in many parts of the country will prolong the growing season, at the same time an increase in the

Table 6. The eigenvalues and described variance for each of the 5 principal components in the situation of climate change (2025, 2050, 2075, and 2100) based on the results of the general circulation model (GCM).

PCA	Eigenvalues				Ratio of total variance				Cumulative ratio of total variance*			
	2025	2050	2075	2100	2025	2050	2075	2100	2025	2050	2075	2100
PCA 1	0.49207	0.50396	0.54910	0.60579	0.49207	0.50396	0.54910	0.60579	25.8314	27.1001	31.020	37.1914
PCA 2	0.94048	0.87647	0.89778	0.89174	0.44841	0.37251	0.34868	0.28595	24.1833	22.1990	20.1212	17.3120
PCA 3	0.96177	0.90782	0.94274	0.94443	0.02129	0.03135	0.04496	0.05269	2.8616	2.0312	2.4511	3.0824
PCA 4	0.97871	0.92186	0.95802	0.95998	0.01694	0.01404	0.01528	0.01555	1.0281	0.8817	0.9142	0.9101

* The cumulative value of the ratio of variance described by successive components.

duration of the dry season will create limitations for new agricultural climate indicators that are not very obvious in the current situation. Confirmation of this conclusion requires further studies on the growth and development responses of crops under the expected future climatic conditions of Iran.

Fig. 1 shows the zoning of stations by PCA in terms of agricultural climate indicators (1990-2019). Based on this, the studied stations are located in 6 classes but the second class was not located in any of the climatic zones. The northern regions of the country were located in class 7 and the southern, southwestern, and southeastern regions were located in class 1. There is climatic diversity in the western and northwestern regions of the country. By crossing the northwest and west of the country to the central, southern, northern, and eastern regions, climate diversity is reduced and the country is divided into two parts including humid (class 7) and very dry (south, center, and east) climates. The southern coastal region, due to rising temperatures and lack of suitable vegetation, and despite its high relative humidity, was located in class 1 (Table 7).

Agricultural climate data for the studied stations were reclassified after determining the PCA under climate change conditions. The position of the stations under climate change conditions is shown in Fig. 2 for the years 2025 (6 zones), 2050 (7 zones), 2075 (6 zones), and 2100 (5 zones) (Table 8). According to these results, under future climatic conditions of the country, the similarity between the climates will increase in terms of ACIs, and in fact, the climatic diversity of the country's agriculture will decline compared to current conditions. Also, with the intensification of future climate change, as shown in Fig. 2, the density of stations within each area increase, confirming the uniformity of conditions in that climate.

Although the effect of climate change on Iran's climate is not certain, the study results of various researchers confirm this (Nassiri et al., 2006). On the one hand, the effect of climate change on agricultural climatic

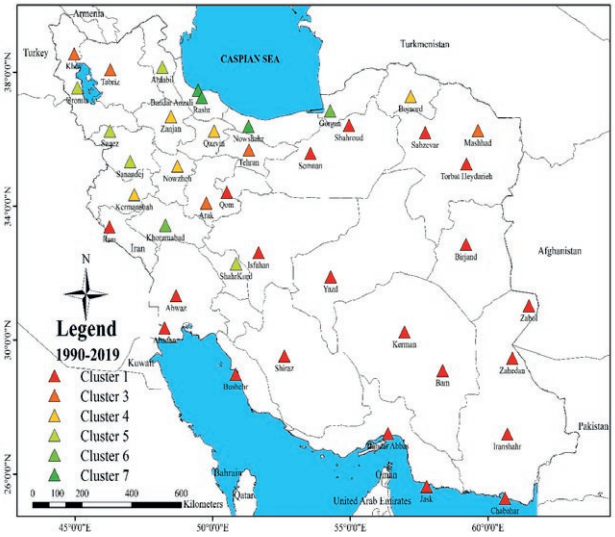

Fig. 1. Map showing the zoning of stations based on PCA (1990-2019).

indicators and finally the displacement of agricultural climatic areas has been reported by some researchers (Antle, 1996; Rosenzweig et al., 1995). For example, Holden and Brereton (2004) and Araya et al. (2010) showed that future climate change would affect agricul-

Table 7. The classification of stations based on PCA (1990-2019).

Class	Stations
1	Abadan, Ahwaz, Bam, Birjand, Bandar Abbas, Bushehr, Chabahar, Ilam, Jask, Qom, Kerman, Sabzevar, Semnan, Shahroud, Shiraz, Tehran, Torbat Heydarieh, Yazd, Zabol, Zahedan, Iranshahr, Isfahan
3	Arak, Khoy, Mashhad, Tabriz
4	Bojnord, Nozheh, Kermanshah, Qazvin, Zanjan
5	Ardabil, Urmia, Saqez, Sanandej, ShahreKurd
6	Gorgan, Khoramabad
7	Bandar Anzali, Rasht, Nowshahr

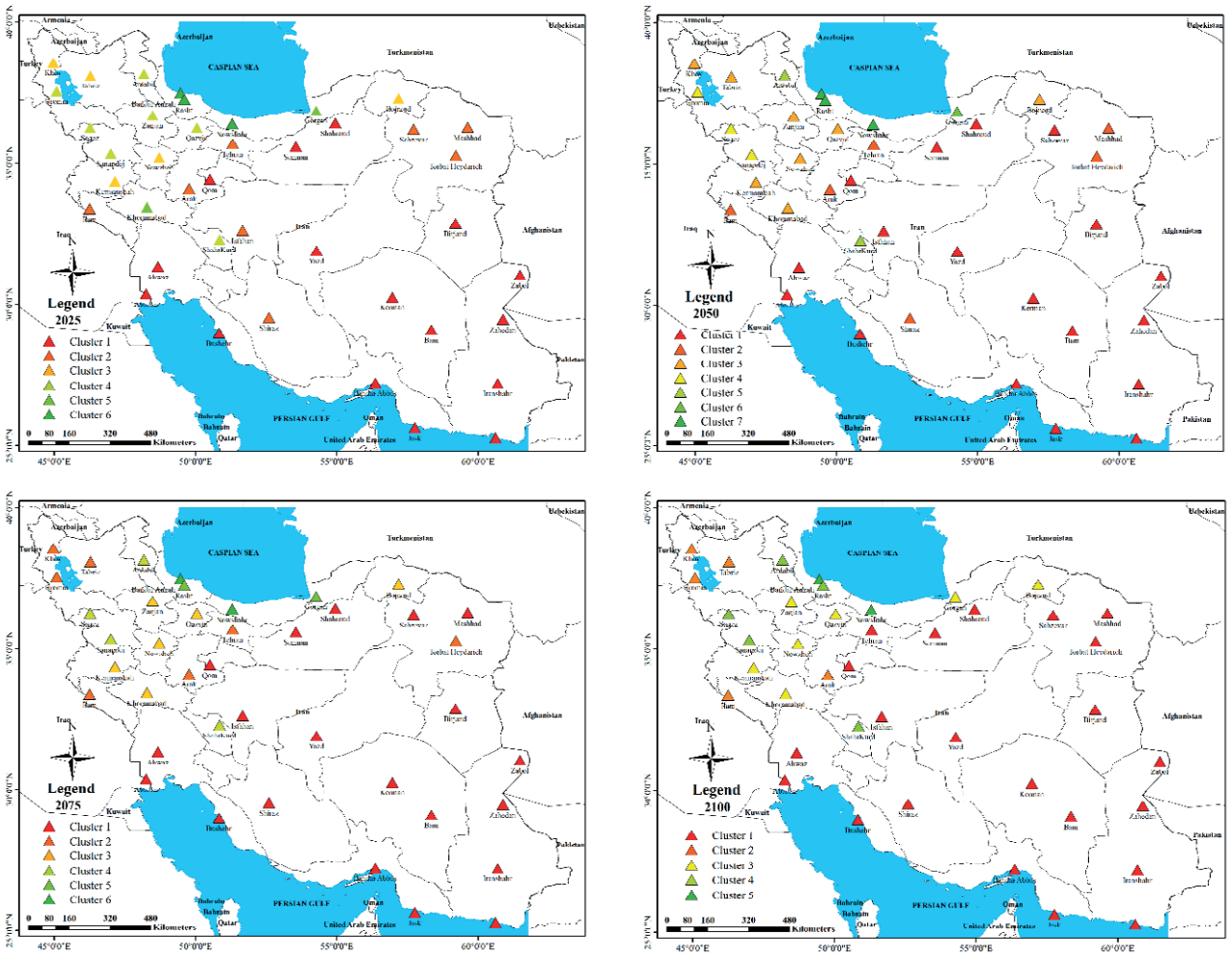

Fig. 2. The predicated maps of climate classification based on PCA for 2025, 2050, 2075, and 2100 in Iran.

tural climate climates, reducing potential crop production in Ireland and Ethiopia, respectively. Solaymani (2018) also showed that climate variables reduce the food security and well-being of poor families, especially in rural areas of Malaysia. Accordingly, and considering the results obtained in the case of Iran, it seems that the effects of climate change on a regional scale along with studies on the physiological consequences of this phenomenon are important and should be considered.

Vaghefi et al. (2019) used five climate models to project temperature and precipitation distribution across Iran. They confirmed that compared to the period of 1980–2004, in the period of 2025–2049, Iran is likely to experience more extended periods of extreme temperatures in the dry and very dry climates (for ≥120 days: precipitation <2 mm, Tmax ≥30°C) as well as humid climates (for ≤3 days: total precipitation ≥110 mm) conditions. Also, Panahi et al. (2020) evaluated data time series of temperature, precipitation, runoff, ET_{ref}, and water storage change, to determine their situation and variations in Iran (1986–2016). They found that the country warmed, precipitation typically decreased, while ET_{ref} increased in dry and very dry climates. Overall, the extra water provided from primarily groundwater depletion has fed and kept ET_{ref} at levels beyond those sustained by the annually renewable water input from precipitation. Therefore, this shows unsustainable water consumption for maintaining and expanding human activities, such as irrigated agriculture.

CONCLUSIONS

The study results show that the PCA method under climate change conditions explained more than 96 percent of the observed changes among the climatic data

Table 8. The predicated stations classification based on PCA for 2025, 2050, 2075 and 2100 in Iran.

Year	Class	Stations
2025	1	Abadan, Ahwaz, Bam, Birjand, Bandar Abbas, Bushehr, Chabahar, Jask, Qom, Kerman, Semnan, Shahroud, Yazd, Zabol, Zahedan, Iranshahr
	2	Arak, Mashhad, Sabzevar, Shiraz, Tehran, Torbat Heydarieh, Ilam, Isfahan
	3	Bojnord, Khoy, Nozheh, Kermanshah, Tabriz
	4	Ardabil, Qazvin, Urmia, Saqez, Sanandej, ShahreKurd, Zanjan
	5	Gorgan, Khoramabad
	6	Bandar Anzali, Rasht, Nowshahr
2050	1	Abadan, Ahwaz, Bam, Birjand, Bandar Abbas, Bushehr, Chabahar, Jask, Qom, Kerman, Sabzevar, Semnan, Shahroud, Yazd, Zabol, Zahedan, Iranshahr, Isfahan
	2	Arak, Mashhad, Shiraz, Tehran, Torbat Heydarieh, Ilam
	3	Bojnord, Qazvin, Nozheh, Khoramabad, Kermanshah, Khoy
	4	Urmia, Saqez, Sanandej
	5	Ardabil, ShahreKurd
	6	Gorgan
	7	Bandar Anzali, Rasht, Nowshahr
2075	1	Abadan, Ahwaz, Bam, Birjand, Bandar Abbas, Bushehr, Chabahar, Jask, Qom, Kerman, Sabzevar, Semnan, Shahroud, Yazd, Zabol, Zahedan, Iranshahr, Isfahan, Mashhad, Shiraz
	2	Arak, Khoy, Urmia, Tabriz, Tehran, Torbat Heydarieh, Ilam
	3	Bojnord, Qazvin, Nozheh, Khoramabad, Kermanshah, Zanjan
	4	Ardabil, ShahreKurd, Saqez, Sanandej
	5	Gorgan, Rasht
	6	Bandar Anzali, Nowshahr
2100	1	Abadan, Ahwaz, Bam, Birjand, Bandar Abbas, Bushehr, Chabahar, Jask, Qom, Kerman, Sabzevar, Semnan, Shahroud, Yazd, Zabol, Zahedan, Iranshahr, Isfahan, Mashhad, Shiraz, Tehran, Torbat Heydarieh
	2	Arak, Khoy, Urmia, Tabriz, Ilam
	3	Bojnord, Qazvin, Nozheh, Khoramabad, Kermanshah, Zanjan, Gorgan
	4	Ardabil, ShahreKurd, Saqez, Sanandej, Rasht
	5	Bandar Anzali, Nowshahr

of the 44 weather nation-wide stations studied. Note that the first two principal components, i.e. temperature and precipitation information and their associated climatic indicators (especially ET_{ref}, which is a combination of all climatic parameters) explained more than 90 percent of the change in the current situation and climate change. However, if future changes occur, the contribution of precipitation to the current situation will increase and the role of the temperature will reduce relatively. According to the results, it seems that under these conditions, Iran's climatic diversity has already been reduced to some extent and the climatic similarity between the areas is increasing. Therefore, given the climatic stability of the country's very dry climates till 2050 and the addition of stations located in dry climate to a very dry climate by 2100, the central, western, and northwestern, eastern, and southeastern regions are expected to be under very dry conditions.

It is necessary to mention that each developed index has advantages and disadvantages and can be used in a limited situation and for specific purposes. High uncertainty, specific and limited application, and overestimation or underestimation are among the most important disadvantages of most agro-climatological indicators. Therefore, confirmation of these results requires more extensive studies (review of more diverse models), especially the growth response of plants in the future climatic conditions of Iran. Given that only one general circulation model was used in the present study, it is suggested that more models be used in future research.

REFERENCES

Allen R.G., Pruitt W.O., Wright J.L., Howell T.A., Ventura F., Snyder R., … & Elliott R., 2006. A recommendation on standardized surface resistance for hourly calculation of reference ETo by the FAO56 Penman-Monteith method, *Agricultural Water Management*, 81(1-2), 1-22.

Antle J.M., 1996. Methodological issues in assessing potential impacts of climate change on agriculture, *Agricultural and Forest Meteorology*, 80(1), 67-85.

Anwar M.R., O'Leary G., McNeil D., Hossain H., Nelson R., 2007. Climate change impact on rainfed wheat in south-eastern Australia, *Field crops research*, 104(1-3), 139-147.

Araya A., Keesstra S.D., Stroosnijder L., 2010. A new agro-climatic classification for crop suitability zoning in northern semi-arid Ethiopia, *Agricultural and forest meteorology*, 150(7-8), 1057-1064.

Blazquez D., Domenech J., 2018. Big Data sources and methods for social and economic analyses, *Technological Forecasting and Social Change*, 130, 99-113.

Briggs R.D., Lemin J.R.C., 1992. Delineation of climatic regions in Maine, *Canadian Journal of Forest Research*, 22(6), 801-811.

Brown M.E., Funk C.C., 2008. Food security under climate change.

Casillas-García L.F., de Anda, J., Yebra-Montes, C., Shear, H., Díaz-Vázquez, D., Gradilla-Hernández, M.S., 2021. Development of a specific water quality index for the protection of aquatic life of a highly polluted urban river, *Ecological Indicators*, 129, 107899.

Celestin S., Qi F., Li R., Yu T., Cheng W., 2020. Evaluation of 32 simple equations against the Penman–Monteith method to estimate the reference evapotranspiration in the Hexi corridor, *Northwest China. Water*, 12(10), 2772.

Challinor A.J., Wheeler T.R., Craufurd P.Q., Slingo J.M., 2005. Simulation of the impact of high temperature stress on annual crop yields, *Agricultural and Forest Meteorology*, 135(1-4), 180-189.

Choudhary JS., Shukla G., Prabhakar C., Maurya S., Das B., Kumar S., 2012. Assessment of local perceptions on climate change and coping strategies in Chotanagpur Plateau of Eastern, *India Journal of Progressive Agriculture*, 3, 8-15.

Doorenbos J., Pruitt W.O., 1977. Guidelines for predicting crop water requirements, Irrigation and drainage paper No 24, 2nd edn, Food and Agriculture Organization, Rome, p 156Fovell RG, Fovell M-YC (1993) Climate zones of the conterminous United States defined using cluster analysis. *Journal of Climate* 6: 2103-2135

Hargreaves G.H., 1975. Moisture availability and crop production, *Transactions of the ASAE*, 18(5), 980-984.

Gholipoor M., 2009. Evaluating the effect of crop residue on water relations of rainfed chickpea Maragheh, Iran, using simulation.

Gholipoor M., 2008. Quantifying the threshold frost hardiness for over-wintering survival of wheat in Iran, using simulation. *International J. Plant Production*, 2(2), 125-136.

Gong L., Xu C.Y., Chen D., Halldin S., Chen Y.D., 2006. Sensitivity of the Penman–Monteith reference evapotranspiration to key climatic variables in the Changjiang (Yangtze River) basin, *Journal of hydrology*, 329(3-4), 620-629.

Güçlü Y.S., Subyani A.M., Şen Z., 2017. Regional fuzzy chain model for evapotranspiration estimation, *Journal of hydrology*, 544, 233-241.

Hammer G.L., Hansen J.W., Phillips J.G., Mjelde J.W., Hill H., Love A., Potgieter, A., 2001. Advances in application of climate prediction in agriculture, *Agricultural systems*, 70(2-3), 515-553.

Holden N.M., Brereton A.J., 2004. Definition of agroclimatic regions in Ireland using hydro-thermal and crop yield data, *Agricultural and Forest Meteorology*, 122(3-4), 175-191.

IPCC., 2014. Intergovernmental Panel on Climate Change. Climate Change 2014: impacts, adaptation, and vulnerability http://www. ipcc.ch/report/ar5/wg2. Accessed 15 May 2015

Jacovides C.P., 1998. Reply to comment on" Statistical procedures for the evaluation of evapotranspiration computing models", *Agricultural water management*, 37(1), 95-97.

Johnson D.E., 1998. Applied multivariate methods for data analysts, Duxbury Resource Center.

Kamali M.R., 2007. World situation of Wheat in the past, present, and future. 10th congress of agronomy and modification of plants, Karaj, Iran. 23-45.

Mohammed R., Scholz M., 2019. Climate variability impact on the spatiotemporal characteristics of drought and Aridityin arid and semi-arid regions, *Water Resources Management*, 33(15), 5015-5033.

Mukherjee N., Siddique G., 2019. Assessment of climatic variability risks with application of livelihood vulnerability indices, *Environment, Development and Sustainability*, 1-27.

Nassiri M., Koocheki A., Kamali G.A., Shahandeh H., 2006. Potential impact of climate change on rainfed wheat production in Iran: (Potentieller Einfluss des Klimawandels auf die Weizenproduktion unter Rainfed-Bedingungen im Iran), *Archives of agronomy and soil science*, 52(1), 113-124.

Newlands N.K., Zamar, D.S., 2012. In-season probabilistic crop yield forecasting, integrating agro-climate, remote-sensing and phenology data.

Ndiaye P.M., Bodian A., Diop L., Deme A., Dezetter A., Djaman K., 2020. Evaluation and Calibration of Alternative Methods for Estimating Reference Evapotranspiration in the Senegal River Basin, *Hydrology*, 7, 24.

Panahi D.M., Kalantari Z., Ghajarnia N., Seifollahi-Aghmiuni S., Destouni G., 2020. Variability and change in the hydro-climate and water resources of Iran over a recent 30-year period. *Scientific reports*, 10(1), 1-9.

Penman H.L., 1948. Natural evaporation from open water, bare soil and grass. Proceedings of the Royal Society of London, Series A. *Mathematical and Physical Sciences*, 193(1032), 120-145.

Rahim S.A., 2014. VIA of climate change on malaysian agriculture systems: Current understanding and plans. University Kebangsaan Malaysia, http://www.ukm.my/seaclidcordex/presentation_rice_project.html.

Rosenzweig C., Ritchie J.T., Jones J.W., Tsuji G.Y., Hildebrand P., 1995. Climate change and agriculture: analysis of potential international impacts. In Symposium on Climate Change and Agriculture: Analysis of Potential International Impacts (No. RESEARCH). Soil Science Society of America.

Saggi M.K., Jain S., 2019. Reference evapotranspiration estimation and modeling of the Punjab Northern India using deep learning, *Computers and Electronics in Agriculture*, 156, 387-398.

Sánchez-Martín, J., Rispail, N., Flores, F., Emeran, A. A., Sillero, J. C., Rubiales, D., Prats, E., 2017. Higher rust resistance and similar yield of oat landraces versus cultivars under high temperature and drought. *Agronomy for sustainable Development*, 37(1), 1-14.

Sarkar C., Abbasi, S.A., 2006. QUALIDEX–a new software for generating water quality indice, *Environmental monitoring and assessment*, 119(1), 201-231.

Schmidhuber J., Tubiello, F.N., 2007. Global food security under climate change, *Proceedings of the National Academy of Sciences*, 104(50), 19703-19708.

Sharafi S., Ghaleni M.M., 2021a. Calibration of empirical equations for estimating reference evapotranspiration in different climates of Iran, *Theoretical and Applied Climatology*, 1-15.

Sharafi S., Ghaleni, M.M., 2021b. Evaluation of multivariate linear regression for reference evapotranspiration modeling in different climates of Iran, *Theoretical and Applied Climatology*, 143(3), 1409-1423.

Sharafi S., Karim N.M., 2020. Investigating trend changes of annual mean temperature and precipitation in Iran, *Arabian Journal of Geosciences*, 13(16), 1-11.

Sharafi S., Ramroudi M., Nasiri M., Galavi M., Kamali G.A., 2016. Role of early warning systems for sustainable agriculture in Iran, *Arabian Journal of Geosciences*, 9(19), 1-17.

Shiri J., Marti P., Karimi S., Landeras G., 2019. Data splitting strategies for improving data driven models for reference evapotranspiration estimation among similar stations, *Computers and Electronics in Agriculture*, 162, 70-81.

Solaymani S., 2018. Impacts of climate change on food security and agriculture sector in Malaysia, *Environment, Development and Sustainability*, 20(4), 1575-1596.

Sun L., Song C., 2008. Evapotranspiration from a freshwater marsh in the Sanjiang Plain, Northeast China, *Journal of Hydrology*, 352(1-2), 202-210.

Sutadian A.D., Muttil, N., Yilmaz, A.G., Perera, B.J.C., 2017. Using the Analytic Hierarchy Process to identify parameter weights for developing a water quality index, *Ecological Indicators*, 75, 220-233.

Torriani D.S., Calanca P., Schmid S., Beniston M., Fuhrer J., 2007. Potential effects of changes in mean climate and climate variability on the yield of winter and spring crops in Switzerland, *Climate Research*, 34(1), 59-69.

Uddin M.G., Nash, S., Agnieszka, I., 2021. A review of water quality index models and their use for assessing surface water quality. *In Ecological Indicators*, 122, p. 107218. DOI: 10.1016/j.ecolind.2020.107218.

Vaghefi S.A., Keykhai M., Jahanbakhshi F., Sheikholeslami J., Ahmadi A., Yang H., Abbaspour K.C., 2019. The future of extreme climate in Iran. *Scientific reports*, 9(1), 1-11.

Zare Feyz Abadi A., Koochaki A., Nassiri Mahalati M., 2006. Trend analysis of yield, production and cultivated area of cereal in Iran during the last 50 years and prediction of future situation, *Iranian Journal of Field Crops Research*, 4(1), 49-70.

Appendix 1. The special vectors of the main components.

Variable	Variable description	PC 1	PCA 2	PCA 3	PCA 4	PCA 5
			Temperature			
VAR1	tmin_minsp	0.16450	0.14441	0.02848	-0.12959	-0.00295
VAR2	tmin_minsu	0.12960	0.05561	0.00245	0.08367	0.04738
VAR3	tmin_minf	0.14060	0.12796	-0.03723	-0.04595	-0.02857
VAR4	tmin_minw	0.11160	0.21297	0.04838	-0.22508	-0.09398
VAR5	tmin_maxsp	0.15854	0.09397	-0.21826	-0.18485	0.00927
VAR6	tmin_maxsu	0.13953	0.02859	-0.22820	-0.00255	0.04716
VAR7	tmin_maxf	0.11035	0.09375	-0.21926	-0.16883	0.01272
VAR8	tmin_maxw	0.13504	0.15051	0.03738	-0.23938	-0.03640
VAR9	tmin_avgsp	0.13949	0.12921	-0.12072	0.00945	-0.00616
VAR10	tmin_avgsu	0.16554	0.02086	-0.26172	-0.01299	0.02835
VAR11	tmin_avgf	0.12383	0.11950	-0.13281	-0.16266	-0.01949
VAR12	tmin_avgw	0.10964	0.22985	0.00949	-0.14321	0.00272
VAR13	tmax_minsp	0.11360	0.01850	0.12050	0.07398	0.00650
VAR14	tmax_minsu	0.16348	-0.05825	0.03838	0.21946	0.09288
VAR15	tmax_minf	0.15027	-0.06380	0.12942	0.08409	-0.01628
VAR16	tmax_minw	0.12897	0.04636	0.21245	-0.07848	-0.03858
VAR17	tmax_maxsp	0.17035	-0.03850	0.03988	0.19298	0.01848
VAR18	tmax_maxsu	0.14478	-0.13740	0.00949	0.20209	0.01949
VAR19	tmax_maxf	0.13894	-0.08450	0.04848	0.18939	0.01849
VAR20	tmax_maxw	0.13034	0.04738	0.31949	-0.01748	-0.00140
VAR21	tmax_avgsp	0.18043	0.00187	0.09844	0.13938	0.02385
VAR22	tmax_avgsu	0.13222	-0.08056	0.02848	0.21041	0.01295
VAR23	tmax_avgf	0.14006	-0.07521	0.09387	0.13939	-0.03925
VAR24	tmax_avgw	0.14039	0.02815	0.34939	-0.02646	-0.04848
VAR25	tavg_minsp	0.14887	0.08386	0.06851	-0.01285	-0.00464
VAR26	tavg_minsu	0.16941	-0.00221	-0.06816	0.12948	0.04839
VAR27	tavg_minf	0.18247	0.04840	0.08738	0.09359	-0.04921
VAR28	tavg_minw	0.11841	0.12960	0.20195	-0.20849	-0.04849
VAR29	tavg_maxsp	0.14847	0.00066	-0.06386	0.12249	0.02858
VAR30	tavg_maxsu	0.11048	-0.04816	-0.11027	0.12939	0.02859
VAR31	tavg_maxf	0.14354	0.08285	-0.07382	0.07377	0.02858
VAR32	tavg_maxw	0.11588	0.11941	0.19384	-0.13939	-0.04849
VAR33	tavg_avgsp	0.13570	0.04840	-0.05463	0.02783	0.02858
VAR34	tavg_avgsu	0.14942	0.02046	-0.02027	0.11409	0.02906
VAR35	tavg_avgf	0.16247	0.01295	-0.00112	0.01946	-0.00927
VAR36	tavg_avgw	0.12360	0.11951	0.11782	-0.09387	-0.10395
			Precipitation			
VAR37	ppt_minsp	-0.08707	0.26999	0.04887	0.14991	0.03001
VAR38	ppt_minsu	-0.11046	0.13127	-0.03981	-0.06542	0.26653
VAR39	ppt_minf	-0.103	0.25092	0.02090	0.12942	0.00538
VAR40	ppt_minw	-0.09034	0.25978	-0.01092	0.27551	-0.04027
VAR41	ppt_maxsp	-0.12041	0.24091	0.02219	0.13090	0.03639
VAR42	ppt_maxsu	-0.13914	0.16592	0.06048	-0.00776	0.19442
VAR43	ppt_maxf	-0.07797	0.22092	-0.00337	0.22082	-0.00548
VAR44	ppt_maxw	-0.07806	0.26507	0.01093	0.25047	-0.06542
VAR45	ppt_avgsp	-0.12313	0.25082	0.03129	0.13092	0.00438
VAR46	ppt_avgsu	-0.13423	0.12002	-0.00897	0.06199	0.23693
VAR47	ppt_avgf	-0.01865	0.27227	-0.00598	0.12783	-0.00819
VAR48	ppt_avgw	-0.09995	0.25548	0.00167	0.25582	-0.09694

			ET_{ref}			
VAR49	eto-minsp	-0.01805	0.24907	0.03588	0.11597	0.03247
VAR50	eto-minsu	-0.14730	0.11586	-0.06691	0.25955	0.23687
VAR51	eto-minf	-0.11508	0.22580	0.01577	0.11162	0.08666
VAR52	eto-minw	-0.10114	0.21505	-0.00797	0.00996	-0.07724
VAR53	eto-maxsp	-0.11319	0.30377	0.03476	0.14958	0.05143
VAR54	eto-maxsu	-0.12194	0.17147	0.06266	0.22705	0.19068
VAR55	eto-maxf	-0.08000	0.25199	-0.03264	0.20395	-0.07998
VAR56	eto-maxw	-0.09242	0.24250	0.01213	0.00977	-0.08323
VAR57	eto-avgsp	-0.11526	0.23413	0.04426	0.14934	0.04450
VAR58	eto-avgsu	-0.13722	0.17167	-0.01058	0.27614	0.22394
VAR59	eto-avgf	-0.10516	0.24775	-0.00915	0.16213	-0.01096
VAR60	eto-avgw	-0.07662	0.22288	0.00303	-0.05244	-0.09554
			GDD			
VAR61	gddsp	0.11312	0.00599	-0.03034	0.13090	0.21253
VAR62	gddsu	0.17077	-0.01446	-0.01383	0.10592	0.08954
VAR63	gddf	0.15094	0.01208	-0.06947	0.08581	0.09602
VAR64	gddw	0.07279	0.07002	0.09964	-0.12650	0.09951
			Frosty days			
VAR65	frz_free	0.11368	0.11417	-0.14843	-0.09487	-0.09497
VAR66	frz_fall	0.13310	0.10408	-0.09587	-0.12554	-0.08497
VAR67	frz_spr	-0.13050	-0.11077	0.12722	0.01679	0.04943

* t; temperature, ppt; precipitation, eto; reference evapotranspiration, min; minimum, max; maximum, avg; average, sp; spring, su; summer, f; fall, w; winter, gdd; growth degree days, frz-free; frostless days, frz-fall; fall frost days, frz-spr; spring frost days.

Italian Journal of Agrometeorology
Rivista Italiana di Agrometeorologia

Firenze University Press
www.fupress.com/ijam

OPEN ACCESS

Citation: D.F. Daniel, R. Dallacort, J.D. Barbieri, M.A.C. De Carvalho, P.S.L. De Freitas, R.C. Tieppo, W. Fenner (2022) Use of microlysimeters to determine soil water evaporation as a function of drainage. *Italian Journal of Agrometeorology* (2): 31-48. doi: 10.36253/ijam-1538

Received: January 12, 2022

Accepted: October 7, 2022

Published: January 29, 2023

Data Availability Statement: All relevant data are within the paper and its Supporting Information files.

Competing Interests: The Author(s) declare(s) no conflict of interest.

ORCID:
DFD: 0000-0003-1743-5089
RD: 0000-0002-7634-8973
JDB: 0000-0002-8251-1255
MACDC: 0000-0003-4966-1013
PSLDF: 0000-0001-6663-2797
RCT: 0000-0001-8132-4813
WF: 0000-0002-3463-9457

Use of microlysimeters to determine soil water evaporation as a function of drainage

Diego Fernando Daniel[1,*], Rivanildo Dallacort[1], João Danilo Barbieri[1], Marco Antonio Camillo De Carvalho[1], Paulo Sérgio Lourenço De Freitas[2], Rafael Cesar Tieppo[1], William Fenner[1]

[1] State University of Mato Grosso/UNEMAT, Department of Agronomy, Graduate Program in Environment and Agricultural Production Systems/PPGASP, Highway MT-358, km 7 - Jardim Aeroporto, 78300-000, Tangará da Serra, MT, Brazil. E-mail address: rivanildo@unemat.br, jdanilob@gmail.com, marcocarvalho@unemat.br, tiepporc@unemat.br, fennerwilliam@gmail.com
[2] State University of Maringá/UEM, Department of Agronomy, Graduate Program in Agronomy/PGA, Colombo Avenue, 5790 - Zona 7, 87020-900, Maringá, PR, Brazil. E-mail address: pslfreitas@uem.br
*Corresponding author. E-mail: diegodaniel.agro@gmail.com

Abstract. The aim of this study was to test two models and two sizes of microlysimeters to determine soil water evaporation as a function of the removal of water by drainage at the bottom of the units. The experiment was conducted at the experimental field of the State University of Mato Grosso (UNEMAT) in Tangará da Serra, Mato Grosso, Brazil. Soil water evaporation was determined using microlysimeters constructed from rigid PVC tubes, of which two models and two sizes were tested. The four microlysimeter treatments were: 100 mm diameter without drainage (ML100WD), 100 mm diameter with drainage (ML100D), 150 mm diameter without drainage (ML150WD), and 150 mm diameter with drainage (ML150D). The microlysimeters were fitted to an irrigation blade of 60 mm and compared to applications with four irrigation blade sizes (15, 30, 45, and 60 mm). Water evaporation from the soil was obtained from the mass variation of the microlysimeters, and was then compared to the soil water evaporation determined using weighing lysimeters. The obtained data were analyzed using descriptive statistical techniques, tests of means, and regression analysis. The soil water evaporation values present significant differences between the two microlysimeter sizes (100 and 150 mm diameter) and the two models (with and without water drainage). Soil water evaporation is affected by the water drainage that occurs at the bottom of the microlysimeters. There was no difference in soil water evaporation between irrigation rates within the same microlysimeter size and model. The two models and the two microlysimeter sizes tested can be used for the quantification of soil water evaporation, due to the high determination coefficients observed when compared to the evaporation observed with the weighing lysimeters.

Keywords: irrigation, lysimeters, mini-lysimeters, water balance, water management.

1. INTRODUCTION

Soil water evaporation corresponds to a portion of evapotranspiration, which is important in the context of agricultural production, as its impact on the hydrological balance can be considerable, especially in situations of conventional cultivation or those with decreased levels of straw in the soil (Facchi et al., 2017). Thus, understanding and quantifying the process of soil water evaporation assists in providing data for many different agricultural crops, which aids in improving the efficiency of irrigation water use (Facchi et al., 2017; Mansour et al., 2022).

Water evaporation at the soil surface is a physical process whereby water changes from a liquid to a gaseous state, resulting in the transfer of water contained in the soil to the atmosphere (Facchi et al., 2017; Heck et al., 2020), without utilizing the transpiration process in plants that produces the same result (Dalmago and Bergamaschi, 2017).

Soil water evaporation generally affects the first 10–15 cm of the soil, although it varies according to soil characteristics such as texture and structure. It also depends on atmospheric conditions, such as air temperature, relative humidity, wind speed, and solar radiation, and soil factors, such as hydraulic properties and soil water volume (Allen et al., 1998; Facchi et al., 2017).

Studies on the quantification of soil water evaporation provide necessary information for several activities, especially those of irrigation use (Wang et al., 2020), agricultural water use efficiency (Barbieri et al., 2020), evapotranspiration component partitioning (Sánchez et al., 2021; Wang et al., 2021), and water balance (Pereira et al., 2020). In addition, soil water evaporation can account for approximately 20–40% of evapotranspiration in agricultural crops grown in the Cerrado regions (Andrea et al., 2019; Barbieri et al., 2020).

Soil water evaporation was originally quantified using lysimeters (Ritchie, 1972; Waggoner and Turner, 1972; Schneider et al., 2021). However, as the process of installing and maintaining lysimeters is complicated and requires considerable time, cost, and specialized labor, researchers have sought new simpler technologies as alternatives to measure and apply methods of soil water evaporation, considering the varied crops and agricultural sectors.

Water loss through evaporation can be quantified using microlysimeters, which have been developed and tested as research has evolved (Boast and Robertson, 1982; Daamen et al., 1993; Yang et al., 2020). They were initially designed by Boast and Robertson (1982) and have since been used to directly determine soil water evaporation in bare soils or those cultivated with agricultural crops (Andrea et al., 2019; Schneider et al., 2021).

Microlysimeters are small tubes filled with undeformed soil samples that are installed at ground level, and periodically weighed to estimate soil water evaporation by temporal mass differences (Flumignan et al., 2012; Facchi et al., 2017). Microlysimeters are based on the same principle as traditional lysimeters and consist of plastic or steel cylinders with diameters of 50–200 mm and heights ranging between 100 and 300 mm (Daamen et al., 1993; Flumignan et al., 2012; Facchi et al., 2017).

Microlysimeters are inserted into the soil, for filled with soil in an undeformed manner (soil monolith), and then weighed at regular intervals to determine of the amount of water evaporated from the soil based on the mass difference. The small size of the devices dictates that several should be installed in the field (which depends on the size of the area) to extend the behavior of soil water evaporation to a larger scale (Yang et al., 2022).

Studies have demonstrated the accuracy of the measurements obtained using microlysimeters by comparing them with the results of classical lysimeters (Flumignan et al., 2012; Ma et al., 2020), and confirming their applicability in different agricultural situations (Lu et al., 2018; Pereira et al., 2020). Several authors have used microlysimeters to determine soil water evaporation. Dalmago and Bergamaschi (2017) evaluated water evaporation in a soil in response to the amount of straw on the surface and atmospheric evaporative demand, and observed that water evaporation on the soil surface is higher in soils subjected to conventional tillage than those with no-till systems. Vieira et al. (2016) determined the evapotranspiration of wheat crops in the region of Maringá, Paraná, Brazil, using microlysimeters to obtain soil water evaporation. Those researchers calculated the coefficient of soil water evaporation (Ke) and revealed that the microlysimeters proved reliable in measuring soil water evaporation.

The determination of soil water evaporation using microlysimeters is possible because the lower part is sealed and the upper surface is open, allowing for water evaporation, which is the only form of water transfer to the atmosphere in this situation. Daamen et al. (1993) stated that drainage could occur at the bottom of the microlysimeter; however, the drained water can be accounted for, and those authors introduced a model of an effective drainage box to measure the water loss.

Microlysimeters that are sealed at the bottom to prevent outflows that may affect soil water evaporation and

its quantification. Therefore, the aim of this study was to test two models and two sizes of microlysimeters to determine soil water evaporation as a function of the drainage of water from the bottom of the units.

2. MATERIALS AND METHODS

2.1 General Description

The experiment was conducted in the experimental field of the Centro Tecnológico de Geoprocessamento e Sensoriamento Remoto (CETEGEO-SR), in the State University of Mato Grosso (UNEMAT), Professor Eugênio Carlos Stieler Campus, Tangará da Serra, Mato Grosso, Brazil. The soil is classified as either dystroferric red latosol with a very clayey texture (Santos et al., 2018) or oxisol (Soil Survey Staff, 2014). The climate is megathermal or tropical with dry winters (Aw), according to the Köppen Climate Classification System (Alvares et al., 2013), with average annual precipitation of 1,830 mm and an average air temperature of 24.4 °C (Dallacort et al., 2011).

An automatic weather station (14°65'00" S, 57°43'15" W, 440 masl) is located near the experimental area and is outfitted with Campbell Scientific Inc. equipment, from which the meteorological data used in this experiment were obtained and the reference evapotranspiration (ETo) was determined, as calculated by the Penman-Monteith method (FAO 56) (Allen et al., 1998).

The evaluated physical and hydraulic characteristics of the soil included texture, soil density, macroporosity, microporosity, total porosity, field capacity, permanent wilting point, soil resistance to penetration, basic infiltration velocity, and available water capacity of the soil (Bernardo et al., 2006; Camargo et al., 2009; Stolf et al., 2012; Teixeira et al., 2017). The dystroferric red latosol of the study site has a very clayey texture, with average values of sand, silt, and clay of 235, 124, and 641 g kg^{-1}, respectively. The soil density averaged 1.172 kg dm^{-3}, which was considered low for the soil studied. The soil moisture at field capacity (θ_{FC}) of the studied area was 0.3490 m^3 m^{-3} and the moisture at the permanent wilting point (θ_{PWP}) was 0.2083 m^3 m^{-3}, with soil presenting an available water capacity (AWC) of 82.45 mm. The average soil resistance to penetration was 1.94 MPa, which is classified as moderate. The basic infiltration velocity (BIV) of the soil was 25.91 mm h^{-1}, which is considered a high value for this soil.

In the previous year of the experiment, some compaction points were found in the studied area, and to homogenize and reduce this compaction, subsoiling was performed in October 2019 with a three-stem subsoiler. Subsequently, an intermediate harrow was used once, followed by a leveling harrow to level and densify the soil. The land was left fallow until July 2020, when the soil was collected for the evaluation and preparation of the microlysimeters.

2.2 Microlysimeter construction process

The process of extracting the undeformed soil (soil monolith) with the microlysimeter is relatively arduous. Therefore, to maintain the soil structure and facilitate the process, the microlysimeter (internal structure) was inserted into the soil with the help of a hydraulic jack with a wedge fixed at the top, and as the jack was activated, the microlysimeter was pushed deeper into the soil. The undeformed samples were then collected, and the soil around the microlysimeter was removed manually and with the aid of a hoe (Fig. 1).

Soil water evaporation was measured using microlysimeters adapted from Boast and Robertson (1982), Flumignan et al. (2012), and Facchi et al. (2017). The microlysimeters were constructed using rigid polyvinyl chloride (PVC) tubes manufactured in two sizes, with the first measuring 100 mm in diameter and 250 mm in height and the second measuring 150 mm in diameter and 250 mm in height. Each microlysimeter size was manufactured both with a drainage system (Fig. 2A) and without drainage (Fig. 2B). For the outer envelope, PVC pipes ranging from 150 to 200 mm in diameter and 320 mm in height were used according to the models described in Fig. 2.

In the model with water drainage, the lower part was not sealed, but covered with a white 80 g TNT fabric (30 × 30 cm) and a 0.1 mm nylon mesh (30 × 30 cm) to prevent the soil from deforming at the bottom of the microlysim-

Fig. 1. Process of inserting the microlysimeter into the soil and collecting the soil to manufacture the microlysimeter with undisturbed soil.

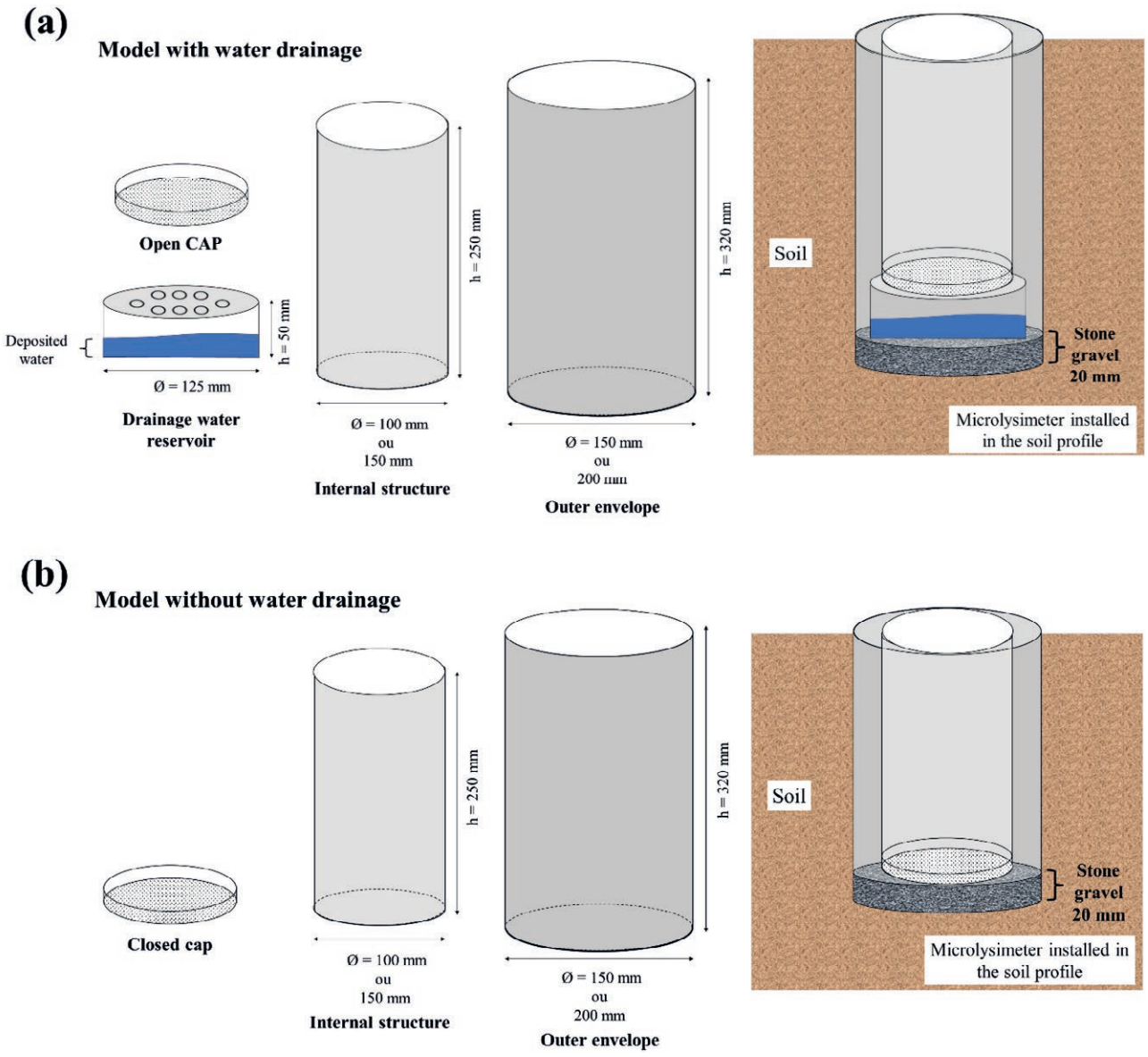

Fig. 2. Microlysimeter models used in the experiment. Microlysimeter with water drainage system at the bottom (A); Microlysimeter without water drainage system at the bottom (B).

eter, while allowing the passage of drainage water (Fig. 3A, 3 B, and 3C). For the model without water drainage, the bottom was sealed using a weldable PVC irrigation CAP (Fig. 3D and 3E). Dalmago et al. (2010) evaluated soil water evaporation by using a similar microlysimeter model to prevent soil loss and facilitate water drainage.

2.3 Tests and data collection methods

Two models and two sizes of the newly manufactured microlysimeters were tested and evaluated with four irrigation blades (15, 30, 45, and 60 mm): 100 mm diameter without drainage (ML100WD), 100 mm diameter with drainage (ML100D), 150 mm diameter without drainage (ML150WD), and 150 mm diameter with drainage (ML150D), with eight repetitions of each.

The collection of soil water evaporation data and that of drained water at the bottom of the microlysimeters was performed during the following periods and days. Test 01 (Single Blade): on Jul 24, 2020, measurements were performed every hour from 06:00 to 18:00, using an irrigation blade of 60 mm with the two models of microlysim-

Fig. 3. Open-bottom microlysimeter model with water drainage (A, B and C); Microlysimeter model with closed bottom without water drainage (D and E). 1 - Internal structure; 2 - Open CAP; 3 - 80 gram white TNT (30 x 30 cm); 4 - 0.1 mm nylon mesh (30 x 30 cm); 5 - Mounting the TNT, the nylon mesh and the CAP on the internal structure; 6 - Bottom of the internal structure of the microlysimeter after it is ready; 7 - PVC closed cap; 8 - Internal structure; 9 - External structure; 10 - Microlysimeter with closed bottom.

eters evaluated. Daily data collection was also performed from Jul 24, 2020 to Jul 30, 2020, at the same times (06:00 and 18:00), to check the variability of evaporation on different days between the microlysimeter models. This irrigation blade was chosen because of the predominance of P75% with less than 60 mm of rainfall in the locality where this study was developed (Fietz et al., 2008; Fietz et al., 2011). Test 02 (Irrigation Blades): On Aug 7, 2020, a second evaluation of evaporation and drainage was conducted with the microlysimeters, performing measurements every hour from 06:00 to 18:00, using four irrigation blades (15, 30, 45, and 60 mm) on the same day. Each treatment consisted of eight microlysimeters, and each irrigation blade was applied to two microlysimeters for each treatment. Daily data collection was performed between Aug 7, 2020 and Aug 13, 2020, at the same times (06:00 and 18:00), to check the variability of evaporation on different days between the models of the microlysimeters with different irrigation blades.

Water drainage was verified in the model of the microlysimeter with drainage (Fig. 2A, 3A, 3 B, and 3C) by collecting water, from the water reservoir where the microlysimeter was placed, in a graduated cylinder with intervals of 1 mL, since it was assumed that 1 mL is equal to 1 g. In the 48 h before the evaluation, all microlysimeters were subjected to a saturation process, whereby they were placed in a 500 L tank, submerged in 1 cm of water at its top, and saturated. Subsequently, they were removed the excess water was drained for 24 h until the field capacity was reached.

The amount of evaporation was obtained from the variation in mass of the microlysimeters, which was determined by manual weighing on a high-precision scale (0.01 g) and noting the values in a spreadsheet. These measurements were used to calculate the variation in mass on a single day and comparing this to the variation on different days. Before weighing, the microlysimeters were cleaned to remove any aggregate material. Soil

water evaporation determination using microlysimeters was calculated according to Eq. 1:

$$E_{ML} = \frac{\Delta M_{ML+P+I}}{A_{ML}} \quad \text{(Eq. 1)}$$

where E_{ML} is the microlysimeter evaporation (mm d^{-1}), $\triangle M_{ML}$ is the microlysimeter mass change (kg), A_{ML} is the microlysimeter surface area (A100 = 0.007854 and A150 = 0.017671 m^2), P is the precipitation (mm), and I is the irrigation (mm).

2.4 Experiment installation and irrigation

On the location for mounting the microlysimeters, four repetitions of microlysimeters were installed in each of the evaluated treatments, with eight units for each treatment, totaling 32 microlysimeters. This number of repetitions was considered sufficient to represent total evaporation and drainage. The microlysimeters were randomly arranged in the experimental area, as shown in Fig. 4.

The irrigation used was a sprinkler system composed of eight sprinklers (Eco232 Frabrimar, Brazil) with 4.0 × 2.8 mm nozzles spaced 12 × 12 m apart, with a Christiansen Coefficient of Uniformity higher than 80%, under a pressure of 30 m.c.a., with an applied water blade of 10.38 mm h^{-1}. The irrigation time was determined such that each treatment would receive the desired irrigation blade. Irrigation was started at the calculated times, and at 06:00, it was turned off, and the desired blade was applied for each test.

2.5 Data analysis and statistics

To compare with microlysimeter evaporation, soil water evaporation from weighing lysimeters (EV_L) was determined. The external dimensions of the lysimeter set were 7.2 m in length and 5.3 m in width, with 1.50 × 1.50 m and 1.20 m depth, with a total area of 2.25 m^2 for each lysimeter. The construction, calibration, and validation methodology was that of Fenner et al. (2019). The weighing lysimeters were connected to a data logger (CR1000, Campbell Scientific Inc., Logan, USA) that was programmed to record data every 30 s and store the average every 15 min. The EV_L values were obtained by converting the lysimeter mass variation into mm, as determined by Eq. 2:

$$EV_L = \frac{\Delta M_{L+P+I}}{A_L} \quad \text{(Eq. 2)}$$

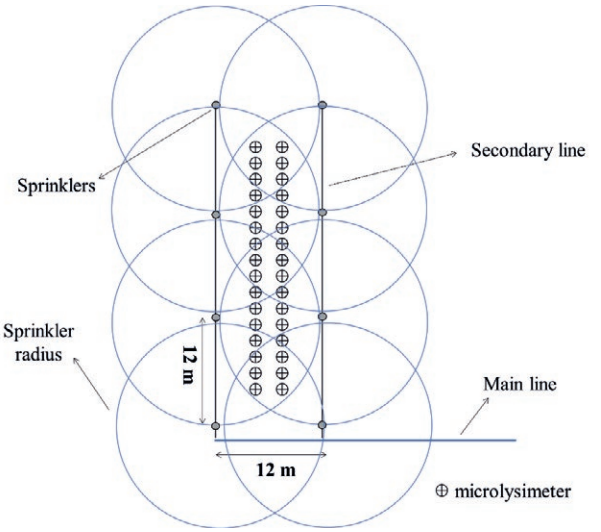

Fig. 4. Sketch of microlysimeters installed in the experimental field and arrangement of the irrigation system.

where EV_L is the soil water evaporation from the lysimeter (mm d^{-1}), $\triangle_{ML}$ is the lysimeter mass variation (kg), A_L is the lysimeter surface area (m^2), P is the precipitation (mm), and I is irrigation (mm).

To calculate the reference evapotranspiration (ETo_{PM}), the Penman-Monteith - FAO 56 methodology was used with Equation 3, as proposed by Allen et al. (1998):

$$ETo_{PM} = \frac{0{,}408\,\Delta\,(Rn - G) + \gamma \frac{900}{T+273} U_2\,(e_s - e_a)}{\Delta + \gamma\,(1 + 0{,}34U_2)} \quad \text{(Eq. 3)}$$

where ETo_{PM} is the reference evapotranspiration (mm d^{-1}), Rn is the net solar radiation of the crop (MJ m^{-2} d^{-1}), G is the soil heat flux density (MJ m^{-2} d^{-1}), T is the air temperature at 2 m above the soil (°C), U_2 is the wind speed at 2 m above the soil (m s^{-1}), e_s is the vapor saturation pressure (kPa) that was estimated through the average of e_s (Tmax) and e_s (Tmin), e_a is the current vapor pressure (kPa), e_s - e_a is the pressure deficit and vapor saturation (kPa $°C^{-1}$), Δ is the vapor pressure curve (kPa $°C^{-1}$), and γ is the psychometric constant (kPa $°C^{-1}$).

Hourly ETo values were accumulated during the same analysis period for both the microlysimeters and lysimeters. A comparison of the drained water from the two microlysimeter sizes and the soil water evaporation between the two sizes and between the models with and without soil water drainage was performed. The data obtained were analyzed by calculating the standard deviation, mean, median, asymmetry coefficient (As), and kurtosis coefficient (Ck).

The mean values of soil water evaporation between treatments were subjected to analysis of variance (ANOVA) using the F test, and the means were compared with the Tukey test at 5% probability. For data analysis, the Sisvar version 5.8 computer program was used (Ferreira, 2011). To evaluate the quality of the microlysimeters for determining soil water evaporation, the averages of the evaporation values of the microlysimeters were compared with those of the lysimeters to observe the correlation between the values, generate a regression equation, and verify the coefficient of determination.

3. RESULTS AND DISCUSSION

3.1 Meteorological elements

The average hourly values of air temperature, relative humidity, precipitation, global solar radiation, and wind speed for the two periods studied (Jul 24, 2020 to Jul 30, 2020 and Aug 7, 2020 to Aug 13, 2020) are shown in Table 1. Solar radiation is the main phenomenon that affects the other climatic variables because the radiant energy that reaches the Earth's surface is used in the convection process, which is related to air heating and heat conduction in the soil, which significantly influences soil water evaporation (Carvalho et al., 2019).

3.2 Water drainage in the microlysimeters

The values of water drainage for the two sizes of microlysimeters with drainage (ML100D and ML150D) were similar on Jul 24, 2020, when the irrigation blade of 60 mm was applied (Test 01) (Fig. 5).

The initial drainage was higher at the beginning of the evaluation and decreased with time. At 07:00, the first drainage evaluation occurred, covering the period from 06:00 to 07:00. At 06:00, when the experiment began, the drainage values were equal to zero and after one hour (07:00), 1.49 and 1.35 mm of drained water were found for the 100- and 150-mm diameter microlysimeters, respectively. Average cumulative drainage values for Jul 24, 2020 were 2.72 mm and 2.44 mm for the 100 mm diameter

Table 1. Daily values of air temperature, relative humidity, precipitation, global solar radiation and wind speed for the two periods studied in Tangará da Serra, Mato Grosso, Brazil.

Test 01 (Single Blade)									
Date	TMean (°C)	TMax (°C)	TMin (°C)	RHMean (%)	RHMax (%)	RHMin (%)	P (mm)	GR (MJ m^{-2} d^{-1})	Wind (m s^{-1})
07/24/2020	26.97	33.69	20.24	55.22	75.57	34.86	0.00	17.89	2.79
07/25/2020	21.05	26.22	15.88	66.30	81.50	51.10	0.00	17.73	4.01
07/26/2020	21.45	31.15	11.74	64.76	93.90	35.62	0.00	19.27	2.26
07/27/2020	24.68	32.90	16.46	55.48	78.53	32.43	0.00	19.75	2.34
07/28/2020	26.53	33.24	19.82	49.40	65.28	33.51	0.00	18.16	2.53
07/29/2020	23.69	29.36	18.01	63.86	81.20	46.52	0.00	18.99	3.48
07/30/2020	20.93	29.04	12.82	65.56	86.10	45.01	0.00	19.55	3.02
Average/Total	23.61	30.80	16.42	60.08	80.30	39.86	0.00	18.76	2.92
Test 02 (Irrigation Blades)									
Date	TMean (°C)	TMax (°C)	TMin (°C)	RHMean (%)	RHMax (%)	RHMin (%)	P (mm)	GR (MJ m^{-2} d^{-1})	Wind (m s^{-1})
08/07/2020	25.33	32.59	18.06	44.67	62.02	27.31	0.00	21.37	3.17
08/08/2020	25.22	32.95	17.49	50.72	73.05	28.39	0.00	21.35	2.95
08/09/2020	25.35	33.36	17.34	45.69	64.51	26.86	0.00	21.36	2.84
08/10/2020	25.93	33.57	18.28	46.85	65.35	28.35	0.00	21.11	2.86
08/11/2020	27.93	35.97	19.88	46.17	63.84	28.50	0.00	19.99	2.56
08/12/2020	28.08	35.88	20.27	48.35	67.16	29.53	0.00	18.94	2.58
08/13/2020	27.38	36.20	18.55	56.38	83.00	29.75	0.00	20.02	2.08
Average/Total	26.46	34.36	18.55	48.40	68.42	28.38	0.00	20.59	2.72

GR = Global solar radiation; TMean = Average air temperature; TMax = Maximum air temperature; TMin = Minimum air temperature; RHMean = Average Relative Humidity; RHMax = Maximum relative humidity; RHMin = Minimum relative humidity; P = Precipitation; Wind = Average wind speed.

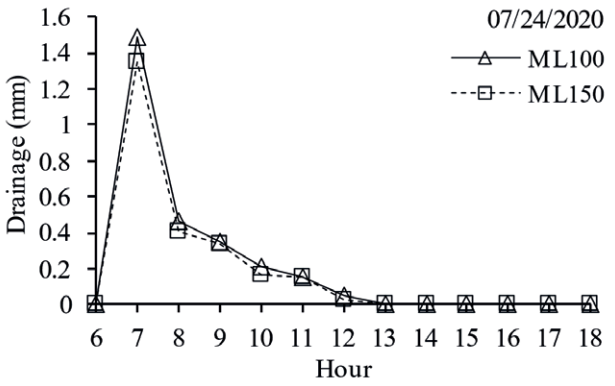

Fig. 5. Water drainage determined in two sizes of microlysimeters (ML100D and ML150D), subjected to an irrigation blade (60 mm) between 6:00 am and 6:00 pm (06:00 to 18:00), observed on Jul 24, 2020. ML100 = 100 mm diameter microlysimeter. ML150 = 150 mm diameter microlysimeter.

and 150 mm diameter microlysimeters, respectively. In this study, we observed that water drainage occurred for a maximum of 7 h, from 06:00 to 13:00, and thereafter, no drainage occurred in either microlysimeter size.

Walker (1983) began to discuss the possible effects of lack of drainage from microlysimeters due to the cap. With the bottom of the microlysimeters remaining sealed, not allowing water to escape, evaporation is the only way to transfer water in this situation to the atmosphere. Thus, a source of error that must be considered when using microlysimeters to quantify soil water evaporation is the possible drainage at the bottom of the soil. However, the measurement of drained water allows this problem to be solved (Daamen et al., 1993).

The values of water drainage for the two sizes of microlysimeters with drainage (ML100D and ML150D) were similar on Aug 7, 2020 (Test 02), when the microlysimeters were subjected to four irrigation blades (15, 30, 45, and 60 mm) (Fig. 6).

Similar to the evaluation performed on Jul 24, 2020, on Aug 7, 2020, the initial drainage was higher at the beginning of the evaluation and decreased with time for all the irrigation blades evaluated. When the experiment began at 06:00, the drainage values were zero and after one hour (at 07:00), 1.27, 1.21, 1.15, and 1.34 mm of drained water was found the 100 mm diameter microlysimeters for the 15, 30, 45, and 60 mm irrigation blades, respectively. For the 150 mm diameter microlysimeters, 1.30, 1.36, 1.22, and 1.41 mm of drained water was observed for the 15, 30, 45, and 60 mm irrigation blades, respectively, at 07:00. For the 60 mm blade, the drainage of water from the soil was greater than that of the other sizes during the day, although not by a large amount. As the microlysimeters were subjected to irrigation at field capacity, there was no marked difference in drainage between the blades.

The average cumulative drainage values on Aug 7, 2020 were 3.12, 3.18, 3.44, and 4.01 mm for the 100 mm diameter microlysimeters with irrigation blades of 15, 30, 45, and 60 mm, respectively. For the microlysimeters with a diameter of 150 mm, the average cumulative drainage values during Aug 7, 2020 were 3.06, 3.48, 3.79, and 4.07 mm for irrigation blades of 15, 30, 45, and 60 mm, respectively Drainage occurred for a maximum of 7 h, from 06:00 to 13:00, similar to that on Jul 24, 2020. Subsequently, no drainage was accounted for in either microlysimeter size (Fig. 6).

3.3 Soil water evaporation

The soil water evaporation values were lower for both sizes of microlysimeters with drainage, with similar evaporation behavior on Jul 24, 2020 (Test 01) (Fig. 7).

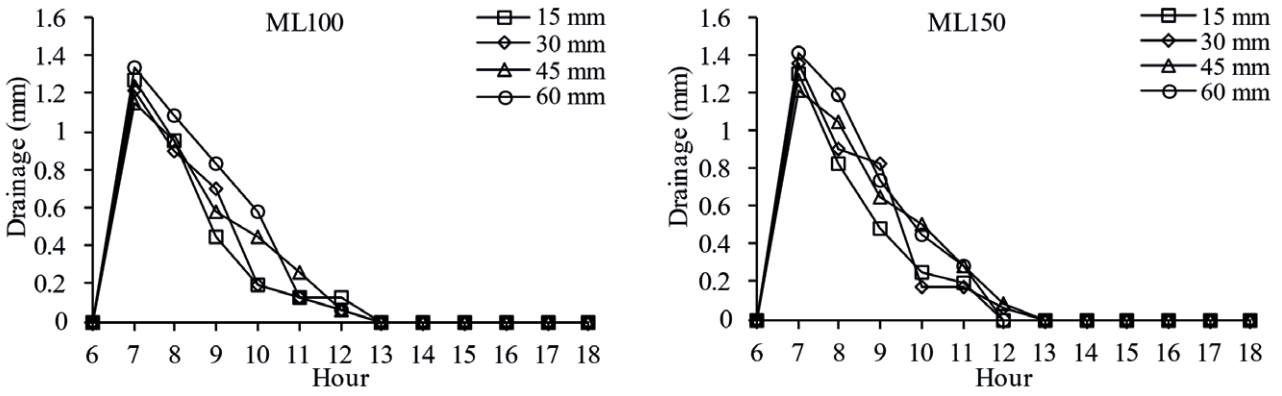

Fig. 6. Water drainage determined in two sizes of microlysimeters subjected to four irrigation blades (15, 30, 45 and 60 mm) between 6:00 am and 6:00 pm (06:00 to 18:00), observed on Aug 7, 2020. ML100 = 100 mm diameter microlysimeter. ML150 = 150 mm diameter microlysimeter.

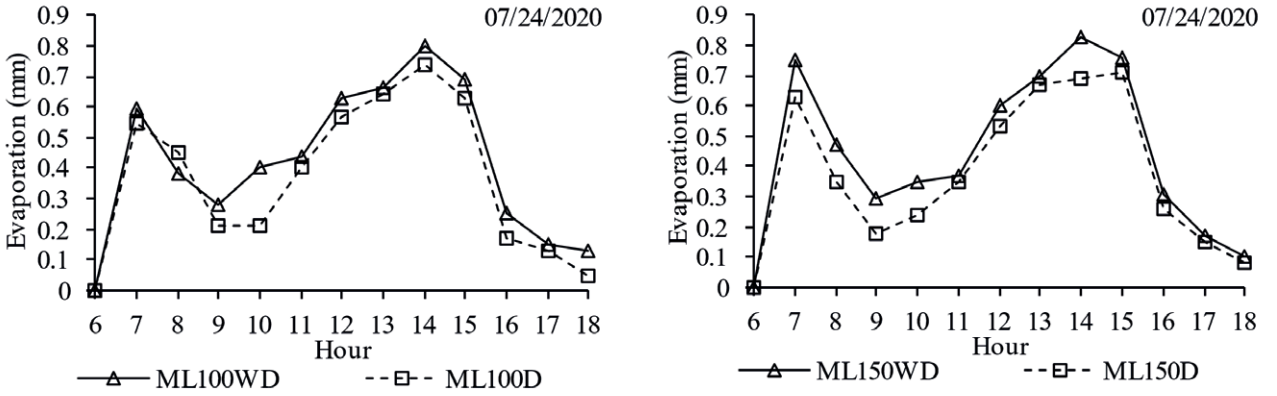

Fig. 7. Hourly soil water evaporation measured by two models and two sizes of microlysimeters between 6:00 am and 6:00 pm (06:00 to 18:00) on Jul 24, 2020. ML100WD = 100 mm microlysimeters without drainage; ML100D = 100 mm microlysimeters with drainage; ML150WD = 100 mm microlysimeters without drainage; ML150D = 100 mm microlysimeters with drainage.

At 07:00, the recorded evaporation was approximately 0.5 to 0.6 mm for the 100 mm diameter microlysimeter and 0.6 to 0.8 mm for the 150 mm diameter unit, with a decrease in values until 09:00. Thereafter, a gradual increase occurred until reaching the peak of evaporation at 14:00 of 0.80 and 0.74 mm for the 100 mm diameter microlysimeters without and with drainage, respectively. The same behavior was observed for the 150 mm diameter microlysimeters without and with drainage, with 0.69 and 0.83 mm of evaporation at 14:00, respectively. Mean cumulative evaporation values during Jul 24, 2020 of 4.75 and 5.40 mm were found for the 100 mm diameter microlysimeter models with and without water drainage, respectively. For the 150 mm diameter microlysimeters, accumulated evaporation during the day was observed to total 4.84 and 5.70 mm for the models with and without water drainage, respectively.

When comparing the soil water evaporation from the two sizes and the two models of microlysimeters subjected to the four blades of irrigation (15, 30, 45, and 60 mm), the same evaporation behavior was observed on Aug 7, 2020 (Test 02) (Fig. 8).

For irrigation blades of 15, 30, and 45 mm, an increase in evaporation was noted from 06:00 until 07:00. The values remained similar until 11:00, when another increase in evaporation occurred with the apex between 13:00 and 14:00 followed by a decrease until 18:00. For the 60 mm blade a gradual increase occurred from 06:00 to 09:00, which remained stable until 14:00, when there was a decrease in soil water evaporation values until 18:00.

Soil water evaporation levels did not vary greatly between the sizes and models of the microlysimeters, or the blade sizes of irrigation. The highest values were observed between 14:00 and 15:00, when they were maintained at approximately 1 mm of evaporation for all irrigation blades, sizes, and microlysimeter models. This apex of soil water evaporation occurred because the solar radiation was at its maximum incidence on the surface (Blight, 2009; Liao et al., 2021), as highlighted in Fig. 8. Thus, the soil reached its maximum evapotranspiration demand.

So far, only a few studies have been carried out to observe the daily or hourly soil water evaporation measured by microlysimeters, highlighting the works of Daamen and Simmonds (1996), Flumignan et al. (2012) and Facchi et al. (2017). The literature does not provide detailed information on how drainage at the bottom of the microlysimeters can affect soil water evaporation and, for this reason, studies such as this one are important to observe the behavior of hourly soil water evaporation.

The evaporation values measured by the lysimeters and by the two models and two sizes of microlysimeters presented the same behavior as the soil water evaporation during the evaluation period in Test 01 (Fig. 9). The soil water evaporation values were generally stable during the evaluation until the fifth day after irrigation, when the measurements decreased both for the lysimeters and microlysimeters due to the drying of the superficial layer of the soil after irrigation. Another factor that influenced the decrease in evaporation values on Jul 29, 2020 and Jul 30, 2020 was the reduction in evapotranspiration demand, which decreased on those days.

During the evaluation period (Jul 24, 2020 to Jul 30, 2020), the average daily reference evapotranspiration observed was 6.56 mm d^{-1}. The average soil water evaporation value between those dates was 3.74 mm d^{-1} for the lysimeters, and 4.03 and 4.31 mm d^{-1} for the 100 mm diameter microlysimeters with and without drain-

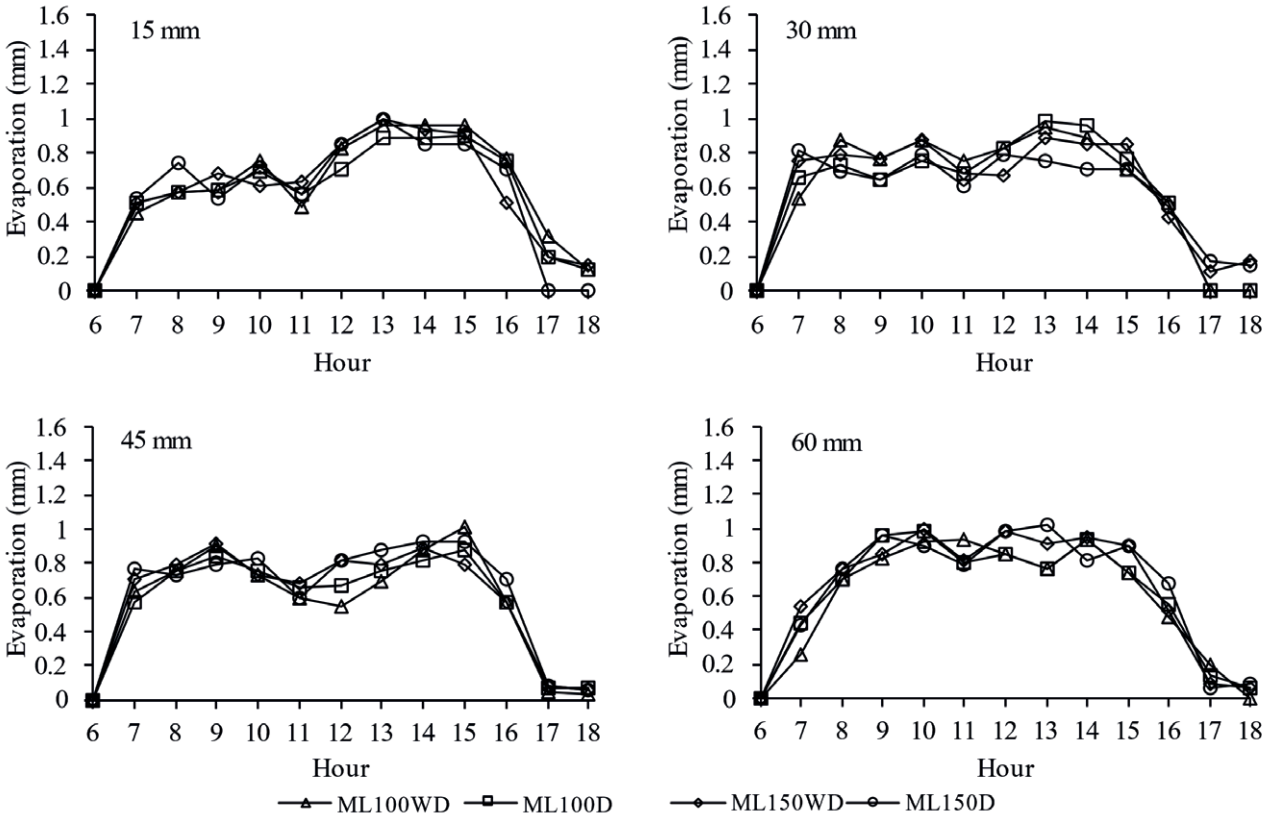

Fig. 8. Hourly soil water evaporation measured by two models and two sizes of microlysimeters subjected to four irrigation blades (15, 30, 45 and 60 mm) between 6:00 am and 6: 00 pm (06:00 to 18:00) on Aug 7, 2020 in Tangará da Serra, Mato Grosso, Brazil.

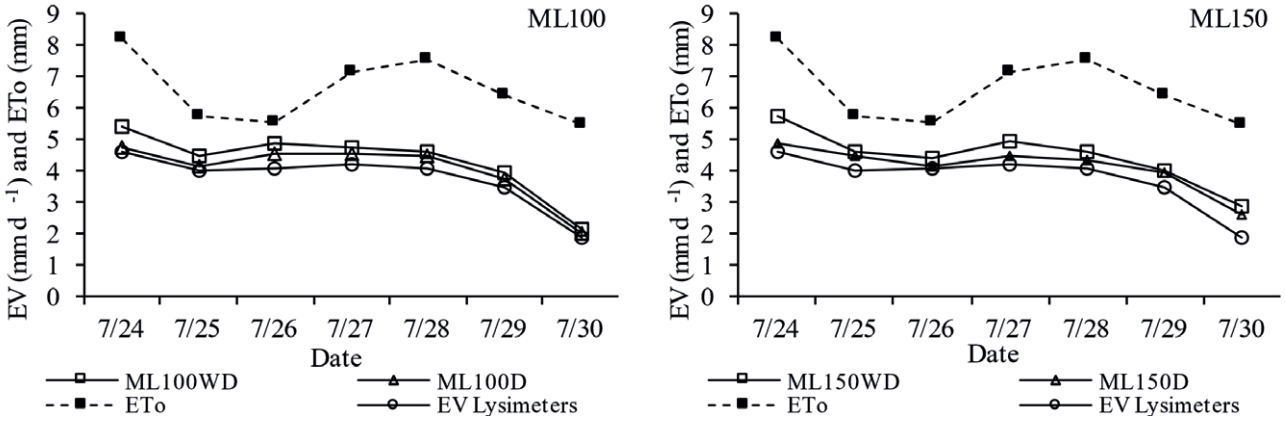

Fig. 9. Reference evapotranspiration (ETo) and daily soil water evaporation (EV) measured by weighing lysimeters (EV Lysimeters) and by two sizes and two models of microlysimeters for the period from Jul 24, 2020 to Jul 30, 2020 in Tangará da Serra, Mato Grosso, Brazil.

age, respectively. For the 150 mm diameter microlysimeters with and without drainage, the average soil water evaporation recorded during those days was 4.11 and 4.43 mm d^{-1}, respectively. The average evaporation of all microlysimeters was 4.22 mm d^{-1}, which was 11.40% higher than the average observed with the lysimeters. The average soil water evaporation for the microlysimeters without drainage was higher than those with water drainage. The values during the period for the 100 mm diameter microlysimeter models with and without water

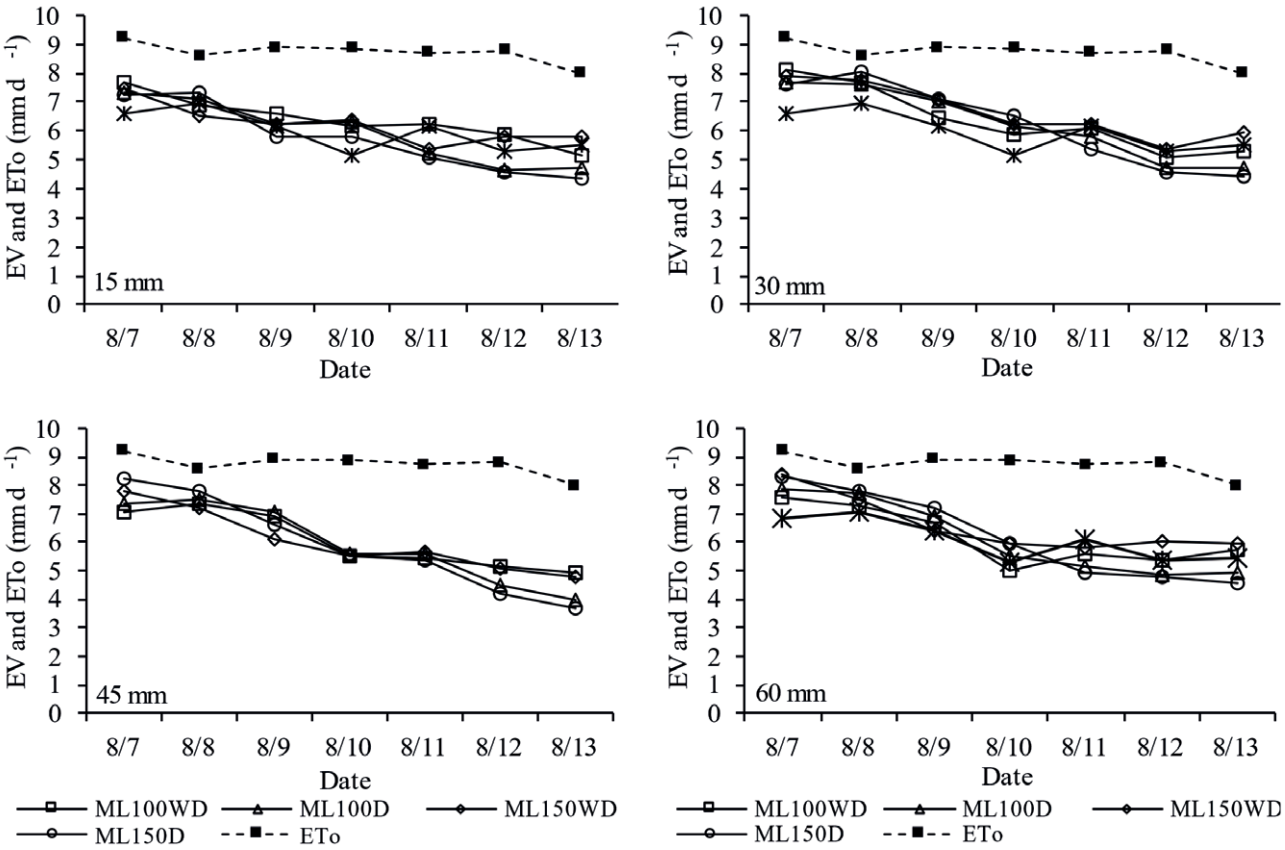

Fig. 10. Reference evapotranspiration (ETo) and daily soil water evaporation (EV) measured by weighing lysimeters (EVL) and two models and two sizes of microlysimeters subjected to 4 irrigation blades (15, 30, 45 and 60 mm) for the period from Aug 7, 2020 to Aug 13, 2020 in Tangará da Serra, Mato Grosso, Brazil.

drainage were 28.19 and 30.15 mm, respectively, while for the 150 mm diameter microlysimeters, the values were 28.79 and 31.04 mm for models with and without water drainage, respectively.

As shown in Fig. 9, soil water evaporation differed between the days evaluated. One explanation is that the response of soil water evaporation to different environmental conditions varies over time, from one locality or region to another (Wei et al., 2015; Wang et al., 2018), and is affected by the evaporative demand of the atmosphere (Tesfuhuney et al., 2015). In addition to these factors influencing soil water evaporation, other authors have reported effects of conditions related to water storage and movement in the soil profile, soil porosity (Gupta et al., 2015; An et al., 2018), and soil cover by straw mulch (Tesfuhuney et al., 2015; Fu et al., 2018; Carvalho et al., 2019).

The soil water evaporation values accounted for by the lysimeters and the two microlysimeter models and sizes, showed the same behavior when subjected to different irrigation blades between Aug 7, 2020 and Aug 13, 2020 (Fig. 10).

The soil water evaporation values showed a slight tendency to decrease over time. The topsoil layer dries, and evaporation moves to Stage 2, according to Lemon (1956), and this stage is less intense because the unsaturated hydraulic conductivity of the soil decreases as the soil dries (Aydin et al., 2005). The process of water evaporation in bare soil is divided into three phases (Ritchie, 1972). The first has a high evaporation potential and is dependent only on the immediate conditions of the atmosphere near the soil. In the second phase, intrinsic soil conditions limit water transport in the profile, and consequently, evaporation. The third phase is characterized by slow water movement toward the surface, due to the low hydraulic conductivity of the soil. Thus, the response over time depends on the phase of the evaporation process.

The high evapotranspiration demand influenced the decrease in evaporation values between Aug 7, 2020 and Aug 13, 2020. During this period, as shown in Table 1, the average air temperature was 26.34 °C and the average solar radiation was 20.59 MJ m^{-2} d^{-1}, and these fac-

tors influenced the high values of soil water evaporation and reference evapotranspiration observed. To reduce the variability of soil water evaporation, straw on the soil surface, which is used in no-till management, is an alternative that can delay soil drying and maintain evaporation at Stage 1 for a longer period (Lemon, 1956). Straw also prevents the direct impact of rainwater or irrigation on the soil, which inhibits surface sealing (Liao et al., 2021). This dry layer breaks the continuity of pores with the rest of the soil profile, thereby affecting evaporation (Aydin et al., 2005).

The soil water evaporation values were lower than the observed reference evapotranspiration values during the evaluated period. The average daily reference value observed was 8.72 mm d^{-1}. The average evaporation amounts of all microlysimeters (averages of the two models and the two sizes) for each irrigation blade were 6.07 mm d^{-1} for the 15 mm blade, 6.38 mm d^{-1} for the 30 mm blade, 5.98 mm d^{-1} for the 45 mm blade, and 6.28 mm d^{-1} for the 60 mm blade. These values were 1.48, 6.27, and 4.78%, higher than the average observed in the lysimeters of 5.98 mm d^{-1} for the 15, 30, and 60 mm blades, respectively. For the 45 mm irrigation blade, the evaporation for all microlysimeters equaled that of the weighing lysimeters.

These results are expected since greater water availability with a longer exposure to atmospheric water demand conditions should result in increased evaporation if there is sufficient energy for the process to occur. The variability of soil water evaporation as a function of measurement time as well as irrigation used before the start of the measurement period affects soil water evaporation (Dalmago et al., 2010; Di et al., 2019).

The comparison between evaporation in lysimeters (EV_L) and microlysimeters (E_{ML}) for the period between Jul 24, 2020 and Jul 30, 2020 (Test 01) is presented in Table 2. There was a significant difference between the treatments on the evaluated days. The average soil water evaporation from the two models and two sizes of microlysimeters differ between treatments, with the lowest evaporation values accounted for with the weighing lysimeters.

The findings revealed that the microlysimeters without drainage at the bottom showed higher soil water evaporation values. This effect is possibly related to the non-outflow of water from the bottom of the units, thereby presenting a greater loss of water to the atmosphere. The soil water evaporation ranges for the four models were as follows: ML100WD: 2.12 – 5.40 mm d^{-1} (average 4.31 mm d^{-1}), ML100D: 2.01 – 4.75 mm d^{-1} (average 4.03 mm d^{-1}), ML150WD: 2.85 – 5.70 mm d^{-1} (average 4.43 mm d^{-1}), and ML150D: 2.62 – 4.84 mm d^{-1} (average 4.11 mm d^{-1}).

Certain factors can be identified as responsible for the differences between treatments, and these can significantly interfere with soil water evaporation in experiments with irrigation (Dalmago et al., 2010; Zhang et al., 2019). For example, when using sprinkler irrigation, because it does not present the same homogeneity of water distribution as rainfall, variability of soil moisture inside the microlysimeters can occur, which affects evaporation (Dalmago et al., 2010; Al-Ghobari et al., 2018). Furthermore, Dalmago et al. (2010) reported that the atmospheric water demand after irrigation is different from that after rainfall, which results in altered evaporation responses.

Table 2. Mean values and descriptive statistics for daily soil water evaporation determined in weighing lysimeters and microlysimeters in Tangará da Serra, Mato Grosso, Brazil.

Date	Soil Water Evaporation (mm d^{-1})					SD	$\bar{X}$	Md	As	Ck
	EVL	ML100WD	ML100D	ML150WD	ML150D					
24/07/2020	4.59b	5.40a	4.75b	5.70a	4.84b	0.47	5.06	4.84	0.66	-1.88
25/07/2020	3.96c	4.46ab	4.16bc	4.58a	4.45ab	0.25	4.32	4.45	-0.75	-1.21
26/07/2020	4.03c	4.88a	4.51ab	4.41bc	4.12bc	0.34	4.39	4.41	0.57	-0.36
27/07/2020	4.21b	4.72a	4.52ab	4.90a	4.49ab	0.26	4.57	4.52	-0.17	0.04
28/07/2020	4.06b	4.62a	4.49a	4.59a	4.34ab	0.23	4.42	4.49	-1.19	0.81
29/07/2020	3.46b	3.95a	3.75ab	4.01a	3.93a	0.22	3.82	3.93	-1.37	1.31
30/07/2020	1.86b	2.12b	2.01b	2.85a	2.62a	0.42	2.29	2.12	0.57	-2.09
Average	3.74c	4.31a	4.03b	4.43a	4.11b	0.27	4.12	4.11	-0.48	-0.14

Means followed by the same lowercase letter on the line do not differ statistically by Tukey's test at the 5% probability of error. EVL = Lysimeters evaporation; ML100WD = 100 mm microlysimeters without drainage; ML100D = 100 mm microlysimeters with drainage; ML150WD = 150 mm microlysimeters without drainage; ML150D = 150 mm microlysimeters with drainage; SD = Standard deviation; $\bar{X}$ = Average; Md = Median; As = Asymmetry; Ck = Kurtosis.

The standard deviation of the treatments varied between 0.22 and 0.47 mm d^{-1}, with an average of 0.27 mm d^{-1} among the days evaluated. EV_L varied between 1.86 and 4.59 mm d^{-1}, with an average of 3.74 mm d^{-1}. This variation is due to the different atmospheric demands on the days evaluated as well as the decreasing water loss to the atmosphere. As shown in Table 2, without making any distinction between the soil water evaporation accounted in the lysimeters and microlysimeters studied, the deviations found between the measurements obtained were generally within the range of ±0.35 mm d^{-1} (71.43% of the data).

The evaporation and lifetime of a microlysimeter are influenced by errors intrinsic to this method, such as drainage limitations, capillary rise caused by bottom closure, degree of soil disturbance caused during extraction, and heat conduction inside the microlysimeter (Daamen et al., 1993; Marek et al., 2019). These factors may explain the higher mean evaporation values found in the 100 and 150 mm diameter microlysimeters without drainage compared to those with water drainage (Table 2). It was observed that until the fifth day after irrigation, the evaporation values recorded in the lysimeters remained similar, and on the sixth day, there was a decrease. The symmetrical set and the microlysimeters should be maintained at close to field capacity so that measurements of soil water evaporation are not lower than those that actually occurred on the day because of the smaller amount of water present in the soil.

Allen (1990) reported that soil water evaporation values in the first few days may be overestimated when microlysimeters are installed soon after precipitation or irrigation has occurred. Thus, it is important that when installing the microlysimeters after an irrigation or rainfall event, the aspects of the water sheet applied to the soil and the water distribution capacity of the soil should be considered (Flumignan et al., 2012; Marek et al., 2019).

When comparing the mean with the median, low variation was observed between the values of soil water evaporation, which indicates that they are close to normal; this was also proven by the value of the asymmetry coefficient, showing positive asymmetry for three days and negative asymmetry for four different days, but values close to 0 (symmetry), with an average of -0.48, which is a good parameter for daily assessment of soil water evaporation (Table 2). Regarding the kurtosis coefficient (Ck), the mean values of soil water evaporation for four of the seven days studied presented a platykurtic distribution ($Ck < 0$), and the other three days presented a leptokurtic distribution ($Ck > 0$), but soil water evaporation distributions were close to normal for all days ($Ck = 0$, mesokurtic). According to Carvalho et al. (2002), asymmetry and kurtosis values ranging between $-3 < 0 > 3$ indicate the normality of the data, which was observed in this study.

The soil water evaporation values from the lysimeters and microlysimeters between Aug 7, 2020 and Aug 13, 2020 (Test 02), where four irrigation blades were applied, are shown in Table 3. The EV_L varied between 5.31 and 6.96 mm d^{-1}, with an average of 5.98 mm d^{-1}.

The soil water evaporation in the ML100WD treatment showed a standard deviation of 0.15 mm d^{-1} between the irrigation blades. The ML100D, ML150WD, and ML150D treatments presented mean deviations of 0.15, 0.29, and 0.24 mm d^{-1} in relation to the irrigation blades, respectively. The mean and median indicated low variation for the soil water evaporation values among the microlysimeter models and sizes and the irrigation blades, indicating that they were close to normal. The trend observed for the low variability of the observed evaporation can be attributed to the short measurement period evaluated and the limited number of days on which evaporation was measured. In addition, irrigation tends to eliminate the differences between treatments and mask the variation in soil water evaporation (Dalmago et al., 2010; Yang et al., 2020).

The average asymmetry for both models and microlysimeter sizes showed negative asymmetry, but the values were close to zero (symmetry). Regarding the kurtosis coefficient (Ck), the mean values of soil water evaporation for the days, microlysimeters, and blades studied mainly showed a leptokurtic distribution ($Ck > 0$), but some days showed a platykurtic distribution ($Ck < 0$), with the distribution of soil water evaporation being close to normal for all days.

3.4 Comparison of soil water evaporation between microlysimeters and lysimeters

The average soil water evaporation values obtained for the 100 mm and 150 mm diameter microlysimeters with and without drainage were subjected to regression analysis, using the evaporation values in the weighing lysimeters (EV_L) as a reference (Fig. 11). The adjusted equations indicate that the soil water evaporation data obtained by the microlysimeters and lysimeters were similar, revealing good agreement between the methods based on the high coefficient of determination (R^2) values. The 100 mm diameter microlysimeters showed R^2 values of 0.9834 and 0.9853 for the models with and without water drainage, respectively, while the 150 mm diameter microlysimeters presented R^2 values of 0.974 and 0.9147, respectively.

Table 3. Mean values and descriptive statistics for daily soil water evaporation determined in lysimeters (EV_L) and microlysimeters (E_{ML}) subjected to four irrigation blades (15, 30, 45 and 60 mm) in Tangará da Serra, Mato Grosso, Brazil.

Date	Soil Water Evaporation (mm d^{-1})					SD	$\bar{X}$	Md	As	Ck
	EVL	ML100WD	ML100D	ML150WD	ML150D					
Irrigation blade - 15 mm										
08/07/2020	6.87	7.70	7.32	7.47	7.27	0.31	7.33	7.32	-0.58	1.17
08/08/2020	7.03	6.88	7.13	6.51	7.36	0.32	6.98	7.03	-0.65	0.78
08/09/2020	6.38	6.62	6.24	6.22	5.80	0.30	6.25	6.24	-0.64	1.48
08/10/2020	5.31	6.18	6.30	6.37	5.80	0.44	5.99	6.18	-1.15	0.28
08/11/2020	6.14	6.24	5.22	5.38	5.09	0.53	5.61	5.38	0.49	-2.89
08/12/2020	5.36	5.86	4.65	5.80	4.56	0.62	5.24	5.36	-0.24	-2.96
08/13/2020	5.41	5.16	4.71	5.80	4.39	0.56	5.09	5.16	-0.05	-1.20
Average	6.07	6.38	5.94	6.22	5.75	0.44	6.07	6.09	-0.40	-0.48
Irrigation blade - 30 mm										
08/07/2020	6.72	8.09	7.70	7.92	7.64	0.53	7.61	7.70	-1.62	3.02
08/08/2020	7.18	7.70	7.58	7.78	8.06	0.32	7.66	7.70	-0.55	1.21
08/09/2020	6.15	6.47	7.07	7.07	7.07	0.43	6.77	7.07	-0.92	-1.55
08/10/2020	5.39	5.86	6.18	6.22	6.51	0.43	6.03	6.18	-0.81	0.45
08/11/2020	6.01	6.11	5.79	6.22	5.38	0.33	5.90	6.01	-1.16	0.97
08/12/2020	5.15	5.09	4.71	5.38	4.61	0.32	4.99	5.09	-0.14	-2.01
08/13/2020	5.31	5.28	4.71	5.94	4.44	0.58	5.14	5.28	0.24	-0.61
Average	5.99	6.37	6.25	6.65	6.24	0.42	6.30	6.43	-0.71	0.21
Irrigation blade - 45 mm										
08/07/2020	6.65	7.07	7.38	7.78	8.21	0.61	7.42	7.38	0.08	-0.88
08/08/2020	6.93	7.38	7.51	7.22	7.78	0.32	7.36	7.38	-0.13	0.06
08/09/2020	6.24	6.94	7.07	6.08	6.65	0.43	6.60	6.65	-0.18	-2.47
08/10/2020	5.24	5.54	5.60	5.52	5.52	0.14	5.48	5.52	-1.88	3.96
08/11/2020	6.23	5.41	5.60	5.66	5.38	0.34	5.66	5.60	1.58	2.70
08/12/2020	5.46	5.16	4.46	5.09	4.19	0.53	4.87	5.09	-0.43	-1.96
08/13/2020	5.49	4.90	4.01	4.81	3.65	0.74	4.57	4.81	-0.15	-1.45
Average	6.03	6.06	5.95	6.02	5.91	0.44	5.99	6.06	-0.16	-0.01
Irrigation blade - 60 mm										
08/07/2020	6.59	7.58	7.89	8.35	8.32	0.72	7.75	7.89	-1.27	1.38
08/08/2020	6.96	7.26	7.70	7.50	7.78	0.34	7.44	7.50	-0.64	-0.92
08/09/2020	6.18	6.68	6.94	6.37	7.19	0.41	6.67	6.68	0.06	-1.68
08/10/2020	5.18	5.03	5.54	5.94	5.97	0.43	5.53	5.54	-0.09	-2.68
08/11/2020	6.14	5.60	5.16	5.80	4.95	0.48	5.53	5.60	0.00	-1.56
08/12/2020	5.31	5.35	4.84	6.03	4.78	0.50	5.26	5.31	0.88	0.49
08/13/2020	5.52	5.72	4.90	5.97	4.56	0.59	5.33	5.52	-0.47	-1.82
Average	5.98	6.17	6.14	6.56	6.22	0.50	6.22	6.29	-0.22	-0.97

EV_L = Lysimeter evaporation; ML100WD = 100 mm microlysimeters without drainage; ML100D = 100 mm microlysimeters with drainage; ML150WD = 150 mm microlysimeters without drainage; ML150D = 150 mm microlysimeters with drainage; SD = Standard deviation; $\bar{X}$ = Average; Md = Median; As = Asymmetry; Ck = Kurtosis.

On a daily basis, the soil water evaporation was on average 15, 8, 18, and 10% higher for ML100WD, ML100D, ML150WD, and ML150D, respectively, when compared to the weighing lysimeter (between ±0.3 and 0.7 mm d^{-1}). Similar results were found by Dalmago et al. (2010), who observed 11% (±0.3 mm d^{-1}) more soil water evaporation from the microlysimeters that had water drainage compared to lysimeters. The high coefficient of determination observed between these measurements demonstrates that the microlysimeter technique

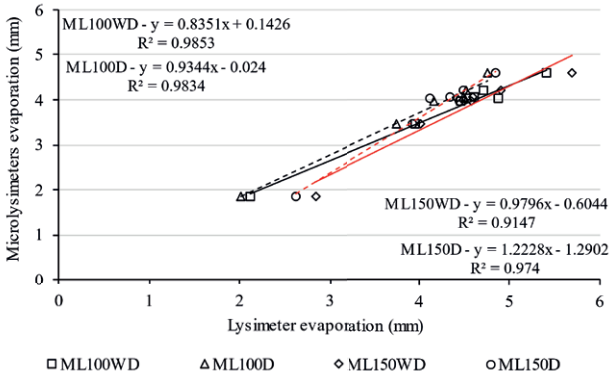

Fig. 11. Linear correlation of soil water evaporation determined by weighing lysimeters and by two sizes of microlysimeters with and without water drainage in Tangará da Serra, Mato Grosso, Brazil.

used in this study can be adopted for soil water evaporation measurements. The significant adjustment of evaporation measured with the microlysimeters relative to that measured with a weighing lysimeter, both in terms of daily and cumulative evaporation, indicates that microlysimeters are suitable for direct measurements of absolute evaporation values in the field.

Similar results were obtained by Dalmago et al. (2010), who evaluated soil water evaporation in soil management systems (no-till and conventional tillage) using microlysimeters of sizes similar to those used in this study. Flumignan et al. (2012) compared soil water evaporation measurements between lysimeters and microlysimeters, and concluded that the use of microlysimeters is valid for soil water evaporation measurements. Facchi et al. (2017) evaluated the performance of microlysimeters for measuring soil water evaporation in rice crops with intermittent irrigation and stated that microlysimeters are effective tools for measuring soil water evaporation.

Care should be taken when using microlysimeters to quantify soil water evaporation, because measurement failures may occur, which, according to Flumignan et al. (2012), can be associated with several factors, such as days with high rainfall, which may cause unevenness of precipitated water reaching the microlysimeter, inhibition of drainage in the microlysimeters, impacts from falling water drops, and removal of soil particles inside the microlysimeters, as well as differences in the amount and intensity of precipitation. The same authors also mentioned that in cultivated soil conditions, the error and variability in evaporation measurements may be greater because the crop canopy intercepts the precipitated water, which is unevenly distributed in the microlysimeters distributed in the soil profile.

The field activities that were developed in this study show that the greatest difficulty in the management of microlysimeters is their fabrication and installation because the soil is very clayey and humid; therefore, this procedure requires care to preserve the extracted soil structure. Flumignan et al. (2012) reported that studies with microlysimeters generally require two people to manufacture and install, but once installed, it only requires the daily presence of one person to perform weighing, which takes little time. In this particular study, where 32 microlysimeters were used, two people over approximately six hours were required to perform the installation in the field, and during data collection, two people were required simultaneously for rapid data collection.

4. CONCLUSIONS

The water drainage at the bottom of the microlysimeters was higher at the beginning of the evaluation and decreased with time. Water drainage occurred for a maximum of 7 h after irrigation, and thereafter, no drainage was observed for the two microlysimeter sizes.

The soil water evaporation values differ significantly between the two microlysimeter sizes (100 and 150 mm diameter) and in the two models (with and without water drainage) and were higher than those observed with the weighing lysimeters. Soil water evaporation is affected by the water drainage that occurs at the bottom of the microlysimeters, with lower evaporation values in the microlysimeter model with drainage compared to those without drainage.

There was no difference between the irrigation blades in terms of soil water evaporation values within the same microlysimeter size and model. The two models and two microlysimeter sizes tested in this experiment can be used for the quantification of soil water evaporation because of the high determination coefficients observed compared to those observed with the weighing lysimeters.

The microlysimeter technique is suitable for measuring soil water evaporation when using irrigation. The high coefficient of determination observed when comparing soil water evaporation between microlysimeters and lysimeters demonstrates that the microlysimeter technique used in this study can be adopted for soil water evaporation measurements.

The study is subject to a specific date and location, needing to assess the effects of drainage on the basis of microlysimeters on soil water evaporation at different locations and assessment times. We emphasize the

importance of studying the functioning of microlysimeters in quantifying soil water evaporation in different types of soil, and these need to be investigated further.

ACKNOWLEDGEMENTS

This study was financed in part by the Coordenação de Aperfeiçoamento de Pessoal de Nível Superior, Brazil (CAPES), Finance Code 001.

REFERENCES

Al-Ghobari, H.M., El-Marazky, M.S., Dewidar, A.Z., Mattar, M.A. 2018. Prediction of wind drift and evaporation losses from sprinkler irrigation using neural network and multiple regression techniques. Agricultural Water Management, 195: 211-221. https://doi.org/10.1016/j.agwat.2017.10.005.

Allen, R.G., Pereira, L.S., Raes, D., Smith, M. 1998. Crop evapotranspiration: Guidelines for computing crop water requirements. FAO Irrigation and drainage paper 56. FAO, Rome, 300: D05109.

Allen, S.J. 1990. Measurement and estimation of evaporation from soil under sparse barley crops in northern Syria. Agricultural and Forest Meteorology 49: 291-309. http://doi.org/10.1016/0168-1923(90)90003-O.

Alvares, C.A., Stape, J.L., Sentelhas, P.C., Gonçalves, J.L.M., Sparovek, G. 2013. Köppen's climate classification map for Brazil. Meteorologische Zeitschrift 22: 711-728. http://dx.doi.org/10.1127/0941-2948/2013/0507.

An, N., Tang, C.S., Xu, S.K., Gong, X.P., Shi, B., Inyang, H.I. 2018. Effects of soil characteristics on moisture evaporation. Engineering Geology 239: 126-135. https://doi.org/10.1016/j.enggeo.2018.03.028.

Andrea, M.C.da.S., Vieira, F.F., Dallacort, R., Barbieri, J.D., Freitas, P.S.L.de., Tieppo, R.C., Zolin, C.A., Krause, W., Daniel, D.F. 2019. Effect of soil coverage on dual crop coefficient of maize in a region of Mato Grosso, Brazil. Journal of Agricultural Science 11: 143-155. http://doi.org/10.5539/jas.v11n13p143.

Aydin, M., Yang, S.L., Kurt, N., Yano, T. 2005. Test of a simple model for estimating evaporation from bare soils in different environments. Ecological Modelling 182: 91-105. http://doi.org/10.1016/j.ecolmodel.2004.07.013.

Barbieri, J.D., Dallacort, R., Daniel, D.F., Dalchiavon, F.C., Freitas, P.S.L.de. 2020. Soil coverage, evapotranspiration and productivity of off-season corn. Cultura Agronômica 29: 76-91. http://dx.doi.org/10.32929/2446-8355.2020v29n1p76-91.

Bernardo, S., Soares, A.A., Mantovani, E.C. 2006. Manual de irrigação. 8th ed. Viçosa: Federal University of Viçosa. 625p.

Blight, G. 2009. Solar heating of the soil and evaporation from a soil surface. Géotechnique 59: 355-363. https://doi.org/10.1680/geot.2009.59.4.355.

Boast, C.W., Robertson, T.M. 1982. A "micro-lysimeter" method for determining evaporation from bare soil: description and laboratory evaluation. Soil Science Society of America Journal 46: 689-696. http://doi.org/10.2136/sssaj1982.03615995004600040005x.

Camargo, O.A., Moniz, A.C., Jorge, J.A., Valadares, J.M.A.S. 2009. Métodos de Análise Química, Mineralógica e Física de Solos do Instituto Agronômico de Campinas. Campinas: IAC. 77p. (Boletim Técnico, 106).

Carvalho, J.R.P.de., Silveira, P.M.da., Vieira, S.R. 2002. Geostatistics to determine spatial variability of soil chemical properties using different preparation systems. Pesquisa Agropecuária Brasileira 37: 1151-1159. http://doi.org/10.1590/S0100-204X2002000800013.

Carvalho, K.S., Vianna, M S., Nassif, D.S., Costa, L.G., Folegatti, M.V., Marin, F.R. 2019. Effect of soil straw cover on evaporation, transpiration, and evapotranspiration in sugarcane cultivation. Australian Journal of Crop Science 13: 1362-1368. https://doi.org/10.21475/ajcs.19.13.08.p1814.

Daamen, C.C., Simmonds, L.P. 1996. Measurement of evaporation from bare soil and its estimation using surface resistance. Water Resources Research 32: 1393-1402. https://doi.org/10.1029/96WR00268.

Daamen, C.C., Simmonds, L.P., Wallace, J.S., Laryea, K.B., Sivakumar, M.V.K. 1993. Use of microlysimeters to measure evaporation from sandy soils. Agricultural and Forest Meteorology 65: 159-173. http://doi.org/10.1016/0168-1923(93)90002-Y.

Dallacort, R., Martins, J.A., Inoue, M.H., Freitas, P.S.L.de., Coletti, A.J. 2011. Rain distribution in Tangará da Serra, mid-northern Mato Grosso state, Brazil. Acta Scientiarum. Agronomy 33: 193-200. http://doi.org/10.4025/actasciagron.v33i2.5838.

Dalmago, G.A., Bergamaschi, H. 2017. Evaporation of the soil water in response to the amount of straw and evaporative demand. Agrometeoros 25: 361-371.

Dalmago, G.A., Bergamaschi, H., Krüger, C.A.M.B., Bergonci, J.I., Comiran, F., Heckler, B.M.M. 2010. Soil surface water evaporation under no-tillage and conventional tillage systems. Pesquisa Agropecuária Brasileira 45: 780-790.

Di, N., Wang, Y., Clothier, B., Liu, Y., Jia, L., Xi, B., Shi, H. 2019. Modeling soil evaporation and the response of the crop coefficient to leaf area index in mature

Populus tomentosa plantations growing under different soil water availabilities. Agricultural and Forest Meteorology 264: 125-137. https://doi.org/10.1016/j.agrformet.2018.10.004.

Facchi, A., Masseroni, D., Miniotti, E.F. 2017. Self-made microlysimeters to measure soil evaporation: a test on aerobic rice in northern Italy. Paddy and Water Environment 15: 669-680. http://doi.org/10.1007/s10333-016-0566-7.

Fenner, W., Dallacort, R., Faria Junior, C.A., Freitas, P.S.L.de., Queiroz, T.M.de., Santi, A. 2019. Development, calibration and validation of weighing lysimeters for measurement of evapotranspiration of crops. Revista Brasileira de Engenharia Agrícola e Ambiental 23: 297-302. http://doi.org/10.1590/1807-1929/agriambi.v23n4p297-302.

Ferreira, D.F. 2011. Sisvar: a computer statistical analysis system. Ciência e Agrotecnologia 35: 1039-1042. http://doi.org/10.1590/S1413-70542011000600001.

Fietz, C.R., Comunello, É., Cremon, C., Dallacort, R. 2008. Estimativa da precipitação provável para o Estado de Mato Grosso. Dourados: Brazilian Agricultural Research Corporation - Embrapa Agropecuária Oeste. 237p.

Fietz, C.R., Comunello, É., Cremon, C., Dallacort, R., Pereira, S.B. 2011. Chuvas intensas no Estado de Mato Grosso. 2nd ed. Dourados: Brazilian Agricultural Research Corporation - Embrapa Agropecuária Oeste. 117p.

Flumignan, D.L., Faria, R.T.de., Lena, B.P. 2012. Test of a microlysimeter for measurement of soil evaporation. Engenharia Agrícola 32: 80-90. http://doi.org/10.1590/S0100-69162012000100009.

Fu, Q., Yan, P., Li, T., Cui, S., Peng, L. 2018. Effects of straw mulching on soil evaporation during the soil thawing period in a cold region in northeastern China. Journal of Earth System Science 127: 1-12. https://doi.org/10.1007/s12040-018-0933-4.

Gupta, B., Shah, D.O., Mishra, B., Joshi, P.A., Gandhi, V.G., Fougat, R.S. 2015. Effect of top soil wettability on water evaporation and plant growth. Journal of Colloid and Interface Science 449: 506-513. http://doi.org/10.1016/j.jcis.2015.02.018.

Heck, K., Coltman, E., Schneider, J., Helmig, R. 2020. Influence of radiation on evaporation rates: a numerical analysis. Water Resources Research, 56: e2020WR027332. https://doi.org/10.1029/2020WR027332.

Lemon, E.R. 1956. The potentialities for decreasing soil moisture evaporation loss. Soil Science Society of America Journal 20: 120-125. http://doi.org/10.2136/sssaj1956.03615995002000010031x.

Liao, Y., Cao, H.X., Liu, X., Li, H.T., Hu, Q.Y., Xue, W.K. 2021. By increasing infiltration and reducing evaporation, mulching can improve the soil water environment and apple yield of orchards in semiarid areas. Agricultural Water Management, 253: 106936. https://doi.org/10.1016/j.agwat.2021.106936.

Lu, Y., Ma, D., Chen, X., Zhang, J. 2018. A simple method for estimating field crop evapotranspiration from pot experiments. Water 10: 1823. https://doi.org/10.3390/w10121823.

Ma, L., Li, Y., Wu, P., Zhao, X., Chen, X., Gao, X. 2020. Coupling evapotranspiration partitioning with water migration to identify the water consumption characteristics of wheat and maize in an intercropping system. Agricultural and Forest Meteorology 290: 108034. https://doi.org/10.1016/j.agrformet.2020.108034.

Mansour, H.A., Gaballah, M.S, Khalil, S.E., Pibars, S.K. 2022. The role of irrigation water management and improving agricultural soils in increasing crop productivity in light of the use of modern technologies. International Journal of Mechanical Engineering 7: 857-865. https://garuda.kemdikbud.go.id/documents/detail/2614550.

Marek, G.W., Colaizzi, P.D., Evett, S.R., Moorhead, J.E., Brauer, D.K., Ruthardt, B.B. 2019. Design, fabrication, and operation of an in-situ microlysimeter for estimating soil water evaporation. Applied Engineering in Agriculture 35: 301-309. https://doi.org/10.13031/aea.13140.

Pereira, L.S., Paredes, P., Jovanovic, N. 2020. Soil water balance models for determining crop water and irrigation requirements and irrigation scheduling focusing on the FAO56 method and the dual Kc approach. Agricultural Water Management, 241: 106357. https://doi.org/10.1016/j.agwat.2020.106357.

Ritchie, J.T. 1972. Model for predicting evaporation from a row crop with incomplete cover. Water Resources Research 8: 1204-1212. http://doi.org/10.1029/WR008i005p01204.

Sánchez, J.M., Simón, L., González-Piqueras, J., Montoya, F., López-Urrea, R. 2021. Monitoring crop evapotranspiration and transpiration/evaporation partitioning in a drip-irrigated young almond orchard applying a two-source surface energy balance model. Water 13: 2073. https://doi.org/10.3390/w13152073.

Santos, H.G.dos., Jacomine, P.K.T., Anjos, L.H.C.dos., Oliveira, V.Á., Lumbreras, J.F., Coelho, M.R., Almeida, J.A.de., Araujo Filho, J.C.de., Oliveira, J.B.de., Cunha, T.J.F. 2018. Brazilian Soil Classification System. 5th ed. Brasília: Brazilian Agricultural Research Corporation.

Schneider, J., Groh, J., Pütz, T., Helmig, R., Rothfuss, Y., Vereecken, H., Vanderborght, J. 2021. Prediction of soil evaporation measured with weighable lysimeters using the FAO Penman–Monteith method in combination with Richards' equation. Vadose Zone Journal 20: e20102. https://doi.org/10.1002/vzj2.20102.

Soil Survey Staff. 2014. Keys to Soil Taxonomy. 12th ed. Washington DC: Natural Resources Conservation Service, United States Department of Agriculture. 372p.

Stolf, R., Murakami, J.H., Maniero, M.A., Soares, M.R., Silva, L.C.F. 2012. Integration of ruler to measure depth in the design of a Stolf impact penetrometer. Revista Brasileira de Ciência do Solo 36: 1476-1482. http://doi.org/10.1590/S0100-06832012000500011.

Teixeira, P.C., Donagemma, G.K., Fontana, A., Teixeira, W.G. 2017. Manual de métodos de análise de solo. 3rd ed. Brasília: Brazilian Agricultural Research Corporation. 574p.

Tesfuhuney, W.A., Van Rensburg, L.D., Walker, S., Allemann, J. 2015. Quantifying and prediction soil water evaporation as influenced by runoff strip lengths and mulch cover. Agricultural Water Management 152: 7-16. http://doi.org/10.1016/j.agwat.2014.11.018.

Vieira, P.V.D., Freitas, P.S.L.de., Silva, A.L.B.R.da., Hashiguti, H.T., Rezende, R., Faria Junior, C.A. 2016. Determination of wheat crop coefficient (Kc) and soil water evaporation (Ke) in Maringa, PR, Brazil. African Journal of Agricultural Research 11: 4551-4558. http://doi.org/10.5897/AJAR2016.11377.

Waggoner, P.E., Turner, N.C. 1972. Comparison of simulated and actual evaporation from maize and soil in a lysimeter. Agricultural Meteorology 10: 113-123. http://doi.org/10.1016/0002-1571(72)90012-X.

Walker, G.K. 1983. Measurement of evaporation from soil beneath crop canopies. Canadian Journal of Soil Science 63: 137-141. https://doi.org/10.4141/cjss83-013.

Wang, Y., Horton, R., Xue, X., Ren, T. 2021. Partitioning evapotranspiration by measuring soil water evaporation with heat-pulse sensors and plant transpiration with sap flow gauges. Agricultural Water Management 252: 106883. https://doi.org/10.1016/j.agwat.2021.106883.

Wang, Y., Li, S., Qin, S., Guo, H., Yang, D., Lam, H.M. 2020. How can drip irrigation save water and reduce evapotranspiration compared to border irrigation in arid regions in northwest China. Agricultural Water Management 239: 106256. http://doi.org/10.1016/j.agwat.2020.106256.

Wang, Y., Yang, J., Chen, Y., Wang, A., De Maeyer, P. 2018. The spatiotemporal response of soil moisture to precipitation and temperature changes in an arid region, China. Remote Sensing 10: 468. https://doi.org/10.3390/rs10030468.

Wei, Z., Paredes, P., Liu, Y., Chi, W.W., Pereira, L.S. 2015. Modelling transpiration, soil evaporation and yield prediction of soybean in North China Plain. Agricultural Water Management 147: 43-53. http://doi.org/10.1016/j.agwat.2014.05.004.

Yang, D., Li, S., Kang, S., Du, T., Guo, P., Mao, X., Ling, T., Hao, X., Ding, R., Niu, J. 2020. Effect of drip irrigation on wheat evapotranspiration, soil evaporation and transpiration in Northwest China. Agricultural Water Management 232: 106001. https://doi.org/10.1016/j.agwat.2020.106001.

Yang, T., Xing, X., Fu, W., Ma, X. 2022. Performances of evaporation and desiccation cracking characteristics for attapulgite soils. Journal of Soil Science and Plant Nutrition 22: 2503–2519. https://doi.org/10.1007/s42729-022-00823-x.

Zhang, G., Shen, D., Ming, B., Xie, R., Jin, X., Liu, C., Hou, P., Xue, J., Chen, J., Shang, W., Liu, W., Wang, K., Li, S. 2019. Using irrigation intervals to optimize water-use efficiency and maize yield in Xinjiang, northwest China. The Crop Journal 7: 322-334. https://doi.org/10.1016/j.cj.2018.10.008.

Italian Journal of Agrometeorology
Rivista Italiana di Agrometeorologia

Firenze University Press
www.fupress.com/ijam

OPEN ACCESS

Citation: A. Irvem, M. Ozbuldu (2022) Evaluation of the performance of CFSR reanalysis data set for estimating reference evapotranspiration (ET_0) in Turkey. *Italian Journal of Agrometeorology* (2): 49-61. doi: 10.36253/ijam-1325

Received: May 31, 2021

Accepted: December 1, 2022

Published: January 29, 2023

Data Availability Statement: All relevant data are within the paper and its Supporting Information files.

Competing Interests: The Author(s) declare(s) no conflict of interest.

Evaluation of the performance of CFSR reanalysis data set for estimating reference evapotranspiration (ET_0) in Turkey

Ahmet Irvem*, Mustafa Ozbuldu

Department of Biosystems Engineering, Faculty of Agriculture, Hatay Mustafa Kemal University, 31040, Antakya, Hatay, Turkey
*Corresponding author. E-mail: airvem@mku.edu.tr

Abstract. Evapotranspiration is a key process and a necessary parameter for hydrological, meteorological, and agricultural studies. However, the calculation of actual evapotranspiration is very challenging and costly. Therefore, reference evapotranspiration (ET_0) calculated using meteorological data is generally preferred over actual evapotranspiration. However, it is challenging to get complete and accurate data from meteorology stations in rural and mountainous regions. This study examined the suitability of the Climate Forecast System Reanalysis (CFSR) reanalysis data set as an alternative to meteorological observation stations to compute seasonal reference evapotranspiration for seven different climatic regions of Turkey. The ET_0 calculations using the CFSR reanalysis dataset for 1987-2017 were compared to data at 259 weather stations observed in Turkey. As a result of statistical evaluations, it has been determined that the most successful predicted season is winter (C' = 0.64-0.89, SPAEF= 0.63-0.81). The most successful estimations for this season were obtained from coastal areas with low elevations. The weakest estimations were obtained for the summer season (C' = 0.52-0.85, SPAEF= 0.59-0.77). These results show that the ET_0 estimation ability of the CFSR reanalysis dataset is satisfactory for the study area. In addition, it has been observed that CFSR tends to overestimate the observation data, especially in the southern and western regions. These findings indicate that the results of the ET_0 calculation using the CFSR reanalysis data set are relatively successful for the study area. However, the data should be evaluated with observation data before being used, especially in the summer models.

Keywords: CFSR reanalysis, Reference evapotranspiration, FAO56-PM, Turkey.

1. INTRODUCTION

Evapotranspiration (ET) is the total amount of water transferred to the atmosphere by evaporation from soil surfaces and transpiration from plant leaves (Tabari et al. 2013; Anderson et al. 2019). ET is the parameter that plays a crucial role in hydrological, meteorological, and agricultural studies, especially in planning water resources, programming irrigation time, and creating models. This parameter is measured in the field with different

methods such as lysimeter (Gebler et al. 2015), Eddy-covariance method (Sun et al. 2008), Bowen ratio energy balance (Shi et al. 2008), scintillometer (Moorhead et al. 2017) and evaporation pans (Conceicao 2002). However, these procedures are quite costly and challenging to apply in wide basin conditions (Latrech et al. 2019).

Reference evapotranspiration (ET_0) is defined as the amount of water that can evaporate when the water in the soil is sufficient to meet the atmospheric moisture demand (Allen et al. 1998). The ET_0 is extremely useful for determining the atmospheric water demand of the area. Therefore, it is widely used in various applications such as irrigation planning, drought monitoring, and understanding the effects of climate change (Lang et al. 2017). Recently, numerous methodologies have been developed to determine ET_0 and actual evapotranspiration using meteorological data (Bandyopadhyay et al. 2012). These methods are mostly based on solar radiation (Priestley Taylor), temperature (Thornthwaite, Hargreaves, and Samani), and a combination of solar radiation and temperature (Penman-Monteith) (Seong et al. 2017; Purnadurga et al. 2019). Compared to other methods, the FAO56-PM method is considered a good way to estimate evapotranspiration globally (Sentelhas et al. 2010; Srivastava et al. 2013; Tabari et al. 2013; Tanguy et al. 2018).

Kite and Drooger (2000) assessed eight different ETo calculation methods and explained that the FAO56-PM method is most compatible with field observations. The FAO56-PM is a combination of physiological and aerodynamic methods that require climate factors like maximum and minimum temperature, wind speed, relative humidity, and solar radiation. However, there are no sufficient meteorological stations providing these data, particularly in developing countries, also these are not distributed uniformly (Alfaro et al. 2020). In addition, setting up and maintaining the meteorological station at these locations is quite costly (Tabari et al. 2013; Lang et al. 2017). Therefore, alternative data sources such as the reanalysis data set can be used to estimate ET_0 in case of a lack of required data. These datasets were generated using data from meteorology observation stations based on data assimilation methods, data from observation satellites, and weather estimate models (Purnadurga et al. 2019).

Reanalysis datasets with high precision and high spatiotemporal resolution have been widely used in recent years. (Alfaro et al. 2020). These are CFSR (Saha et al. 2010), NCEP/DOE (Kanamitsu et al. 2002), and NCEP/NCAR (Kalnay et al. 1996) datasets produced by NCEP, ERA-15 (Bromwich et al. 2005), ERA40 (Uppala et al. 2005) and ERA-Interim (Dee et al. 2011) datasets produced by ECMWF, JRA-55 (Ebita et al. 2011) datasets from the Japanese meteorology agency, and MERRA (Rienecker et al. 2011) datasets by NASA. The NCEP-CFSR uses numerical weather prediction techniques to identify atmospheric conditions with a resolution of 0.3125° x 0.3125° (~ 38 km). (Fuka et al. 2013). The most crucial advantage of CFSR is that it provides complete and continuous recording of climate data such as precipitation, temperature, solar radiation, relative humidity, and wind speed since 1979 (Auerbach et al. 2016).

Laurie et al. (2014) used reanalysis data as input in a hydrological model for the Mekong basin. They evaluated CFSR temperature data and model results. They indicated that CFSR temperature data gave satisfactory model results and it could be used for hydrological modeling studies if data is lacking. Tian et al. (2014) examined the usability of CFSv2 for seasonal estimation of evapotranspiration in different states of the USA. They explained that CFSv2-based ET estimations are more successful in cold seasons than warm seasons. Dile and Srinivasan (2014) assessed whether or not the CFSR dataset is appropriate for hydrologic modeling in their research in the Blue Nile River Basin. As a result of their study, the modeling with CFSR temperature and precipitation data gave similar results to the modeling using the data obtained from the observation stations and reported that the CFSR data set could be used in basins in the absence of observation stations. In another study, Alemayehu et al. (2015) evaluated the ability to calculate evapotranspiration with sufficient accuracy using different reanalysis datasets. They compared the ET_0 estimates calculated using the CFSR dataset with the results of the observation stations and reported that the CFSR dataset is a good alternative. Anderson et al. (2019) evaluated the usability of the CFSR reanalysis dataset in the context of a satellite-based remote sensing framework to map ET at high spatiotemporal resolution. They explained that the CFSR data has sufficient accuracy for use in ET modeling studies. Alfaro et al. (2020) calculated the evapotranspiration required for hydrological modeling with their study's CFSR reanalysis data set. They explained that the predictive performance of the CFSR dataset was good by evaluating the results obtained.

These studies show that reanalysis datasets such as CFSR are of sufficient quality and resolution to be used as inputs in basin modeling studies. In addition, this dataset can be an important alternative for overcoming problems encountered in obtaining meteorological observation data. This study aims to investigate the accuracy and usability of the CFSR reanalysis dataset to calculate ET_0 using the FAO56-Penman method in Turkey.

2. MATERIAL AND METHODS

2.1. Study area and meteorological data

Turkey is located between 36°-42° N and 26°-45° E. The total area is 779.452 square kilometers and the average altitude is 1141 meters. Turkey's climate is located between the temperate and sub-tropical zones. In the country, temperature and precipitation vary according to region due to factors such as the rugged terrain, the direction of the mountains, the fact that seas surround it on three sides, and the elevation increases from west to east. These factors cause different climate types to be seen. Depending on this situation, it has been traditionally accepted by Turkish climatologists since the beginning of the 20th century that there are seven climate regions in Turkey (Erinç, 1984). The locations of these regions are given in Figure 1.

Climate is generally harsh and cold in winter, especially in the Eastern Anatolia region, because of the high-pressure system from Siberia and the low-pressure system from Iceland. In summer, tropical air masses are generally more dominant by the effect of polar air masses moving towards northern latitudes. The Azores high-pressure system from the west of Europe and the Basra low-pressure system from the Persian Gulf are pretty effective in the summer season (Türkeş 2020).

The western and southern parts of the country have a Mediterranean climate, where precipitation peaks at the end of both winter and spring. Other parts generally have a continental climate with the highest precipitation in late spring or early summer. Annual precipitation varies from 295 to 2220 mm having an annual average of 648 mm (Deniz et al. 2011). The Black Sea and Mediterranean regions have more precipitation with the effect of air masses coming over the seas than the inner regions because the amount of precipitation decreases with the effect of the North and South Anatolian mountain ranges. The lowest temperatures are seen in the Eastern Anatolia Region due to the altitude, and the maximum temperatures are seen in the southern parts and the Mediterranean coasts (Katipoglu et al. 2021).

In this study, the calculated ET_0 using the FAO56-PM method, for each station was obtained from the "Vegetable Water Consumption Guide" published by the General Directorate of State Hydraulic Works and Agricultural Research and Policies (TAGEM). TAGEM used 30-year (1987-2017) daily minimum temperature, daily average temperature, daily maximum temperature, daily relative humidity, daily precipitation, daily wind speed,

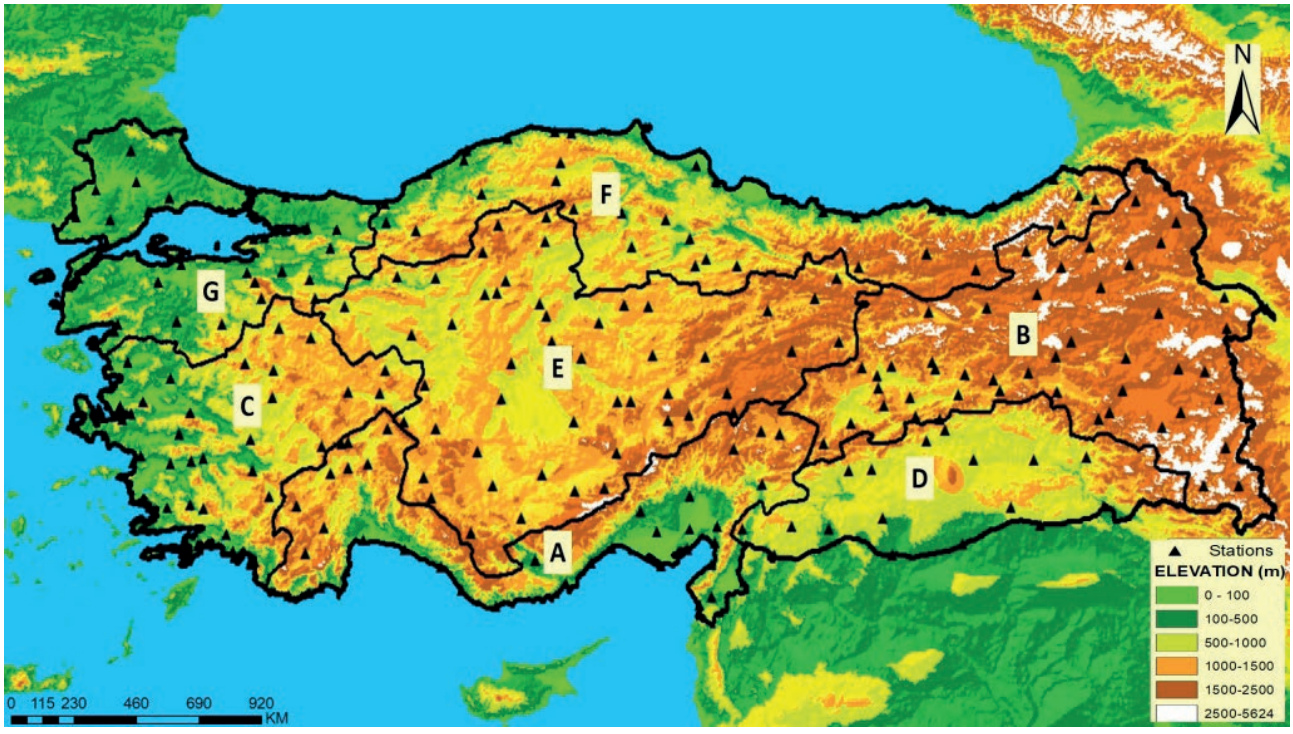

Figure 1. Location of meteorological stations and climate regions (The Mediterranean region (A), The Eastern Anatolia region (B), The Aegean region (C), The South-Eastern Anatolia region (D), The Central Anatolia region (E), The Black Sea region (F), The Marmara region (G)).

daily sunshine duration, and daily intensity of insolation data to calculate the ET_0. All data was obtained from 259 stations belonging to the General Directorate of Meteorology. The location of these stations is given in Figure 1. TAGEM declared that the daily data obtained from the observation stations were subjected to quality control and completed the missing data (TAGEM 2017).

2.2. CFSR reanalysis dataset

The CFSR reanalysis dataset contains the maximum and minimum temperatures (°C), precipitation (mm), wind speed (m s-1), relative humidity (%), and solar radiation (MJ m-2) from any location in the world (Dile and Srinivasan 2014; Irvem and Ozbuldu 2019). The spatial and temporal resolution of the CFSR is 0.35° (nearly 38 km) and 6 hours, respectively. CFSR datasets for Turkey (1987–2017) were obtained via the internet (https://rda.ucar.edu/).

2.3. FAO56-PM method

Penman (1948) developed an evaporation formula for open water surfaces based on climatic data. Monteith (1976) adjusted this formula by adding aerodynamics and surface strength factors and called the Penman-Monteith equation (PM). PM calculated using the given equation.

$$ET_0 = \frac{0.408\,\Delta\,(R_n - G) + \frac{900\,\gamma}{T+273}\,u_2\,(e_s - e_a)}{\Delta + \gamma\,(1 + 0.34\,u_2)} \quad (1)$$

where; ET_0 is daily referenced ET (mm day^{-1}), Δ is the slope of the relationship between saturation vapor pressure and mean daily air temperature (kPa $°C^{-1}$), R_n is the net radiation at the crop surface (MJ m^{-2} day^{-1}), G is the soil heat flux density (MJ m^{-2} day^{-1}), γ is the psychrometric constant which depends on the altitude of each location (kPa $°C^{-1}$), T is the mean daily air temperature (°C), u_2 is the wind speed at 2 m height (m s^{-1}); e_s is the saturation vapor pressure (kPa); e_a is the actual vapor pressure (kPa).

2.4. Evaluation criteria

The five statistical measures were used to evaluate the accuracy of the ET_0 estimation by comparing the calculated ET_0 using CFSR dataset against the calculated ET_0 using meteorological station data. These are the coefficient of determination (R^2), root-mean-square error (RMSE), PBias (percent bias), and the performance index (C') and SPAtial Efficiency (SPAEF).

R^2 shows to what extent the ET_0 estimates calculated with the CFSR dataset are similar to the ET_0 values calculated with the observation data. R^2 varies between 0 and 1, higher values indicate less error variation. Generally, values above 0.50 are considered acceptable (Santhi et al. 2001; Moriasi et al. 2007) and calculated based on Eq 2.

$$R^2 = \left(\frac{n\sum(O_i M_i) - (\sum O_i)(\sum M_i)}{\sqrt{(n(\sum O_i^2) - (\sum O_i)^2)(n(M_i^2) - (\sum M_i)^2)}} \right)^2 \quad (2)$$

The value of RMSE should always be positive and it is desired to be close to zero. This indicates that the lower the value, the better the model will perform. RMSE provides performance information for correlations by comparing the difference between model results and observed values (Piñeiro et al. 2008). RMSE is calculated by Eq. 3.

$$RMSE = \sqrt{\frac{1}{n}\sum(Predict_i - Obs_i)^2} \quad (3)$$

PBias is used to determine how far the model predicted values are in the negative or positive direction from the observed values. Whereas positive values indicate that the observed values are higher than the simulated values, negative values indicate the opposite situation (Gupta et al. 1999). PBias is determined by Eq. 4.

$$PBias = 100\,(\sum Obs_i - Predict_i \,/\, \sum Obs_i\,) \quad (4)$$

The performance index (C') was calculated by combining accuracy and precision criteria into the relationship between the model and the predictive data. The Pearson linear correlation coefficient, which measures the degree and direction of distribution among variables, was used as a precision criterion. The Willmott's index of agreement was chosen as an accuracy criterion because it measures the degree of fit between the predicted and observed data. The performance index of the model was computed by Eq. 5 and evaluated using Table 1 (Santos et al. 2020).

C' = Correlation Coefficient (CC) * Willmott's index of agreement(*d*) (5)

The Willmott index of agreement (d) shows the degree of fit between observed and predicted measurements between 0 and 1. The closer the result is to 1, the better the model performance is determined (Willmott 1981; Tran et al. 2020). It is calculated by Eq. 6.

Table 1. Model performance evaluation table (Moriasi et al. 2007; Santos et al. 2020).

Classification	C'	PBias
Very Good	0.75 - 1.00	< 10
Good	0.65 - 0.75	10 - 15
Satisfactory	0.55 - 0.65	15 - 25
Unsatisfactory	< 0.55	> 25

$$d = \frac{\sum(Obs_i - Predict_i)^2}{\sum([Predict_i - Obs_{mean}] + [Obs_i - Obs_{mean}])^2} \quad (6)$$

SPAEF was developed by Demirel et al. (2018) as a holistic and balanced assessment method that uses various aspects for a comprehensive assessment. SPAEF value is between $-\infty$ and 1. The closer the result is to 1, the higher the prediction success. The SPAEF values are computed by Eq. 7.

$$SPAEF = 1 - \sqrt{(\alpha - 1)^2 + (\beta - 1)^2 + (\gamma - 1)^2}$$

$$\alpha = \rho(obs, sim), \beta = \left(\frac{\sigma_{sim}}{\mu_{sim}}\right) \Big/ \left(\frac{\sigma_{obs}}{\mu_{obs}}\right), \gamma = \frac{\sum_{j=1}^{n} \min(K_j, L_j}{\sum_{j=1}^{n} K_j} \quad (7)$$

where, α represents the Pearson correlation coefficient, β is the fraction of the coefficient of variation representing spatial variability, γ is the histogram intersection for the given histogram K of the observed pattern and the histogram L of the simulated pattern, each containing n bins (Swain and Ballard, 1991). Correlation is a statistical measure that allows two variables to be compared. The CV ratio indicates whether the spatial variability is adequately represented. Histo match value is an indicator of spatial variability that is not present in high and low areas despite satisfactory correlation and spatial variability (Koch et al. 2018).

3. RESULTS AND DISCUSSION

The mean seasonal and mean annual ET_0 were estimated for each observation station using CFSR reanalysis data set which consists of the daily meteorological data from 1987 to 2017. These estimates were compared with the ET_0 values calculated by TAGEM using data from meteorological ground observation stations. The accuracy and usability of the CFSR reanalysis dataset were evaluated using different statistical evaluation criteria. In addition, maps were created using the IDW interpolation technique to show the areal distributions of long-term annual averages of ET_0 results for different seasons.

3.1. Results of ET_0 estimates for the winter season

The ETo estimation results obtained using the CFSR data set for the winter season (December, January, and February) were compared with the observed data separately for each climate region. The performance evaluation results are given in Table 2.

Results show that the estimation performance is higher in regions close to the sea and lower in regions with high elevation. The Performance Index (C') was calculated as 0.89 in the Mediterranean region at the highest, and 0.64 in the Eastern Anatolia region at the lowest. In general, the performance of ET_0 estimations using CFSR data for the winter season was determined to be high (C' > 0.65).

Similar to the Performance Index results, the highest SPAEF values were calculated at 0.81, 0.75, and 0.73 for the Mediterranean, the Black Sea, and the Aegean regions, respectively. Thus, the best estimations of ET_0 for the winter season have been seen in the coastal regions in terms of spatial variability and distribution.

Spatial distribution of estimated and observed ET_0 values for the winter season were classified into 6 categories between 20 and 250 mm as shown in the map (Fig. 2).

Table 2. Performance evaluation results for the winter season.

Regions	R^2	RMSE (mm season^{-1})	PBias (%)	d	C'	SPAEF
The Mediterranean region	0.87	14.87	-5.46	0.96	0.89	0.81
The Eastern Anatolia region	0.72	16.09	23.03	0.76	0.64	0.63
The Aegean region	0.82	20.01	-13.92	0.88	0.80	0.73
The South-Eastern Anatolia region	0.72	8.25	-2.35	0.91	0.78	0.63
The Central Anatolia region	0.76	10.18	3.39	0.90	0.79	0.64
The Black Sea region	0.84	9.27	-0.15	0.96	0.88	0.75
The Marmara region	0.77	5.50	-7.68	0.92	0.81	0.65

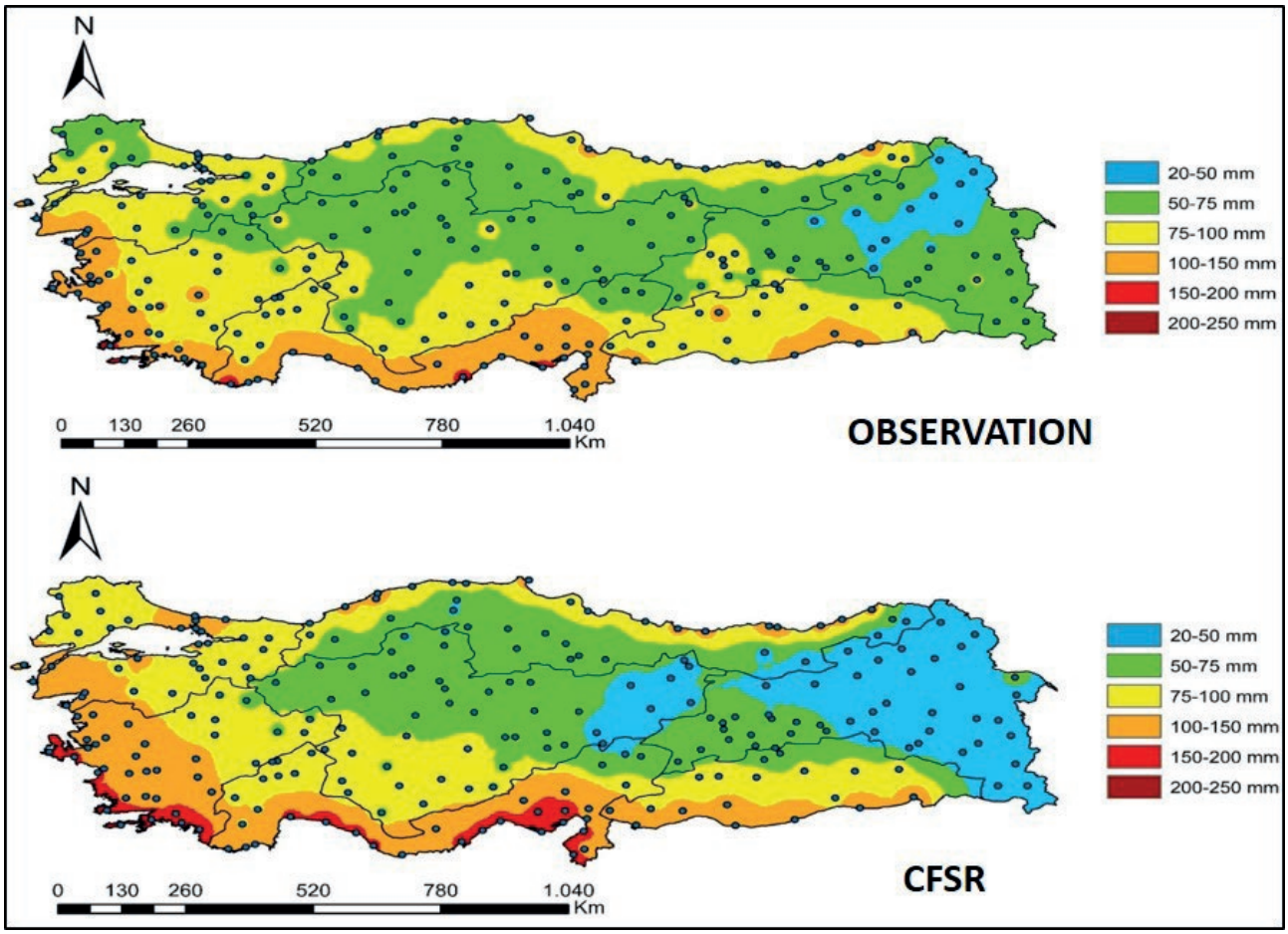

Figure 2. Average long-term ET_0 map for the winter season a) observation b) CFSR.

The CFSR reanalysis dataset has relatively high temperature and solar radiation data in the south and west regions, unlike the eastern region. Consequently, the results of CFSR estimations are better in regions having higher temperatures and solar radiation. PBias values for most stations are negative. ET_0 estimation using CFSR in five regions was overestimated for the winter season. On the other hand, it was underestimated in the Eastern Anatolia (23.03) and Central Anatolia (3.39) regions. Bhattacharya et al. (2020) evaluated reanalysis and global meteorological products in the Beas River Basin of Northwestern Himalaya. They compared CFSR and observed temperature data and explained that the temperature differences between CFSR and observed temperature data are less in the western region where the temperature is higher than in the eastern region.

The R^2 value calculated between 0.72-0.87 as seen in Table 2. This shows that the CFSR reanalysis dataset has a good correlation with the observation data. R^2 values between 0.50-0.99 are considered good estimates for hydrological studies (Alfaro et al. 2020).

3.2. Results of ET_0 estimates for the spring season

The ET_0 estimation results obtained using the CFSR data set for the spring season (March, April, and May) were compared with the observed data separately for each climate region. The performance evaluation results for the spring are given in Table 3.

Performance Index (C') was calculated as 0.81 in the Black Sea region at the highest, and 0.72 in the The South-Eastern Anatolia region at the lowest. In general, the performance of ET_0 estimations using CFSR data for the spring season was determined to be high (C' > 0.70).

Similar to the Performance Index results, the highest SPAEF values were calculated at 0.84, 0.79, and 0.72 for the Black Sea, the Marmara and the Central

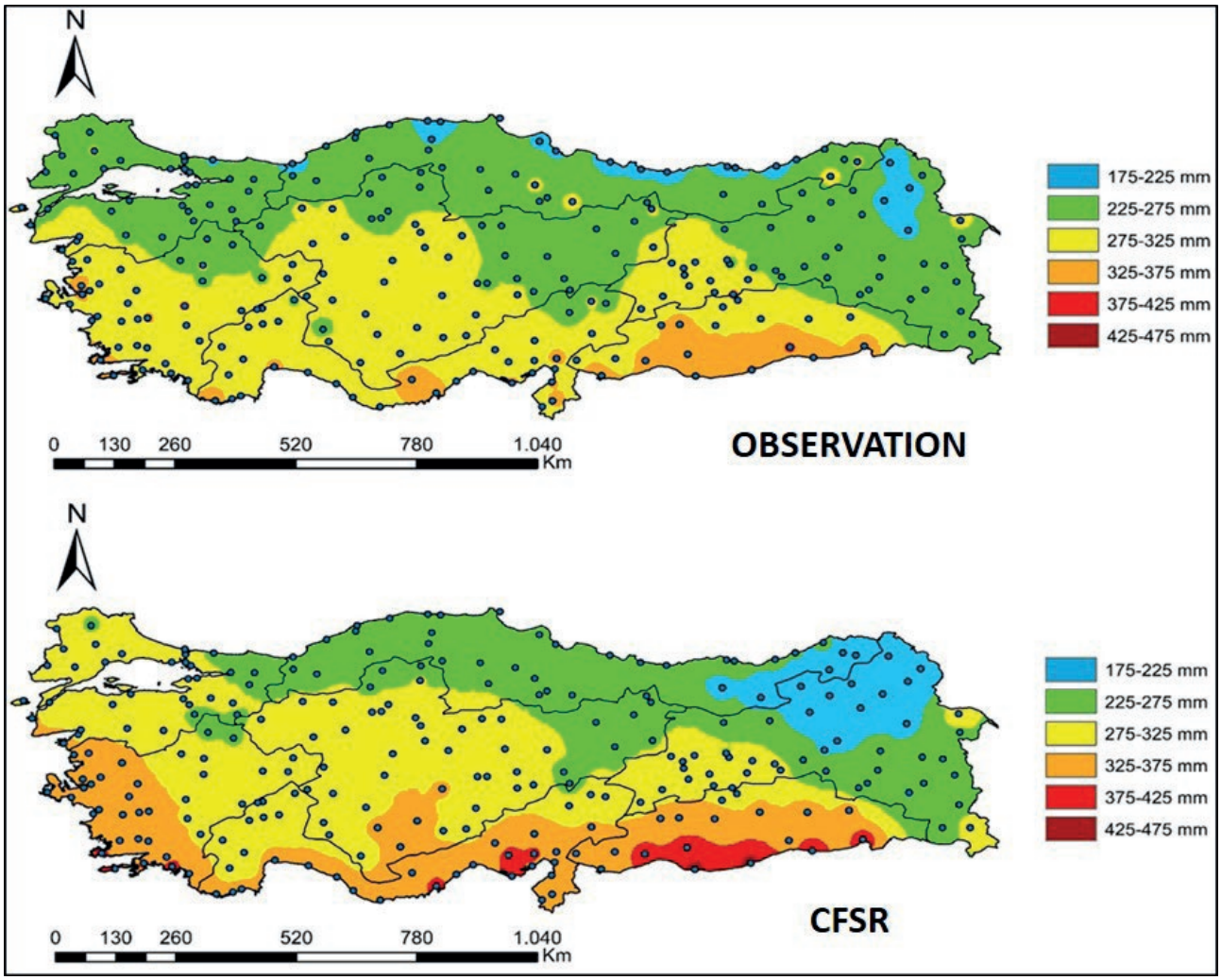

Figure 3. Average long-term ET_0 map for the spring season a) observation b) CFSR.

Table 3. Performance evaluation results for the spring season.

Regions	R2	RMSE (mm season-1)	PBias (%)	C'	SPAEF
The Mediterranean region	0.75	15.40	-3.69	0.77	0.67
The Eastern Anatolia region	0.72	22.23	-5.15	0.73	0.63
The Aegean region	0.75	20.34	-4.61	0.79	0.63
The South-Eastern Anatolia region	0.70	15.27	-5.47	0.72	0.55
The Central Anatolia region	0.77	14.75	-0.78	0.79	0.72
The Black Sea region	0.82	19.30	-2.01	0.81	0.84
The Marmara region	0.79	21.28	-2.64	0.75	0.79

Anatolia regions, respectively. Thus, the best estimations of ET_0 for the spring season have been seen in the northern regions in terms of spatial variability and distribution.

Spatial distribution of estimated and observed ET_0 values for the spring season were classified into 6 categories between 175 and 475 mm as shown in the map (Figure 3). Same as winter season, the results of CFSR

Table 4. Performance evaluation results for the summer season.

Regions	R^2	RMSE (mm season^{-1})	PBias	C'	SPAEF
The Mediterranean region	0.69	72.27	-12.10	0.53	0.61
The Eastern Anatolia region	0.63	76.47	-11.07	0.61	0.59
The Aegean region	0.74	41.06	-7.34	0.71	0.70
The South-Eastern Anatolia region	0.67	69.98	-13.04	0.52	0.61
The Central Anatolia region	0.75	38.96	-6.17	0.74	0.74
The Black Sea region	0.82	22.38	-2.50	0.85	0.77
The Marmara region	0.71	32.90	-2.17	0.75	0.66

estimations for spring are better in regions having higher temperatures and solar radiation. PBias values for most stations are negative. ET_0 estimation using CFSR in all regions was overestimated for the spring season. The R^2 values calculated between 0.70-0.82 as seen in Table 3. This shows that the CFSR reanalysis dataset has a good correlation with the observation data for spring season.

3.3. Results of ET_0 estimates for the summer season

The ET_0 estimation results obtained using the CFSR data set for the winter season (June, July, and August) were compared with the observed data separately for each climate region. The performance evaluation results are given in Table 4.

The Performance Index (C') was calculated as 0.85 in the Black sea region at the highest, and 0.52 in the The South-Eastern Anatolia region at the lowest. In general, the performance of ET_0 estimations using CFSR data for the summer season was determined to be acceptable (C' > 0.55) in five regions but two region have poor estimation performance. These two regions Mediterranean and The South-Eastern Anatolia regions have relatively higher temperature.

Similar to the Performance Index results, the highest SPAEF values were calculated at 0.77, 0.74, and 0.70 for the Black Sea, The Central Anatolia and the Aegean regions, respectively. Thus, the best estimations of ET_0 for the summer season have been seen in the Northern regions in terms of spatial variability and distribution. Spatial distribution of estimated and observed ET_0 values for the winter season were classified into 6 categories between 300 and 900 mm as shown in the map (Figure 4).

When the predictions made by the CFSR for the summer season are compared with the observation data, the differences between the results are higher than in other seasons as seen in Figure 4. The reason for this thought is that temperature and solar radiation increase considerably in the summer months and the CFSR reanalysis data set cannot accurately predict these changes. Tian et al. (2014) reported that the estimates obtained for the winter season were more successful than the summer seasons. They explained that this is due to the fact that more convective heating occurs in summer than in winter. Because this type of convection can produce different weather conditions on a small scale, it may not be detected by reanalysis due to coarse solubility. PBias value was calculated from -2.17 to 12.10 for the summer season. It shows that the CFSR reanalysis made higher estimates in summer than winter and spring, but estimated ET_o for the summer is still in acceptable (<± 25) ranges.

The R^2 values calculated between 0.63-0.82 as seen in Table 4. This shows that the CFSR reanalysis dataset has a good correlation with the observation data for summer season. Although ET_o estimates are acceptable in terms of R^2 (>0.50), the ET_o estimation of the CFSR reanalysis dataset underperforms in the summer due to the decrease in solar radiation and temperature prediction capabilities (Bhattacharya et al. 2020). The reason can be explained that more convective warming occurs in summer compared to other seasons. This type of convection may cause the formation of different weather conditions on a small scale that CFSR cannot predict due to its coarse resolution (Tian et al., 2014). Using the CFSR data set directly on models for the summer months will result in unsuccessful simulation results. For this reason, preliminary procedures that will reduce this dataset to a regional scale should be applied and re-evaluated before using it.

3.4. Results of ET_0 estimates for the autumn

The ET_0 estimation results obtained using the CFSR data set for the autumn season (September, October, and November) were compared with the observed data separately for each climate region. The performance evaluation results are given in Table 5.

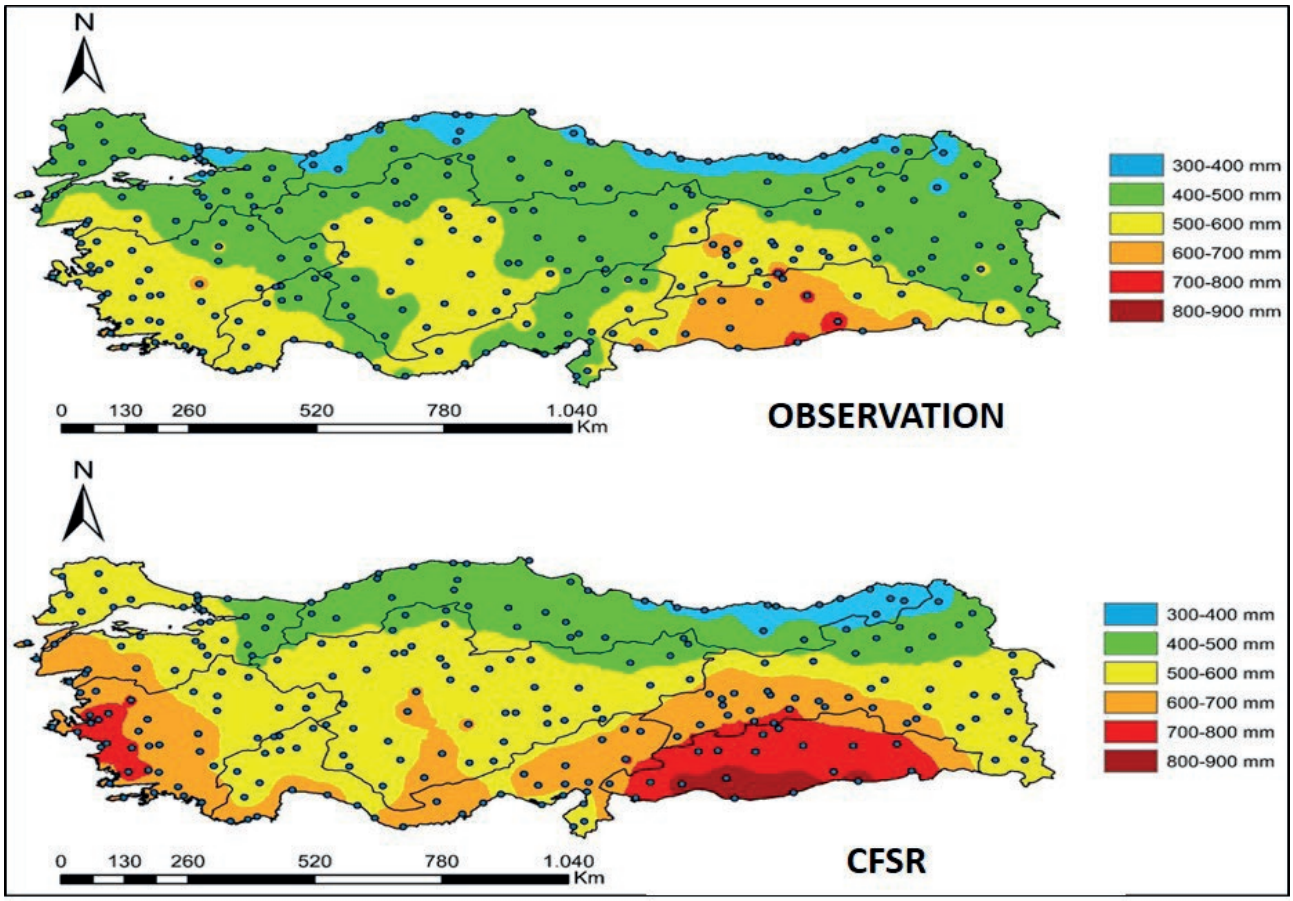

Figure 4. Average long-term ET_0 map for the summer season a) observation b) CFSR.

Performance Index results (C') was calculated as 0.86 in the Black Sea region at the highest, and 0.69 in The South-Eastern Anatolia region at the lowest. In general, the performance of ET_0 estimations using CFSR data for the autumn season was determined to be high (C' > 0.65). Similar to the Performance Index results, the highest SPAEF values were calculated at 0.80, 0.77, and 0.73 for the Mediterranean, the Black Sea, and the Marmara regions, respectively. Thus, the best estimations of ET_0 for the autumn season have been seen in the coastal regions in terms of spatial variability and distribution.

Spatial distribution of estimated and observed ET_0 values for the winter season were classified into 6 categories between 300 and 900 mm as shown in the map (Figure 5). PBias value was calculated from -0.31 to -8.83 for the autumn season. The R^2 values calculated between

Table 5. Performance evaluation results for the autumn season.

Regions	R^2	RMSE (mm season^{-1})	Pbias (%)	C'	SPAEF
The Mediterranean region	0.85	11.16	-4.54	0.84	0.80
The Eastern Anatolia region	0.68	22.52	-8.83	0.72	0.58
The Aegean region	0.80	15.73	-5.83	0.77	0.70
The South-Eastern Anatolia region	0.75	28.73	-4.60	0.69	0.60
The Central Anatolia region	0.84	21.09	-6.50	0.84	0.72
The Black Sea region	0.89	15.45	-0.31	0.86	0.77
The Marmara region	0.77	12.09	-2.82	0.82	0.73

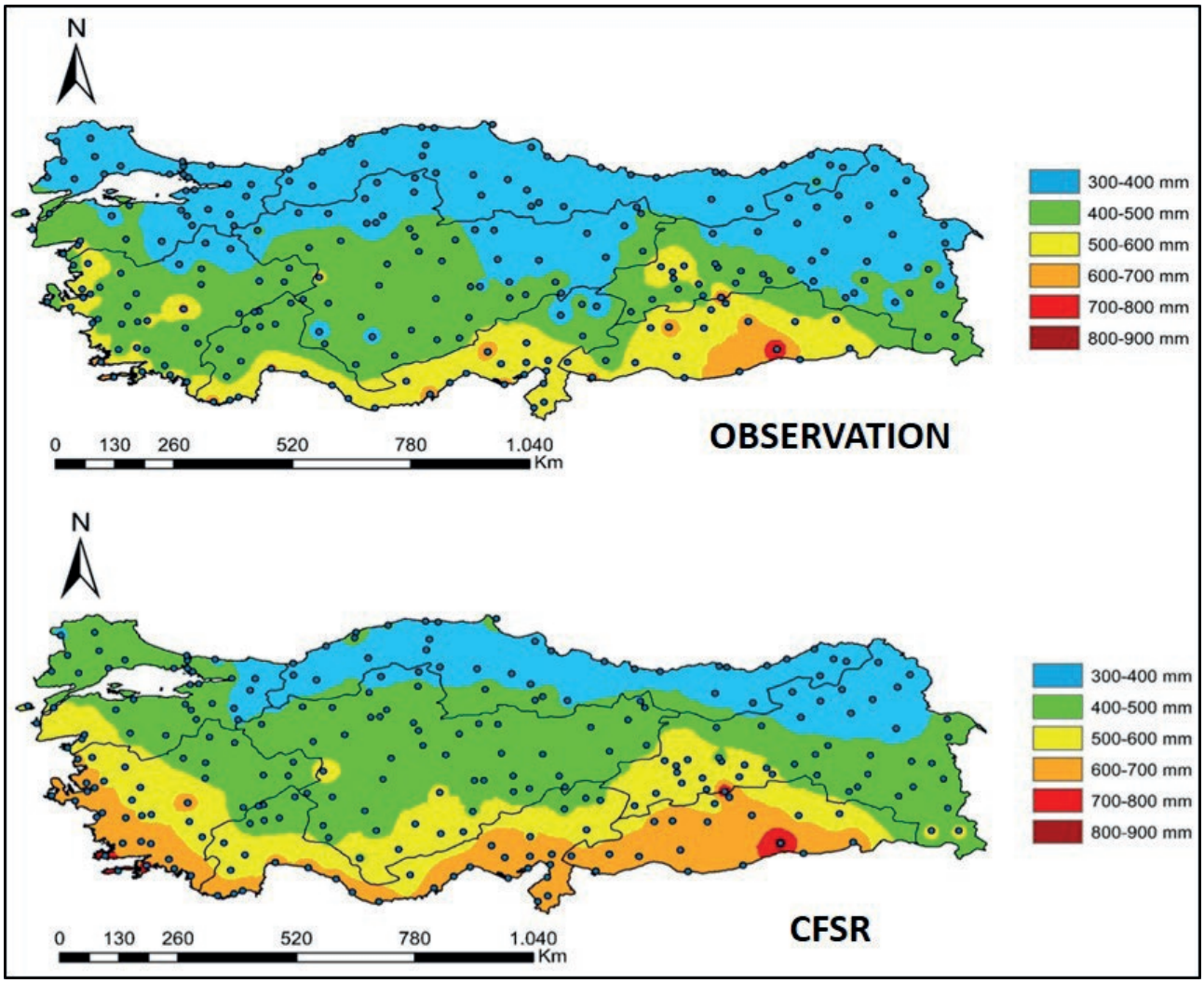

Figure 5. Average long-term ET_0 map for the autumn season a) observation b) CFSR.

0.68-0.89 as seen in Table 5. This shows that the CFSR reanalysis dataset has a good correlation with the observation data for autumn season.

When evaluated in general, it was determined that the ETo estimations for the winter and autumn seasons were more successful than the spring and summer seasons. Tian et al. (2014) explained that the ETo estimations are performed more accurately in the winter season using the CFSR data set for regions with missing ET_o.

While the ET_0 estimations calculated for the coastal regions during the cold seasons performed better, the estimation performance was found to be low in the inner regions with high altitudes. In the spring and summer seasons, the estimate performance was generally lower due to the higher temperature and solar radiation. Especially in summer, estimate performance was underestimated in the southern regions. The CFSR reanalysis dataset tends to overestimate ET_o than the observation data due to increased temperature and solar radiation (Srivastava et al., 2013; Paredes et al., 2017; Tian et al., 2018).

The best estimation performance results are obtained for the coastal regions because the temperature differences in these regions are less than in inner regions due to the effect of the sea in winter. On the other hand, it was understood that the worst estimation results were obtained, especially in the Eastern Anatolia region, due to the difference in temperature values depending on the altitude Bhattacharya et al. (2020) were found similar results in their study carried out in the Beas River Basin of Northwestern Himalaya. It was determined that CFSR was more successful in estimating ETo for north-

ern regions in the spring season. It has been understood that the temperature difference in these regions is less in March, April, and May than in the southern regions, which affects the accuracy of the estimations

4. CONCLUSION

ETo is a very important parameter for hydrological, meteorological, and agricultural studies. However, it is very difficult to obtain the meteorological data for the calculation or estimation of this parameter in developing countries for the required regions. In this study, ETo was estimated by the FAO56-PM method using observed and CFSR data set for Turkey. The accuracy of the seasonal estimations was evaluated statistically by comparing it with the ETo calculated with the meteorological ground observation station data by TAGEM.

As a result of regional evaluations, it has been determined that the most successful predicted season is winter. The most successful estimations for this season were obtained from coastal areas with low elevation. The weakest estimations were obtained for the summer season. Especially with the higher temperature and the solar radiation, very poor estimates were obtained in the southern regions. The ETo estimation ability of the CFSR reanalysis dataset is generally satisfactory for the study area. PBias value was calculated as negative for almost all seasons.

It has been observed that CFSR tends to overestimate the observation data, especially in the southern and western regions. According to all results, the CFSR reanalysis data set is a good potential data source. However, it is recommended to evaluate the data with observation data before being used especially in summer seasons and to be used after regionalization with downscaling methods before being used in models.

REFERENCES

Alemayehu T, van Griensven A, Bauwens W (2016) Evaluating CFSR and WATCH data as input to SWAT for the estimation of the potential evapotranspiration in a data-scarce Eastern-African catchment. J Hydrol Eng 21(3):1–16. https://doi.org/10.1061/(ASCE)HE.1943-5584.0001305

Alfaro MDM, Lopes I, Montenegro AAA, Leal BG (2020) CFSR- NCEP performance for weather data forecasting in the Pernambuco Semiarid, Brazil. DYNA 87(215):204-213. http://doi.org/10.15446/dyna.v87n215.89952

Allen RG, Pereira SL, Raes D, Smith M (1998) Crop evapotranspiration. Guidelines for computing crop water requirements. FAO Irrigation and Drainage Paper 56, Rome, pp 300

Anderson M, Diak G, Gao F, Knipper K, Hain C, Eichelmann E, Hemes K, Baldocchi D, Kustas W, Yang YJRS (2019) Impact of insolation data source on remote sensing retrievals of evapotranspiration over the California Delta. Remote Sens 11:216. https://doi.org/10.3390/rs11030216

Auerbach DA, Easton ZM, Walter MT, Flecker AS, Fuka DR (2016) Evaluating weather observations and the Climate Forecast System Reanalysis as inputs for hydrologic modelling in the tropics. Hydrol Process 30(19):3466–3477. https://doi.org/10.1002/hyp.10860

Bandyopadhyay A, Bhadra A, Swarnakar RK, Raghuwanshi NS, Singh R (2012) Estimation of reference evapotranspiration using a user-friendly decision support system: DSS_ET. Agr Forest Meteorol 154:19–29. https://doi.org/10.1016/j.agrformet.2011.10.013

Bromwich DH, Wang SH (2005) Evaluation of the NCEP-NCAR and ECMWF 15- and 40-yr reanalyses using rawinsonde data from two independent Arctic field experiments. Mon Weather Rev 133:3562–3578. https://doi.org/10.1175/MWR3043.1

Conceição MAF (2002) Reference evapotranspiration based on Class A-pan evaporation. Sci Agric. 59(3):417-420. https://doi.org/10.1590/S0103-90162002000300001

Dee DP, Uppala S, Simmons A, Berrisford P, Poli P, Kobayashi S, Andrae U, Balmaseda M, Balsamo G, Bauer P (2011) The ERA-Interim reanalysis: Configuration and performance of the data assimilation system. Q J Roy Meteor Soc 137:553–597. https://doi.org/10.1002/qj.828

Demirel MC, Mai J, Mendiguren G, Koch J, Samaniego L, Stisen S (2018) Combining satellite data and appropriate objective functions for improved spatial pattern performance of a distributed hydrologic model. Hydrol Earth Syst Sci 22(2): 1299–1315. https://doi.org/10.5194/hess-22-1299-2018

Deniz A, Toros H, Incecik S (2011) Spatial variations of climate indices in Turkey. Int J Clim. 31(3): 394–403. https://doi.org/10.1002/joc.2081

Dile YT, Srinivasan R (2014) Evaluation of CFSR Climate Data for Hydrologic Prediction in Data-Scarce Watersheds: An Application in the Blue Nile River Basin. J Am Water Resour As 50:1226–1241. https://doi.org/10.1111/jawr.12182

Ebita A, Kobayashi S, Ota Y, Moriya M, Kumabe R, Onogi K, Harada Y, Yasui S, Miyaoka K, Takahashi K, Kamahori H, Kobayashi C, Endo H, Soma M,

Oikawa Y, Ishimizu T (2011) The Japanese 55-year Reanalysis "JRA-55": An interim report. SOLA 7:149–152. https://doi.org/10.2151/sola.2011-038

Erinc S. (1984). Climatology and its methods, 3rd edition. Istanbul, Gur-ay Pres Inc. (in Turkish)

Fuka DR, Walter MT, MacAlister C, Degaetano AT, Steenhuis TS, Easton ZM (2013) Using the Climate Forecast System Reanalysis as weather input data for watershed models. Hydrol Process 28:5613–5623. https://doi.org/10.1002/hyp.10073

Gebler S, Hendricks Franssen HJ, Putz T, Post H, Schmidt M, Vereecken H (2015) Actual evapotranspiration and precipitation measured by lysimeters: A comparison with eddy covariance and tipping bucket. Hydrol Earth Syst Sc 19:2145–2161. https://doi.org/10.5194/hess-19-2145-2015

Gupta HV, Sorooshian S, Yapo PO (1999) Status of automatic calibration for hydrologic models: comparison with multilevel expert calibration. J Hydrol Eng 4(2):135–143. https://doi.org/10.1061/(ASCE)1084-0699(1999)4:2(135)

Irvem A, Ozbuldu M 2019 Evaluation of Satellite and Reanalysis Precipitation Products Using GIS for All Basins in Turkey. Adv Meteorol 2019(4820136):1–11. https://doi.org/10.1155/2019/4820136

Kalnay E, Kanamitsu M, Kistler R, Collins W, Deaven D, Gandin L, Iredell M, Saha S, White G, Woollen J, Zhu Y, Chelliah M, Ebisuzaki W, Higgins W, Janowiak J, Mo KC, Ropelewski C, Wang J, Leetmaa A, Reynolds R, Jenne R, Joseph D (1996) The NCEP NCAR 40-year reanalysis project. B Am Meteorol Soc 77:437–472. https://doi.org/10.1175/1520-0477

Kanamitsu M, Ebisuzaki W, Woollen J, Yang SK, Hnilo JJ, Fiorino M, Potter GL (2002) NCEP–DOE amip-ii reanalysis (r-2). B Am Meteorol Soc 83(11):1631–1644. https://doi.org/10.1175/BAMS-83-11-1631

Katipoglu OM, Acar R, Senocak S (2021) Spatio-temporal analysis of meteorological and hydrological droughts in the Euphrates Basin, Turkey. Water Supp, ws2021019. https://doi.org/10.2166/ws.2021.019

Kite GW, Droogers P (2000) Comparing evapotranspiration estimates from satellites, hydrological models and field data. J Hydrol 229:3–18. https://doi.org/10.1016/S0022-1694(99)00193-6

Koch J, Demirel MC, Stisen S (2018) The SPAtial EFficiency metric (SPAEF): multiple-component evaluation of spatial patterns for optimization of hydrological models. Geosci Model Dev 11: 1873–1886. https://doi.org/10.5194/gmd-11-1873-2018.

Lang D, Zheng J, Shi J, Liao F, Ma X, Wang W, Chen X, Zhang M (2017) A comparative study of potential evapotranspiration estimation by eight methods with FAO Penman–Monteith Method in Southwestern China. Water 9:1–18. https://doi.org/10.3390/w9100734

Latrech B, Ghazouani H, Lasram A, M'hamdi BD, Mansour M, Boujelben A (2019) Assessment of different methods for simulating actual evapotranspiration in a semi-arid environment. Ital J Agrometeoro 2:21-34. https://doi.org/10.13128/ijam-650

Lauri H, Räsänen TA, Kummu M (2014) Using reanalysis and remotely sensed temperature and precipitation data for hydrological modeling in monsoon climate: Mekong River case study. J Hydrometeorol 15:1532–1545. https://doi.org/10.1175/JHM-D-13-084.1

Moorhead JE, Marek GW, Colaizzi PD, Gowda PH, Evett SR, Brauer DK, Marek TH, Porter DO (2017) Evaluation of sensible heat flux and evapotranspiration estimates using a surface layer scintillometer and a large weighing lysimeter. Sensors 17:2316–2350. https://doi.org/10.3390/s17102350

Moriasi DN, Arnold JG, Van Liew MV, Bingner RL, Harmel RD, Veith TL (2007) Model evaluation guidelines for systematic quantification of accuracy in watershed simulations. T ASABE 50(3):885–900. https://doi.org/10.13031/2013.23153

Paredes P, Martins DS, Pereira LS, Cadima J, Pires C (2017) Accuracy of daily PM-ETo estimations with ERA-Interim reanalysis products. Euro Water 59:239-246.

Piñeiro G, Perelman S, Guerschman JP, Paruelo JM (2008) How to evaluate models: observed vs. predicted or predicted vs. observed? Ecol Model 216(3-4):316–322. https://doi.org/10.1016/j.ecolmodel.2008.05.006

Purnadurga G, Kumar TL, Rao KK, Barbosa H, Mall RK (2019) Evaluation of evapotranspiration estimates from observed and reanalysis data sets over Indian region. Int J Clim 39(15):5791–5800. https://doi.org/10.1002/joc.6189.

Rienecker MM, Suarez MJ, Gelaro R, Todling R, Bacmeister J, Liu E, Bosilovich MG, Shubert SD, Takacs L, Kim GK, Bloom S, Chen J, Collins D, Conaty A, Silva AD, Gu W, Joiner J, Koster RD, Luccesi R, Molod A, Owens T, Pawson S, Pegion P, Redder CR, Reichle R, Robertson FR, Ruddick AG, Sienkiewicz M, Woollen J (2011) MERRA: NASA's modern-era retrospective analysis for research and applications. J Clim 24:3624–3648. https://doi.org/10.1175/JCLI-D-11-00015.1

Saha S, Moorthi S, Pan HL, Wu X, Wang J, Nadiga S, Tripp P, Kistler R, Woollen J, Behringer D, Liu H, Stokes D, Grumbine R, Gayno G, Wang J, Hou YT, Chuang HY, Juang HMH, Sela J, Iredell M, Treadon R, Kleist D, van Delst P, Keyser D, Derber J, Ek

M, Meng J, Wei H, Yang R, Lord S, van den Dool H, Kumar A, Wang W, Long C, Chelliah M, Xue Y, Huang B, Schemm JK, Ebisuzaki W, Lin R, Xie P, Chen M, Zhou S, Higgins W, Zou CZ, Liu Q, Chen Y, Han Y, Cucurull L, Reynolds RW, Rutledge G, Goldberg M (2010) The NCEP Climate Forecast System Reanalysis. B Am Meteorol Soc 91:1015–1058. https://doi.org/10.1175/2010BAMS3001.1

Salekin S, Burgess J, Morgenroth J, Mason E, Meason D (2018) A comparative study of three non-geostatistical methods for optimising digital elevation model interpolation. ISPRS Int Geo-Inf 7(8):300. https://doi.org/10.3390/ijgi7080300

Santhi C, Arnold JG, Williams JR, Dugas WA, Srinivasan R, Hauck ML (2001) Validation of the SWAT model on a large river basin with point and nonpoint sources. J American Water Resources Assoc 37(5): 1169-1188.

Santos JFS, Leite DC, Severo FAS, Naval LP (2020) Validating the Mark-HadGEM2-ES and Mark-MIROC5 climate models to simulate rainfall in the last agricultural frontier of the Brazilian North and North-East Savannah. Adv Res 21(8):43-54. https://doi.org/10.9734/air/2020/v21i830225

Sentelhas PC, Gillespie TJ, Santos EA (2010) Evaluation of FAO Penman-Monteith and alternative methods for estimating reference evapotranspiration with missing data in Southern Ontario, Canada. Agr Water Manage 97:635-644. https://doi.org/10.1016/j.agwat.2009.12.001

Seong C, Sridhar V, Billah MM (2018) Implications of potential evapotranspiration methods for streamflow estimations under changing climatic conditions. Int J Climatol 38 (2):896–914. https://doi.org/10.1002/joc.5218

Shi TT, Guan DX, Wu JB, Wang AZ, Jin CJ, Han SJ (2008) Comparison of methods for estimating evapotranspiration rate of dry forest canopy: Eddy covariance, Bowen ratio energy balance, and Penman-Monteith equation. J Geophys Res 113(D19):D19116. https://doi.org/10.1029/2008JD010174

Srivastava PK, Han D, Ramirez MAR, Islam T (2013) Comparative assessment of evapotranspiration derived from NCEP and ECMWF global datasets through Weather Research and Forecasting model. Atmos Sci Lett 14:118–125. https://doi.org/10.1002/asl2.427

Sun G, Noormets A, Chen J, McNulty SG (2008) Evapotranspiration estimates from eddy covariance towers and hydrologic modeling in managed forests in Northern Wisconsin, USA. Agr Forest Meteorol 148:257-267.

Tabari H, Grismer ME, Trajkovic S (2013) Comparative analysis of 31 reference evapotranspiration methods under humid conditions. Irrigation Sci 31:107–117. https://doi.org/10.1007/s00271-011-0295-z

TAGEM (2017) Türkiye'de sulanan bitkilerin bitki su tüketimleri. https://www.tarimorman.gov.tr/TAGEM/Belgeler/yayin/Tu%CC%88rkiyede%20Sulanan%20Bitkilerin%20Bitki%20Su%20Tu%CC%88ketimleri.pdf. Accessed: 16 March 2021

Tanguy M, Prudhomme C, Smith K, Hannaford J (2018) Historical gridded reconstruction of potential evapotranspiration for the UK. Earth Syst Sci Data 10(2): 951–968. https://doi.org/10.5194/essd-10-951-2018

Tian D, Martinez CJ, Graham WD (2014) Seasonal prediction of regional reference evapotranspiration based on Climate Forecast System Version 2. J Hydrometeorol 15:1166–1188. https://doi.org/10.1175/JHM-D-13-087.1

Tian Y, Zhang K, Xu YP, Gao X, Wang J (2018) Evaluation of potential evapotranspiration based on CMADS reanalysis dataset over China. Water 10:1126. https://doi.org/10.3390/w10091126

Tran TMA, Eitzinger J, Manschadi AM (2020) Response of maize yield under changing climate and production conditions in Vietnam. Ital J Agrometeorol, 1: 73-84. https://doi.org/10.13128/ijam-764

Türkeş 8M, (2020) Climate and Drought in Turkey. In: Harmancioglu, N., Altinbilek, D. (eds) Water Resources of Turkey. World Water Resources, vol 2. Springer, Cham. https://doi.org/10.1007/978-3-030-11729-0_4

Uppala SM, Kallberg PW, Simmons AJ, Andrae U, Bechtold VDC, Fiorino M, Gibson JK, Haseler J, Hernandez A, Kelly GA, Li X, Onogi K, Saarinen S, Sokka N, Allan RP, Andersson E, Arpe K, Balmaseda MA, Beljaars ACM, Berg LVD, Bidlot J, Bormann N, Caires S, Chevallier F, Dethof A, Dragosavac M, Fisher M, Fuentes M, Hagemann S, Hólm E, Hoskins BJ, Isaksen L, Janssen PAEM, Jenne R, Mcnally AP, Mahfouf JF, Morcrette JJ, Rayner NA, Saunders RW, Simon P, Sterl A, Trenberth KE, Untch A, Vasiljevic D, Viterbo P, Woollen J (2005) The ERA-40 re-analysis. Q J Roy Meteor Soc 131:2961–3012. https://doi.org/10.1256/qj.04.176

Willmott CJ (1981) On the validation of models. Phys Geogr 2(2):184–194. https://doi.org/10.1080/02723646.1981.10642213

Italian Journal of Agrometeorology
Rivista Italiana di Agrometeorologia

Firenze University Press
www.fupress.com/ijam

Citation: S. Banerjee, R. Biswas, A. Mukherjee, A. Sattar (2022) Simulating the impact of elevated thermal condition on wet-season rice grown in Eastern India by different crop growth models. *Italian Journal of Agrometeorology* (2): 63-71. doi: 10.36253/ijam-758

Received: December 9, 2019

Accepted: November 25, 2022

Published: January 29, 2023

Data Availability Statement: All relevant data are within the paper and its Supporting Information files.

Competing Interests: The Author(s) declare(s) no conflict of interest.

Simulating the impact of elevated thermal condition on wet-season rice grown in Eastern India by different crop growth models

Saon Banerjee[1,*], Ria Biswas[2], Asis Mukherjee[3], Abdus Sattar[4]

[1] *Professor, Department of Agril. Meteorology and Physics, Bidhan Chandra Krishi Viswavidyalaya, Mohanpur, Nadia, West Bengal-741 252. India*
[2] *Guest Lecturer, Department of Agril. Statistics, Bidhan Chandra Krishi Viswavidyalaya, Mohanpur, Nadia, West Bengal-741 252. India*
[3] *Assistant Professor, Department of Agril. Meteorology and Physics, Bidhan Chandra Krishi Viswavidyalaya, Mohanpur, Nadia, West Bengal-741 252. India*
[4] *Agrometeorologist, Agrometeorology Division, Dr. Rajendra Prasad Central Agricultural University, Pusa, Samastipur, Bihar-848 125. India*
*Corresponding author. E-mail: sbaner2000@yahoo.com

Abstract. Elevated thermal condition caused by global warming is a threat to major crops grown in India as well as other Asian and tropical countries, as it negatively affects the crop phenology, growth, dry-matter production and yield. The present research work aims to assess the impact of elevated temperature on rice production using three crop growth simulation models, namely, DSSAT, WOFOST and InfoCrop. Field experimental data-set of rice for seven years was used for model calibration and validation. After validation, three models were used to predict the yield under 1, 2 and3^{0}C rise over normal maximum and minimum temperature. The models were also used to assess the thermal impact on leaf area indices (LAI) and crop duration. It was observed that the crop duration was shortened by almost 10 days for 3^{0}C enhancement over normal and the LAI was also reduced considerably. The wet-season rice yield may be reduced by 8.7% for 1^{0}C, 12.5% for2^{0}C and 21.1% for 3^{0}C increase of normal temperature. Use of combination of more than one crop models can predict the climate change impact on rice production more reliably.

Keywords: rice, climate change, temperature, simulation technique, crop growth models.

1. INTRODUCTION

In most of the Asian countries including India, agriculture is expected to be adversely affected by the impact of climate change (IPCC, 2007). The increased climatic variability and anticipated temperature increase caused by global warming are the prime concern of rice crop scientists of Southeast Asia. The elevated thermal condition poses serious threat to rice productivity, which in turn disturb the socio-economic stability of different rice growing

countries (Krishnan, et al., 2007). Globally rice is grown in 154 million ha land, out of which 137 million ha is grown in Asia alone. In Southeast Asia, rice is cultivated in 48 million ha land, i.e., 31 percent of the world rice is grown in this region (FAOSTAT, 2012). In India, rice is the most important food-grain, and it is cultivated in 43.8 million hectares land with 99.50 million tons of total national production (CRRI, 2011). Like all other crops, rice production is also dependent on prevailing weather situation to a considerable extent and therefore any changes in global climate will have major impact on rice production and productivity, causing socio-economic disturbance in Southeast Asia. Hence, in the present paper, rice crop has been chosen to observe the impact of elevated thermal conditions.

Significant warming trend in the tune of 0.51°C per 100 year has been observed in Indian sub-continent for the period 1901-2007(Kothawale et al., 2010). The regional climate models also predict increasing temperature trends for future. The all-India summer monsoon rainfall may increase 3 to 7% in the 2030's compared to 1970's (MoEF, 2010). Rice is water-loving crop and grown under stagnant water condition, hence the probability of getting reduced production under elevated rainfall situation will be less compared to elevated thermal condition. It was found that climate change is likely to reduce the yields of wheat, corn, and rice in Asia by 18.26, 45.10, and 36.25% until 2100 (Zhang, 2017). IFAD (2019) also reported that smallholder farmers cultivating rice will be the most vulnerable community due to climate change. On the contrary, few scientists reported that rice will perform better under elevated thermal condition if sown in optimal time (Devkota et al., 2013; Malhi et al., 2021). Although the impacts of climate change on crop production in Asia will vary by region, most of the regions will experience a decline in production level (IPCC, 2013). To assess the variations in climatic parameters on crop performance, Crop Growth Simulation Models (CGSMs)can be used very accurately, which are dynamic in nature (Hoogenboom et al., 1999; Jones et al., 1998). In near future, simulation will be used more extensively to assess the effects of climate change on agriculture and to find out the suitable adaptation options (Banerjee et al., 2014; Arbuckle et al., 2015). Many scientists are also working on comparison of various CGSMs to assess model's applicability and their interrelationship (Pirttioja et al., 2015; Sandor et al., 2017; Fronzek et al., 2018; Harkness et al. 2020). In this research paper the simulation results will provide some indication on change of LAI, maturity period, and overall yield of wet season rice under elevated thermal condition. Moreover, the calibration and validation processes for three important crop growth models are the part of the present research work.

2. MATERIALS AND METHODS

2.1 Study area

The study area was located under the New Alluvial Agro-climatic Zone of West Bengal, India. The zone is a part of lower Gangetic plain of India, where the climate is typically subtropical – hot and humid. Field experimentation was carried out at Agricultural University Farm of Kalyani (22.57°N, 88.20°E and 7.8 m above mean sea level), Nadia District, West Bengal. The characteristics of the region's climate are hot summers and moderately cool winters. The mean annual rainfall ranges from 140.0 to 160.0 cm. The potential evapotranspiration (PET) varies from 110.0 to 140.0 cm and the water deficit is about 40.0 cm. The length of crop-growing period is greater than 270 days. The seasons of this zone can broadly be divided into five main categories: spring, summer, rainy season, autumn, and winter. The autumn here is comparatively shorter than other parts of India, lasting only from beginning of October to the middle of November. The summer season is typically hot and the maximum temperature ranges between 38°C and 45°C, while the minimum is around 20°C. The monsoon season is observed during June to September and more than 75% of annual rainfall is received during the season. The wet-season rice is grown in this season. Mild winter in December-January is observed here with average minimum temperatures being somewhere around 15°C. Alluvium-derived soil is predominant in the region. The texture of the soil was sandy loam, with moderately well drainage capacity. The bulk density is around 1.55 g cm^{-3} and only 0.5 % soil organic carbon is observed here. The soil of this zone has high water holding capacity and it is less acidic.

2.2 Database generated for model calibration and validation

The crop data was generated through field experimentation under "All India Coordinated Research Program on Agrometeorology" (AICRPAM) of Kalyani center. The most popular rice cultivar of West Bengal State, namely, *Swarna* was grown with different dates of sowing during 2007 to 2013. Data on phenology, crop height, LAI, biomass and yield were recorded from the experiment field for the whole study period (2007 to 2013). Actual observation on phenology, especially days to crop maturity was recorded for all the treatments. The

crop height and LAI were measured for different phonological stages along with final above ground biomass and yield. Data sets of 2007 and 2008 were considered for model calibration (done by simple trial-and-error or iteration method) and the remaining data sets were used for model validation. The weather data of nearby Meteorological Observatory, situated less than 50 m away from experimental field, were used as weather inputs. Soil-data inputs were taken from Annual Progress Report (APR) of FASAL Project (FASAL, 2013). The crop management inputs for the model (such as sowing dates, seed rate, irrigation scheduling, fertilizer applications, etc.) were considered as per State recommendation. With all the input parameters, the rice yield was simulated and compared with actual yield.

2.3 Description of models

In the present paper three models are used to simulate the rice yield, namely DSSAT (Version 4.5), WOFOST (Version 7.1), and Info Crop(Version 1.0). The "Decision support system for agrotechnology transfer" (DSSAT) was developed by the network of scientists associated with International Benchmark Sites Network for Agrotechnology Transfer project (IBSNAT, 1993; Jones et al., 1998). DSSAT is built with a modular approach, with different options available to represent such processes as evapotranspiration and soil organic matter accumulation, which facilitates testing different representations of processes important in crop growth. DSSAT typically requires input parameters related to soil condition, weather, and management practices, such as fertilizer use and irrigation, and characteristics of the crop variety being grown. DSSAT model is driven by CO_2, solar radiation, temperature and rainfall. In this model water level can be maintained like field level under management option interface. The InfoCrop model simulates daily dry matter production as a function of irradiance, maximum and minimum temperatures, water, nitrogen and biotic stresses (Aggarwal et al., 2006). The model provides integrated assessment of the effect of weather, variety, soil and management practices on crop growth and yield along with soil nitrogen and organic carbon dynamics. The WOFOST model computes the instantaneous photosynthesis, where irradiance plays the vital role (Boogaard et al., 1998). After subtracting the maintenance respiration, which described as a function of temperature, assimilates are partitioned over roots, stems, leaves and grains as a function of the development stage of the crop. The effect of soil moisture on crop growth is not considered and a continuously moist soil is assumed.

2.4 Future temperature scenarios

IPCC Fifth Assessment Report (IPCC AR5 WG1) has projected mean temperature increase in the tune of 1°C for RCP 2.6 and 2°C for RCP 8.5 during 2046-2065. During 2081-2100, the mean temperature may be enhanced by 3.6°C for RCP 8.5 (IPCC, 2013). Boomiraj et al., 2010 indicated that mean temperature increase in Eastern India will be about 1°C for 2020 and 3°C in 2050 if A2 scenario is considered. In view of the above referred climate change projections, the impact of 1°C, 2°C and 3°C temperature rise over normal temperature condition on production of wet-season rice has been assessed for Kalyani. The average weather data of thirty years (1981 to 2010) of Kalyani weather station was taken as normal weather data. Then 1°C, 2°C and 3°C were added with both normal maximum and minimum temperature to obtain elevated thermal regime. This regime was used to observe the effect of increased temperature on crop production.

2.5 Statistical procedure

The model performance was worked out using some statistical parameters, such as Coefficient of determination (R^2), Standard Error (SE), Root Mean Square Error (RMSE) and others, which were used to compare the simulated yield, biomass, LAI and crop duration with observed data (Fox, 1981). The linearity between simulated and actual values is denoted by R^2whereas the mean absolute deviation between the said values is described by RMSE. The combination of lower RMSE, higher R^2 values and lower SE indicates the accuracy of simulation model. The bias was also evaluated for testing reliability of the model. Bias indicates the extent up to which the prediction process can be trusted. In the present study, the used statistical tools are given below (Gordon and Shykewich, 2000):

(a) Bias indicates the mean of the predicted value minus the mean of observed value.

$$\text{Bias} = \frac{1}{N}\sum_{i\,1}^{N}(\text{fi} - \text{Oi}) \quad (1)$$

Here, N is observation numbers, fi is the predicted yield and Oi is the observed yield.

(b) Mean absolute error (MAE) is the average of the absolute difference between predicted yield and observed yield.

$$\text{MAE} = \frac{1}{N}\sum_{i\,1}^{N}(|fi - Oi|) \quad (2)$$

(c) Standard error (SE) can be calculated through comparing actual value (x) and predicted value (y). The

equation of SE of the predicted yield value is as follows:

$$SE = \sqrt{\frac{1}{(N-2)}\left[\sum(y-y')^2 - \frac{[\sum(x-x')(y-y')]^2}{\sum(x-x')^2}\right]} \quad (3)$$

and are the average of $y_{i\text{-}N}$ and $x_{i\text{-}N}$ respectively.

(d) The mean of squares of the "errors" is termed as Mean Square Error (MSE).

$$\text{MSE} = \frac{1}{\text{N}}\sum_{\text{i}=1}^{\text{N}}(\text{fi}-\text{Oi})^2 \quad (4)$$

(e) Root mean square error (RMSE) has the advantage over other error estimation methods as the RMSE is measured in the same units as the unit used in the data-set, rather than in squared units.

$$\sqrt{\frac{1}{\text{N}}\sum_{\text{i}=1}^{\text{N}}(\text{fi}-\text{Oi})^2} \quad (5)$$

3. RESULT AND DISCUSSION

3.1 Comparison between simulated and observed yield of wet-season rice by different models

All the three models were used to simulate the rice yield for various dates of sowing. Before working out the simulated yield [termed as Forecast (F)], the genetic coefficients of the said variety were adjusted using iteration or 'trial-and-error' method. The derived genetic coefficients for DSSAT, WOFOST and InfoCrop are enumerated in Table 1, 2 and 3 respectively. The units of different coefficients are also included in the description. The variations of observed and simulated yield for different dates of sowing are shown in Table 4, 5 and 6 for DSSAT, WOFOST and InfoCrop models respectively. For DSSAT model, the difference between forecasted yield (F) and observed yield (O), i.e. bias was minimum compared to other two CGSMs. The highest correlation coefficient values and considerably lower RMSE also indicated the correctness of DSSAT simulated yield (Table 4). WOFOST model was used to predict the early and late transplanted wet season rice for two years. The WOFOST model slightly over-predicted the rice yield (Table 5). Here the RMSE value was more than DSSAT and InfoCrop models, although bias and SE were considerably low. The InfoCrop model output showed the lowest RMSE value indicating that the model can also provide near reliable yield (Table 6). Considering the R^2value, bias, SE and RMSE together, it is concluded that DSSAT and InfoCrop worked better in the study region.

The DSSAT model considers the maximum numbers of input-parameters for predicting the production, hence its performance is better than other two models. In this model, the crop growth rate is modified by stress-parameters like temperature; water deficit, nutrient defi-

Table 1. Genetic coefficients of *Swarna* Cultivar generated through iteration method in DSSAT Model.

Symbol	Description	Values
Juvenile phase coefficient (P1)	Time period (expressed as growing degree days [GDD] in °C over a base temperature of 9 °C) from seeding emergence during which the rice plant is not responsive to changes in photoperiod. This period is also referred to as the basic vegetative phase of the plant.	880
Critical photoperiod (P2O)	Critical photoperiod or the longest day length (in hours) at which the development occurs at a maximum rate. At values higher than P2O development rate is slowed, hence there is delay owing to longer day lengths.	140
Photoperiodism coefficient (P2R)	Extent to which phasic development leading to panicle initiation is delayed (expressed as GDD in °C) for each hour increase in photoperiod above P2O.	200
Grain filling Duration coefficient (P5)	Time period in GDD (°C) from beginning of grain filling (3–4 days after flowering) to physiological maturity with a base temperature of 9 °C. Growth aspects	11.8
Spikelet number coefficient (G1)	Potential spikelet number coefficient as estimated from the number of spikelets per g of main culm dry (less lead blades and sheaths and spikes) at anthesis	54
Single grain weight (G2)	Single grain weight (g) under ideal growing conditions, i.e. non-limiting light, water, nutrients, and in the absence of pests and diseases	0.024
Tillering coefficient (G3)	Tillering coefficient (scaler value) relative to IR64 cultivar under ideal conditions. A higher tillering cultivar would have a coefficient greater than 1.0.	1
Temperature tolerance coefficient (G4)	Temperature tolerance coefficient. Usually 1.0 for varieties growth in normal environments. G4 for japonica-type rice growing in a warmer environment would be 1.0 or greater. Likewise, the G4 value for indica-type rice in very cool environments or season would be less than 1.0	0.9

Table 2. Genetic coefficients of *Swarna* Cultivar generated through iteration method in WOFOST Model.

Symbol	Description	Values
DLO	Optimum daylength for development (Hr)	10.5
TSUM1	Temperature sum from emergence to anthesis (cel d)	1723
TSUM2	Temperature sum from anthesis to maturity (cel d)	526
TDW1	Initial total crop dry weight (kg ha^{-1})	50.00
CVL	Efficiency of conversion into leaves (kg kg^{-1})	0.754
CVO	Efficiency of conversion into storage organ (kg kg^{-1})	0.600
CVR	Efficiency of conversion into roots (kg kg^{-1})	0.754
CVS	Efficiency of conversion into stems (kg kg^{-1})	0.754

Table 3. Genetic coefficients of *Swarna* Cultivar generated through iteration method in InfoCrop Model.

Description	Values
Thermal time for sowing to germination (^{0}C days)	50
Thermal time for germination to 50% flowering (^{0}C days)	1650
Thermal time for 50% flowering to physiological maturity (^{0}C days)	430
Optimum temperature (^{0}C)	32.0
Maximum temperature (^{0}C)	45.0
Sensitivity to photoperiod	1.0
Relative growth rate of leaf area (^{0}C $days^{-1}$)	0.009
Specific leaf area (dm^2mg^{-1})	0.0022
Index of greenness of leaves	1.0
Extinction coefficient of leaves at flowering	0.6
Radiation use efficiency (g MJ^{-1} day^{-1})	2.6
Root growth rate (mm day^{-1})	12.0
Sensitivity of crop to flooding scale	1.0
Index of N fixation	1.0
Slope of storage organ number/m^2 to dry matter during storage organ formation (storage organ/kg^{-1} day^{-1})	56000
Potential storage organ weight (mg^{-1} $grain^{-1}$)	26
Nitrogen content of storage organ (fraction)	0.012
Sensitivity of storage organ setting to low temperature	1.0
Sensitivity of storage organ setting to high temperature	1.0

ciency and many others (Dhakar et al., 2018). Jain et al., 2018 compared the DSSAT with InfoCrop model and opined that production potential under DSSAT model is very high as compared to InfoCrop model. The absence of tillage effects in the InfoCrop model may be another reason for which the R^2 value between observed and predicted yield is less in InfoCrop compared to other two models. In general, the InfoCrop model utilizes the radiation use efficiency (RUE)-based approach for dry matter production and WOFOST calculates dry matter production as a function of gross canopy photosynthesis. The sensitivity of all the three used models to change in ambient temperature and radiation is not similar, which is reflected in the simulated results. Tapio et al., 2016 emphasized development of robust procedures for parameterizing the models, which is observed in all the models used in the present study. The procedural accuracy is reflected through very low RMSE value. Only 3.2%, 6.6% and 1.8% RMSE values (in respect to average actual yield) were observed for DSSAT, WOFOST and InfoCrop models, respectively. Up to 15% grain RMSE is well accepted (Tovihoudji et al, 2019) and the present predicted result is well within acceptable limit.

3.2 Thermal sensitivity of crop growth models

It is well known fact that the crop duration is highly dependent on prevailing temperature and with the temperature enhancement the crop duration decreases (Fatima et al., 2020). This section shows how different models can assess the impact of thermal imbalance on crop duration or other important growth parameter, like LAI. The DSSAT output showed the simulated LAI would decrease with increase of temperature. The decrease of LAI would be more in PI, heading and grain filling stages (**Fig. 1**). The lower LAI throughout the crop growth stages and shorter duration may be the main cause of yield reduction of wet-season rice under elevated thermal condition. **Figure 2** shows the decrease in crop duration for 1^0, 2^0 and 3^0C temperature enhancement over normal. DSSAT model predicted highest decrease in crop duration (10 days for NT + 3°C). On the contrary for 3°C enhancement, InfoCrop predicted only 5 days reduction in crop duration.

3.3 Production of wet-season rice under elevated thermal condition

The normal weather data of the region were used to simulate the yield. To run the model, the normal DOS (4^{th} week of May) were considered, and the common management practices were taken into account. Although higher temperature in the future climatic scenario alters the sowing window of most of the crops (Perego et al., 2014), the wet-season rice sowing in Gangetic West Bengal mainly depends on monsoon rainfall. Hence, for simulating the rice yield for the future, same sowing time has been considered. 1^0C rise in temperature showed around 235 kg ha^{-1} yield reduction through DSSAT and WOFOST models and around 380 kg ha^{-1} yield reduction through InfoCrop model. For enhancement of 1°C rise in temperature, the crop duration will be decreased by 4

Table 4. Comparison between simulated and observed yield of wet-season rice for different sowing dates using DSSAT Model.

Treatments (Sowing date)	Forecast (F)	Observed (O)	F-O	Abs (F-O)	(F-O)^2	R^2	SE	RMSE
26.05.2010	4502	4750	-248	248	61504			
22.06.2010	4107	3940	167	167	27889			
24.05.2011	4156	4084	72	72	5184			
23.06.2011	4014	3943	71	71	5041			
17.05.2012	4610	4730	-120	120	14400			
01.06.2012	4195	4209	-14	14	196			
	4264.0 (Average)	4276.0 (Average)	-12.0 (Bias)	115.3 (ME)	19035.7 (MSE)	0.97	56.3	138

Table 5. Comparison between WOFOST simulated yield and observed yield of wet-season rice.

Treatments	Forecast (F)	Observed (O)	F-O	Abs (F-O)	$(FW-O)^2$	R^2	SE	RMSE
2012 d_0	4360	4469.5	-109.5	109.5	11990.25			
2012 d_1	4178	3663	515	515	265225			
2013 d_0	4541	4707.5	-166.5	166.5	27722.25			
2013 d_1	4287.5	4162.5	125	125	15625			
	4341.62 (Average)	4250.62 (Average)	91 (Bias)	229 (ME)	80140.63 (MSE)	0.95	58.2	283.09

d_0 = Early transplanting (15th June transplanted).
d_1 = Late transplanting (15th July transplanted).

Table 6. Measured and InfoCrop simulated yield of wet-season rice for different years.

Treatments (Days of sowing)	Forecast (F)	Observed (O)	F-O	Abs (F-O)	(F-O)^2	R^2	SE	RMSE
26.05.2009	4480	4375	105	105	11025			
09.06.2009	4710	4660	50	50	2500			
22.06.2009	4084	4105	-21	21	441			
26.05.2010	4637	4750	-113	113	12769			
09.06.2010	4212	4290	-78	78	6084			
22.06.2010	3853	3940	-87	87	7569			
	4329.3 (Average)	4353.3 (Average)	-24.0 (Bias)	75.7 (ME)	6731.3 (MSE)	0.94	95.1	82

days in DSSAT model. Sarath Chandran et al. (2021) also observed similar result for New Alluvial Zone of West Bengal. The reduction in crop duration has resulted less biomass accumulation and eventually lesser yield. Moreover, the higher photorespiration due to higher temperature is one of the major causes of yield reduction under elevated thermal condition. As discussed earlier, for enhancement of 3°C rise in temperature, the crop duration may decrease in the tune of 10 days which is reflected in yield reduction. More than 21% yield reduction is possible for 3°C temperature enhancement compared to normal condition. The InfoCrop predicted the highest yield reduction compared to other two models. Lowering of LAI mainly caused such reduction in InfoCrop, as the model proved less sensitive in case of crop duration. The LAI is another determining factor for yield prediction as pointed out by different scientists. For example, Pagani et al. (2019) used the assimilation of RS-derived LAI as an input parameter to improve the forecasting capability. All the three models' output under elevated thermal condition is shown in Table 7. At least 5% yield reduction would be observed for 1°C rise of normal temperature (NT + 1°C) and 10% yield would be decreased for 2^0C temperature rise (NT + 2°C).

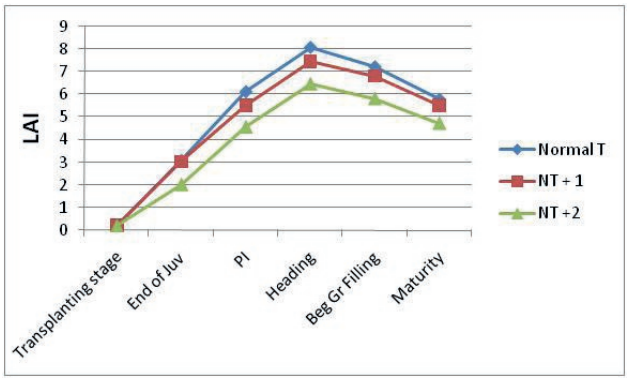

Fig. 1. Change of LAI at different crop growth stages under normal temperature and elevated thermal condition.

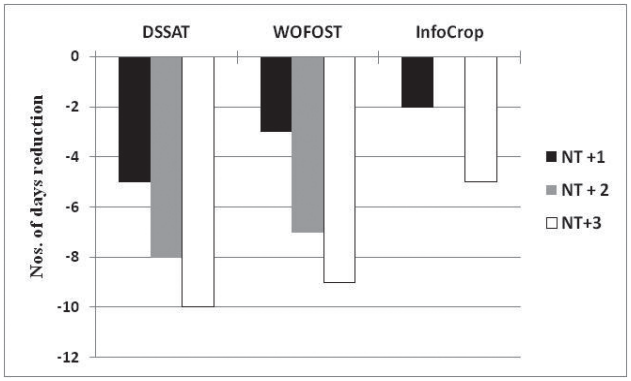

Fig. 2. Reduction in maturity period due to temperature increase (1°C, 2°C and 3°C) over normal temperature (NT).

Table 7. Rice yield under elevated thermal condition.

Models	Yield				% yield reduction		
	NT*	NT+1^{0}C	NT+2^{0}C	NT+3^{0}C	NT+1^{0}C	NT+2^{0}C	NT+3^{0}C
DSSAT	4145.0	3909.3	3625.3	-	5.7	12.5	-
WOFOST	4238.6	4006.5	3784.2	-	5.5	10.7	-
InfoCrop	4380.0	3997.6	-	3455.2	8.7	-	21.1

*Simulate yield under normal temperature (NT) condition

4. CONCLUSIONS

Due to temperature enhancement, the crop duration will be shortened by 2 to 10 days as simulated by different crop growth models. Due to early maturity of rice, farmers can grow short duration leafy vegetables (like spinach, coriander, etc., which takes only 40 days) and then sow the winter vegetables in mid-November. This may be regarded as the positive impact of climate change. There will be enhanced photorespiration and LAI will be reduced if temperature increases. These are the main reasons for reduction of simulated yield under elevated thermal condition. While developing new varieties, the plant breeders must look into these physiological factors to evolve climate resilient variety. All the three models under study predicted lower yield when higher temperature scenario was considered compared to normal weather situation of the study region. For one degree temperature rise, 5 to 8 percent yield will be reduced, whereas for two-degree temperature rise the reduction will be more than 10 percent. The adaptation options, such as added irrigation and fertilizer, choice of varieties, proper sowing window, etc., must be taken care of to reduce the negative impact of elevated thermal condition. DSSAT and InfoCrop models perform better for predicting the yield of wet-season rice in the Lower Gangetic Plains of West Bengal, India. The DSSAT model, being the most robust one, is recommended to assess the climate change impact and adaptation studies for most of the major crops.

ACKNOWLEDGEMENT

The help received from Ms Renaissance for editing the English language of the paper is duly acknowledged. The help and encouragement received from Honorable Vice Chancellor, BCKV and Director of Research, BCKV are gratefully acknowledged. The Mohanpur Centre of AICRP on Agrometeorology, ICAR provided the basic dataset and weather data to run the crop growth models.

REFERENCES

Aggarwal, P.K., Banerjee, B., Daryaei, M.G., Bhatia, A., Bala, A., Rani, S., Chander, S., Pathak, H., Kalra, N. 2006. InfoCrop: a dynamic simulation model for the assessment of crop yields, losses due to pests, and

environmental impact of agro-ecosystems in tropical environments. I. Model description. Agric Syst, 89: 1-25.

Arbuckle, J.G., Morton, L.W., Hobbs, J. 2015. Understanding farmer perspectives on climate change adaptation and mitigation: The roles of trust in sources of climate information, climate change beliefs, and perceived risk. Environ. Behav. 47: 205-234.

Banerjee, S., Das, S., Mukherjee, A., Mukherjee, A. and Saikia, B. 2014. Adaption strategies to combat climate change effect on rice and mustard in Eastern India. *Mitig Adapt Strateg Glob Change*, doi: 10.1007/s11027-014-9595-y.

Boogaard, H.L., van Diepen, C.A., Roetter, R.P., Cabrera, J.M.C.A.,Laar, H.H.V.1998. WOFOST 7.1 : user's guide for the WOFOST 7.1 crop growth simulation model and WOFOST Control Center 1.5. Technical document / DLO Winand Staring Centre; 52. DLO Winand Staring Centre, Wageningen

Boomiraj, K., Chakrabarti, B., Aggarwal, P. K., Choudhary, R.,Chander, S. 2010. Assessing the vulnerability of Indian mustard to climate change. Agric Ecosys and Environ, 138: 265-273.

CRRI 2011. Vision, 2030: Central Rice Research Institute. ICAR, Cuttack, Odisha, India, p. 33.

Devkota, K. P., Manschadi, A. M., Devkota, M., Lamers, J. P. A., E. Ruzibaev, O. Egamberdiev, E. Amiri, P. L. G. Vlek. 2013. Simulating the Impact of Climate Change on Rice Phenology and Grain Yield in Irrigated Drylands of Central Asia. J. Appl. Meteor. Climatol. 52: 2033-2050. doi: http://dx.doi.org/10.1175/JAMC-D-12-0182.1.

Dhakar, R., Sarath Chandran, M. A. Nagar, S., Visha Kumari, V., Subbarao, A. V. M., Bal, S. K., Vijaya Kumar, P. 2018.Field Crop Response to Water Deficit Stress: Assessment Through Crop Models, Advances in Crop Environment Interaction, 287-315. https://doi.org/10.1007/978-981-13-1861-0_11.

FAOSTAT 2012.FAOSTAT Agricultural Production (available at: www.faostat.fao.org/).

FASAL 2013. Annual progress report of FASAL project of Kalyani centre, Directorate of Research, BCKV, pp 4.

Fatima, Z., Ahmed, M., Hussain, M. et al. 2020. The fingerprints of climate warming on cereal crops phenology and adaptation options. Sci Rep, 10: 18013. https://doi.org/10.1038/s41598-020-74740-3

Fox, D. G. 1981.Judging air quality model performance: a summary of the AMS workshop on dispersion model performance. Bull Am Meterol Soc 62: 599-609.

Fronzek, S., Pirttioja, N., Carter, T. R., Bindi, M., Hoffmann, H., Palosuo, T., … &Asseng, S. 2018. Classifying multi-model wheat yield impact response surfaces showing sensitivity to temperature and precipitation change. Agricultural Systems 159: 209-224.

Gordon, N.,Shykewich, J. 2000.Guidelines on performance assessment of public weather service. WMO / TDNO. 1023 pp 9-10.

Harkness, C., Semenov, M. A., Areal, F., Senapati, N., Trnka, M., Balek, J., & Bishop, J. 2020. Adverse weather conditions for UK wheat production under climate change. Agricultural and Forest Meteorology, 282, 107862.

Hoogenboom, G., Wilkens, P. W., Thornton, P.K., Jones, J.W., Hunt, L.A., Imamura, D.T. 1999. Decision support system for agrotechnology transfer v3.5. In: Hoogenboom, G., Wilkens, P.W., Tsuji, G.Y. (Eds.), DSSAT version 3, vol. 4 (ISBN 1-886684-04-9). University of Hawaii, Honolulu, HI, pp. 1-36.

IFAD 2019. Assessing and managing agricultural risk in developing countries. http://www.ifad.org/in.

IBSNAT 1993. The IBSNAT (International Benchmark Sites Network for Agrotechnology Transfer)Decade. Department of Agronomy and Soil Science, College of Tropical Agriculture and Human Resources, University of Hawaii, Honoluly, Hawaii.

IPCC 2007. Climate Change 2007: The Physical Science Basis. Contribution of Working Group I to the Fourth Assessment Report of the Intergovernmental Panel on Climate Change. Solomon S, Qin D, Manning M, Chen Z, Marquis M, Averyt KB, Tignor M, Miller HL (eds) Cambridge University Press, Cambridge, United Kingdom and New York, NY, USA

IPCC 2013.Summary for Policymakers. In: Climate Change 2013: The Physical Science Basis. Contribution of Working Group I to the Fifth Assessment Report of the Intergovernmental Panel on Climate Change [Stocker, T.F., D. Qin, G.-K. Plattner, M. Tignor, S.K. Allen, J. Boschung, A. Nauels, Y. Xia, V. Bex and P.M. Midgley (eds.)]. Cambridge University Press, Cambridge, United Kingdom and New York, NY, USA.

Jain, S., Sastri, A.S.R.A.S., Kumar, B. 2018. Comparison of DSSAT and InfoCrop simulation model for rice production under irrigated and rainfed conditions. International Journal of Chemical Studies, 6(4): 665-669

Jones, J.W., Tsuji, G.Y., Hoogenboom, G., Hunt, L.A., Thornton, P.K., Wilkens, P.W., Imamura, D.T., Bowen, W.T., Singh, U. 1998. Decision support system for agrotechnology transfer; DSSAT v3. In: Tsuji GY, Hoogenboom G, Thornton PK. (Eds.), Understanding Options for Agricultural Production. Kluwer Academic Publishers, Dordrecht, the Netherlands, pp. 157-177.

Kothawale, D. R., Munot, A. A., Krishna Kumar, K. 2010. Surface air temperature variability over India during 1901–2007 and its association with ENSO. Climate Research 42: 89-104. doi.org/10.3354/cr00857.

Krishnan, P., Swain, D.K., Chandra Bhaskar, B., Nayak, S.K., R.N. Dash. 2007. Impact of elevated CO_2 and temperature on rice yield and methods of adaptation as evaluated by crop simulation studies. Agriculture, Ecosystems and Environment, 122: 233-242

Malhi, G.S., Kaur, M., Kaushik, P., 2021. Impact of Climate Change on Agriculture and Its Mitigation Strategies: A Review. Sustainability, 13: 1318. https://doi.org/ 10.3390/su13031318

MoEF (2010) Climate change and India: a 4 × 4 assessment – A sectoral and regional analysis for 2030s. Ministry of Environment and Forests (MoEF), Government of India.

Pagani, V., Guarneri, T., Busetto, L., Ranghetti, L., Boschetti, M., Movedi, E., Ricciardelli, E. 2019. A high-resolution, integrated system for rice yield forecasting at district level. Agricultural systems 168: 181-190.

Perego, A., Sanna, M., Giussani, A., Chiodini, M. E., Fumagalli, M., Pilu, S. R., Acutis, M. 2014. Designing a high-yielding maize ideotype for a changing climate in Lombardy plain (northern Italy). Science of the total environment 499: 497-509.

Pirttioja, N., Carter, T.R., Fronzek, S., Bindi, M., Hoffmann, H., Palosuo, T., Ruiz-Ramos, M., Tao, F., Trnka, M., Acutis, M., Asseng, S., Baranowski, P., Basso, B., Bodin, P., Buis, S., Cammarano, D., Deligios, P., Destain, M.F., Dumont, B., Ewert, F., Ferrise, R., François, L., Gaiser, T., Hlavinka, P., Jacquemin, I., Kersebaum, K.C., Kollas, C., Krzyszczak, J., Lorite, I.J., Minet, J., Minguez, M.I., Montesino, M., Moriondo, M., Müller, C., Nendel, C., Öztürk, I., Perego, A., Rodríguez, A., Ruane, A.C., Ruget, F., Sanna, M., Semenov, M.A., Slawinski, C., Stratonovitch, P., Supit, I., Waha, K., Wang, E., Wu, L., Zhao, Z., Rötter, R.P., 2015. Temperature and precipitation effects on wheat yield across a European transect: A crop model ensemble analysis using impact response surfaces. Clim. Res. 65: 87-105. doi: https://doi.org/10.3354/cr01322.

Sándor, R., Barcza, Z., Acutis, M., Doro, L., Hidy, D., Köchy, M., Minet, J., Lellei-Kovács, E., Ma, S., Perego, A., Rolinksi, S., Ruget, F., Sanna, M., Seddaiu, G., Wu, L., Bellocchi, G., 2017. Multi-model simulation of soil temperature, soil water content and biomass in Euro-Mediterranean grasslands: Uncertainties and ensemble performance. Eur. J. Agron. 88: 22-40. https://doi.org/10.1016/j.eja.2016.06.006.

Sarath Chandran, M.A., Banerjee, S., Mukherjee, A., Nanda, M. K., Mondal, S. and Visha Kumari, V. 2021. Evaluating the impact of projected climate on rice-wheatgroundnut cropping sequence in lower Gangetic plains of India: a study using multiple GCMs, DSSAT model, and longterm sequence analysis. Theoretical and Applied Climatology, https://doi.org/10.1007/s00704-021-03700-2

Tapio J. Salo, TaruPalosuo, Kurt Christian Kersebaum, ClaasNendel, Carlos Angulo, et al.. 2016. Comparing the performance of 11 crop simulation models in predicting yield response to nitrogen fertilization. Journal of Agricultural Science 154(7): 1218-1240. DOI: 10.1017/s0021859615001124

Tovihoudji Pierre G., Akponikpè P. B. Irénikatché, Agbossou Euloge K., Bielders Charles L. 2019. Using the DSSAT Model to Support Decision Making Regarding Fertilizer Microdosing for Maize Production in the Sub-humid Region of Benin. Frontiers in Environmental Science 7: 13. DOI: 10.3389/fenvs.2019.00013

Zhang, P., Zhang, J., Chen, M., 2017. Economic impacts of climate change on agriculture: The importance of additional climatic variables other than temperature and precipitation. J. Environ. Econ. Manag. 83: 8-31.

Finito di stampare da
Logo s.r.l. – Borgoricco (PD) – Italia

RIGOROUS PEER REVIEW
Each submission to IJAm is subject to a rigorous quality control and peer-review evaluation process before receiving a decision. The initial in-house quality control check deals with issues such as competing interests; ethical requirements for studies involving human participants or animals; financial disclosures; full compliance with IJAm's data availability policy, etc.
Submissions may be returned to authors for queries, and will not be seen by our Editorial Board or peer reviewers until they pass this quality control check.
Each paper is subjected to critical evaluation and review by Field Editors with specific expertise in the different areas of interest and by the members of the international Editorial Board.

OPEN ACCESS POLICY
The Italian Journal of Agrometeorology provides immediate open access to its content. Our publisher, Firenze University Press at the University of Florence, complies with the Budapest Open Access Initiative definition of Open Access: By "open access", we mean the free availability on the public internet, the permission for all users to read, download, copy, distribute, print, search, or link to the full text of the articles, crawl them for indexing, pass them as data to software, or use them for any other lawful purpose, without financial, legal, or technical barriers other than those inseparable from gaining access to the internet itself. The only constraint on reproduction and distribution, and the only role for copyright in this domain is to guarantee the original authors with control over the integrity of their work and the right to be properly acknowledged and cited. We support a greater global exchange of knowledge by making the research published in our journal open to the public and reusable under the terms of a Creative Commons Attribution 4.0 International Public License (CC-BY-4.0). Furthermore, we encourage authors to post their pre-publication manuscript in institutional repositories or on their websites prior to and during the submission process and to post the Publisher's final formatted PDF version after publication without embargo. These practices benefit authors with productive exchanges as well as earlier and greater citation of published work.

COPYRIGHT NOTICE
Authors who publish with IJAm agree to the following terms:
Authors retain the copyright and grant the journal right of first publication with the work simultaneously licensed under a Creative Commons Attribution 4.0 International Public License (CC-BY-4.0) that allows others to share the work with an acknowledgment of the work's authorship and initial publication in IJAm.
Authors are able to enter into separate, additional contractual arrangements for the non-exclusive distribution of the journal's published version of the work (e.g., post it to an institutional repository or publish it in a book), with an acknowledgment of its initial publication in this journal.
Authors are allowed and encouraged to post their work online (e.g., in institutional repositories or on their website) prior to and during the submission process, as it can lead to productive exchanges, as well as earlier and greater citation of published work (See The Effect of Open Access).

PUBLICATION FEES
Unlike many open-access journals, the Italian Journal of Agrometeorology does not charge any publication fee.

WAIVER INFORMATION
Fee waivers do not apply at Firenze University Press because our funding does not rely on author charges.

PUBLICATION ETHICS
Responsibilities of IJAm's editors, reviewers, and authors concerning publication ethics and publication malpractice are described in IJAm's Guidelines on Publication Ethics.

CORRECTIONS AND RETRACTIONS
In accordance with the generally accepted standards of scholarly publishing, IJAm does not alter articles after publication: "Articles that have been published should remain extant, exact and unaltered to the maximum extent possible". In cases of serious errors or (suspected) misconduct IJAm publishes corrections and retractions (expressions of concern).

Corrections
In cases of serious errors that affect or significantly impair the reader's understanding or evaluation of the article, IJAm publishes a correction note that is linked to the published article. The published article will be left unchanged.

Retractions
In accordance with the "Retraction Guidelines" by the Committee on Publication Ethics (COPE) IJAm will retract a published article if:
- there is clear evidence that the findings are unreliable, either as a result of misconduct (e.g. data fabrication) or honest error (e.g. miscalculation)
- the findings have previously been published elsewhere without proper crossreferencing, permission or justification (i.e. cases of redundant publication)
- it turns out to be an act of plagiarism
- it reports unethical research.
- An article is retracted by publishing a retraction notice that is linked to or replaces the retracted article. IJAm will make any effort to clearly identify a retracted article as such.

If an investigation is underway that might result in the retraction of an article IJAm may choose to alert readers by publishing an expression of concern.

ARCHIVING
IJAm and Firenze University Press are experimenting a National legal deposition and long-term digital preservation service.

SUBMITTING TO IJAm
Submissions to IJAm are made using FUP website. Registration and access are available at: https://riviste.fupress.net/index.php/IJAm/submission
For more information about the journal and guidance on how to submit, please see https://riviste.fupress.net/index.php/IJAm/index

Principal Contact
Simone Orlandini, University of Florence
simone.orlandini@unifi.it

Support Contact
Alessandro Pierno, Firenze University Press
alessandro.pierno@unifi.it

GUIDE FOR AUTHORS
1. Manuscript should refer to original researches, not yet published except in strictly preliminary form.
2. Articles of original researches findings are published in Italian Journal of Agrometeorology (IJAm), subsequent to critical review and approval by the Editorial Board. External referees could be engaged for particular topics.
3. Three types of paper can be submitted: original paper, review, technical note. Manuscript must be written in English. All pages and lines of the manuscript should be numbered.
4. First Name, Last Name, position, affiliation, mail address, telephone and fax number of all the Co-Authors are required. Corresponding Authors should be clearly identified.
5. The abstract should be no longer than 12 typed lines.
6. Full stop, not comma, must be used as decimal mark (e.g. 4.33 and not 4,33).
7. Figures, tables, graphs, photos and relative captions should be attached in separate files. All images must be vector or at least 300 effective ppi/dpi to ensure quality reproduction.
8. Captions should be written as: Fig. x – Caption title, Tab. x – Caption title. Images should be referred to in the text as (Fig. x), (Tab. x).
9. Proof of the paper (formatted according to the Journal style) will be sent to the Corresponding Author for proof reading just one time. Corrections can be made only to typographical errors.
10. All the references in the text must be reported in the "References" section and vice-versa. In the text, only the Author(s) last name must be present, without the name or the first letter of the name (e.g. "Rossi, 2003" and not "Federico Rossi, 2003" or "F. Rossi, 2003"). If two authors are present, refer to them as: "Bianchi and Rossi, 2003" in the text (do not use "&" between the surnames). If more than two Authors are present, refer to them as: "Bianchi et al., 2003" in the text.
For journals, references must be in the following form:
Bianchi R., Colombo B., Ferretti N., 2003. Title. Journal name, number: pages.
For books:
Bianchi R., Colombo B., Ferretti N., 2003. Book title. Publisher, publishing location, total number of pages pp.
Manuscripts "in press" can be cited.

BECOME A REVIEWER
Peer review is an integral part of the scholarly publishing process. By registering as a reviewer, you are supporting the academic community by providing constructive feedback on new research, helping to ensure both the quality and integrity of published work in your field. Once registered, you may be asked to undertake reviews of scholarly articles that match your research interests. Reviewers always have the option to decline an invitation to review and we take care not to overburden our reviewers with excessive requests.
You must login before you can become a reviewer.
If you don't want to be a reviewer anymore, you can change your roles by editing your profile.

COMPETING INTERESTS
You should not accept a review assignment if you have a potential competing interest, including the following:
- Prior or current collaborations with the author(s)
- You are a direct competitor
- You may have a known history of antipathy with the author(s)
- You might profit financially from the work

Please inform the editors or journal staff and recuse yourself if you feel that you are unable to offer an impartial review.
When submitting your review, you must indicate whether or not you have any competing interests.

Italian Journal of Agrometeorology

Rivista Italiana di Agrometeorologia

n. 2 – 2022

Table of contents